ASSESSING THE POTENTIAL FOR URBAN WIND ENERGY IN CAPE TOWN

MATTHEW BRIAN GOUGH

A thesis submitted for the Degree of Master of Science in Sustainable Energy Engineering

Energy Research Centre
Department of Mechanical Engineering
University of Cape Town

Supervisor: Dr Amos Madhlopa
Co-Supervisor: Professor Azeem Khan

DECLARATION

I know the meaning of plagiarism and declare that all the work in the document, save for that which is properly acknowledged, is my own. This thesis/dissertation has been submitted to the Turnitin module (or equivalent similarity and originality checking software) and I confirm that my supervisor has seen my report and any concerns revealed by such have been resolved with my supervisor.

Pretoria, December 2017

Signed by candidate

Matthew Brian Gough

ABSTRACT

As the demand for alternative and renewable sources of energy grows worldwide, small-scale Urban Wind Energy (UWE) has drawn attention from various researchers as having the potential to generate enough energy to meet a significant portion of the electricity demand for urban areas. However, there is currently a lack of academic research surrounding the realisable potential for UWE, especially in the South African context.

In order to gain a better understanding of the potential of UWE and the barriers acting against its widespread uptake, it is essential to first quantify the resource potential. This study aims to appraise and evaluate the UWE resource potential at six locations in Cape Town, South Africa in order to gain an understanding of the UWE resource potential.

In order to meet the research objectives, wind data was obtained from the South African Weather Service for six locations in Cape Town at five minute recording intervals spanning a period of two years. These locations were: The Royal Cape Yacht Club located in the Table Bay harbour, the Astronomical Observatory located in Observatory, and the Kirstenbosch Botanical Gardens located in Kirstenbosch, the Molteno reservoir located in Oranjezicht, the Automatic Weather station located near the Cape Town International Airport as well as the Cape Town Weather Office (WO) station which is also located at the Cape Town International Airport. The data sets were then analysed using a script written in the programming language *R* in order to quantify the wind energy resource potential of the chosen locations. The wind energy resource potential of each site was combined with the power curves of four commercially available wind turbines in order to calculate the expected annual energy production values of the various turbines at the each of the locations. In order to investigate at which periods of the day a typical turbine is expected to generate electricity, wind data with an interval of five minutes for two days of the year (June 21 and December 21) was used in conjunction with a typical turbine power curve to calculate the electricity generated from a typical turbine over a typical day at a chosen location.

Results from this study highlight the significant variability resource potential of the wind regime that occurs between the six locations. The lowest yearly average wind speed was 2.04m/s which was recorded at the Kirstenbosch recording station, while the highest average wind speed was 5.06m/s which was recorded at the WO station. The average of all six stations for the two year period was 3.24m/s. Therefore the WO station had the highest energy potential with a value of 1474

kWh/m²/year and the station with the lowest energy potential was the Kirstenbosch station with a value of 80 kWh/m²/year. Combining these resource potential values with power curves from four commercially available wind turbines yields the Annual Energy Production (AEP) values for the chosen site and wind turbine. These AEP values also varied drastically with the high of 4304 kWh/year being calculated for the SkyStream turbine at the WO station and a low of just 0.66 kWh/year being calculated at the Kirstenbosch station with the Turby turbine. The wind resource assessment shows that the wind resource potential from one area cannot be reliably used to infer the wind resource potential at another nearby site. This is likely to hinder the uptake of small scale wind power in Cape Town.

The results from the daily generation analysis showed that, during summer, a small scale wind turbine generates the majority of its electricity during the day which resembles the typical South African electricity demand profile. However, during winter, the electricity is mainly generated in the early hours of the morning which does not coincide with the typical load demand profile.

The results of a Levelized Cost of Electricity analysis using the costs associated with the Kestrel e230i turbine show that electricity generated from small scale wind turbines is significantly more expensive than existing domestic electricity rates charged by the City of Cape Town (which are approximately R 2.34/ kWh for households that use more than 600 kW per month) or even the costs of installing rooftop residential PV. The LCOE values calculated in this study range from R 4.11/kWh to R 354.27/kWh. In this study the Horizontal Axis Wind Turbines (HAWTs) had higher calculated values for their Annual Energy Production (AEP) than the Vertical Axis Wind Turbines (VAWTs).

The conclusions of this study show that the UWE resource potential in Cape Town is characterised by high resource variability between the various locations. This study has identified the major challenges associated with UWE to be turbulence, lower hub heights of the wind turbines (this study used 20m as the standard hub height), and variability of the wind regime between locations. These factors, combined with the results of the Levelized Cost of Electricity analysis show that, currently, the use of small scale wind turbines is not a viable or cost competitive form of generating electricity in Cape Town.

ACKNOWLEDGMENTS

I would like to acknowledge and thank the following people who have assisted me in writing this thesis:

- My supervisors, Dr Amos Madhlopa and Professor Azeem Khan, for their guidance and assistance
- The staff at the Energy Research Center for their suggestions and advice during the thesis writing process
- Musa Mkhwanazi and Elsa de Jager at the South African Weather Services for providing the six wind data sets. Your assistance and professionalism is greatly appreciated
- I would like to thank the University of Cape Town's post-graduate funding office who, through the Ada & Bertie Levenstein bursary, provided partial funding for the year 2016 and the National Research Foundation for their funding for the year 2017 through their Renewable and Sustainable Energy Scholarships
- My family and friends who have supported me through the process of writing this thesis
- I would like to thank the R Development Core Team for maintaining and developing R and specifically Christian Graul and Carsten Poppinga who developed the bReeze package for wind resource assessments
- This document has been written in LyX and the formatting is based on André Miede's classic thesis style
- Last but definitely not least, Raquel Jones for her editing, patience, and proofreading skills. Adoro-te.

CONTENTS

LIST OF FIGURES

LIST OF TABLES

ACRONYMS

AEP Annual Energy Production

AWS Automatic Weather Station

AWS Automatic Weather Station

CFD Computational Fluid Dynamics

EEM Equivalent Energy Mehod

GM Graphical Method

GW Gigawatts

HAWT Horizontal Axis Wind Turbine

KIR Kirstenbosch Botanical Gardens

KWH Kilowatt hour

LCOE Levelized Cost of Electricity

MLM Maximum Lilelihood Method

MOL Molteno Reservoir

MOM Moment Method

MW Megawatts

NMT Normal Turbulence Model

OBS South African Astronomical Observatory

PV Photovoltaic

PWMBP Probability Weighted Moments Based on Power density Method

RCYC Royal Cape Yacht Club

REIPPPP Renewable Energy Independant Power Producer Procurement Program

RMSE Root Mean Square Error

SAWS South African Weather Services

TI Turbulence Intensity

TSR Tip Speed Ratio

UWE Urban Wind Energy

VAWT Vertical Axis Wind Turbine

WASA Wind Atlas of South Africa

WO Cape Town Weather Office

WO Weather Office

NOMENCLATURE

A Cross sectional area (m^2/s)

A_{turb} Average turbine availability (%)

C_P Power coefficient (Dimensionless)

C Weibull scale parameter (m/s)

CF Capacity factor (Dimensionless)

E_k Kinetic energy (J)

I Turbulence intensity (%)

K Weibull shape factor (Dimensionless)

M Mass (kg)

P_0 Theoretical available power (W)

p_{pc} Air density at which the turbine's power curve was developed (kg/m^3)

P Power (W)

P_{rated} Rated power of the turbine (W)

P(v_b) Power output at selected wind speed bin (W)

$\boldsymbol{R^2}$ Coefficient of Determination

R Rotor diameter (m)

U Weibull location factor (m/s)

v_b Velocity of chosen wind speed bin b (m/s)

v_{in} Turbine cut in wind speed (m/s)

v_{out} Turbine cut out wind speed (m/s)

V Velocity (m/s)

V Volume flow rate (m^3/s)

V_w Wind speed (m/s)

W(v_b) Probability of chosen wind speed bin occurring (%)

X_{obs} Observed data point

X_{pre} Predicted data point

λ Tip speed ratio (Dimensionless)

ρ Air density (kg/m^3)

ω Rotational speed (rad/s)

1

INTRODUCTION

This chapter provides an introduction to the research undertaken to assess the Urban Wind Energy (UWE) potential in Cape Town. A background section details the global use of wind energy over the years, followed by the problem statement, the scope of the study as well as a section detailing the aims and objectives of the study. This chapter also describes the use of wind energy in South Africa and discusses the subject of small-scale urban wind turbines.

1.1 BACKGROUND

Since the turn of the 21st century, wind power as a form of electricity generation has seen considerable growth worldwide: between the year 2000 to the end of 2016,the amount of globally installed wind generating capacity grew from just under 24GW to reach a recorded total of 486 GW (Global Wind Energy Council, 2016). This growth has enabled wind energy to become a major resource for electricity generation in the renewable energy sector.

Wind as a leading renewable energy resource has predominantly secured its position within the sector through the use of large-scale wind farms which export the electricity into extensive, centralised transmission and distribution grids. Recently , however, the proliferation of distributed energy resources, in particular small-scale rooftop solar photovoltaic (PV) systems, has attracted a significant amount of attention from all spheres to the potential of renewable energy solutions on a smaller scale. Compared to PV systems, the generating potential of small-scale wind turbines has not experienced the same level of research interest.

Research undertaken indicates that while the resource potential for solar PV does not differ greatly between non-urban and urban settings, the differences between non-urban and urban wind energy resources can vary significantly (Karthikeya et al., 2015; Fields et al., 2016). The variations in wind direction and speed in the urban setting are attributed to the effect of buildings and other obstacles on the wind flow. It is this researcher's belief that a deeper understanding of the urban wind regime is required in order to effectively utilise this resource to its full potential on both large and small scales.

The large-scale wind energy sector has also seen considerable growth in South Africa. This growth has been attributed to the success of the Renewable Energy Independent Power Producer Procurement Program (REIPPPP) which has resulted in the procurement of

a total of 2422 MW of wind energy capacity since 2011 and the bidding process has driven down the cost of wind energy by close to 60% since 2011 (Eberhard et al, 2014). Of the 2422 MW of procured capacity, 1472 MW is fully operational as of March 2017 (Energy Blog, 2017). This growth in the wind energy sector has been largely driven by the development of large-scale wind farms along the southern coastline of South Africa.

This growth in large scale wind energy has been driven by robust and detailed wind resource mapping. These maps are generally based on wind data that are recorded at various heights in various non-urban locations around South Africa. The Wind Atlas of South Africa (WASA) is the most recent example of large scale wind resource mapping in South Africa. While there is significant data available concerning non-urban applications of wind energy, there is a shortage of information regarding the potential for small-scale urban wind energy. The urban wind energy regime in South Africa is thus characterised by significant uncertainty. The research undertaken in this thesis aims to assess the energy potential of Cape Town's urban wind regime.

1.2 PROBLEM STATEMENT

It is possible that a substantial percentage of urban electricity demand may be satisfied through the harnessing of wind energy in an urban environment (Yang et al., 2016). Though there are many advantages associated with the harnessing of wind energy in urban areas, the implementation of wind energy technology faces several challenges. One of the main challenges identified by researchers is the uncertainty and complexity surrounding the urban wind regime (Karthikeya et al., 2015; Simões & Estanqueiro, 2015). Driving this complexity is the effect of the surrounding buildings on the wind resource, the varying roughness of the materials used in the urban environment as well as the varying temperature zones in the urban environment (Simões & Estanqueiro, 2015). Additionally, the variance in the wind resource makes reliable data collection difficult (and costly) in the urban environment.

These challenges have meant that there is relatively little reliable urban wind speed data available when compared to the data available for non-urban wind energy applications. This is especially evident in South Africa where there is substantial wind resource data available for large-scale, non-urban wind applications (Hagemann, 2008; South African National Energy Development Institute (SANEDI), 2015), whereas, apart from one feasibility study at a single location in Cape Town (Brosius, 2009), there was no other research available regarding the urban wind energy potential in South African cities at the time of this study.

Even though urban wind energy may have the potential to provide a sizeable portion of the electricity demand for urban areas (Simões & Estanqueiro, 2015), recent research has shown that it may not be able to fully exploit its potential due to a multitude of factors such as: the effects of surrounding buildings; the high levels of turbulence; and the overestimation of the wind resource potential of a particular site, among other factors (Fields et al., 2016). It is therefore imperative that a robust study of urban wind potential in South Africa is carried out to fully understand this potential energy resource. A better understanding of the resource potential of urban wind energy would open the field to further research and provide potential guidelines for further policy discussions and creation.

1.3 SCOPE OF STUDY

The wind resource assessment was undertaken using data supplied by the South African Weather Service (SAWS) for six locations in the Cape Town area. These locations are:

1. The Royal Cape Yacht club located at the Table Bay harbour;
2. The South African Astronomical Observatory located in Observatory;
3. The weather station in the Kirstenbosch Botanical Gardens;
4. The Automatic Weather Station located near the Cape Town International Airport;
5. The Molteno reservoir weather station located in Oranjezicht;
6. The Cape Town Weather Office (WO) located at the Cape Town International Airport.

These sites were chosen as they are spread across various areas of Cape Town and they offer a variety of different wind regimes. Three of these sites (Observatory, Kirstenbosch, and Molteno) are located in residential suburbs of Cape Town and thus are representative of the wind regimes of their respective suburbs. These three locations provided information on the potential for residential scale wind turbines. The three other locations (Royal Cape Yacht Club, the AWS station, and the WO station) are located in more industrial and non-residential areas. These three non-residential locations provided data on the wind energy potential for industrial or commercial clients.

The sites were also chosen based on consultation with the South African Weather Service and these sites have high data availability and a proven track record of providing accurate wind measurements. To this end, all of the six locations have passed their most recent Verification, Conformance and Maintenance report carried out by the

South African Weather Services (South African Weather Services, 2017). These reports are carried out in accordance with the relevant international requirements for the maintenance of instruments as laid out by the World Meteorological Organisation (South African Weather Service, 2017). The data sets all passed the South African Quality Control standard for MetCap data (this standard is discussed in Chapter 3).As this study was limited to just six locations in Cape Town its results may not be relevant to other areas of South Africa. The data from the six locations was recorded over the period from the 1st of January 2015 up to the 31st of December 2016 at 5 minute recording intervals. The length of recording period accounts for the seasonal fluctuations in the wind patterns around the six locations.

1.4 AIMS AND OBJECTIVES

The main aim of the study was to assess the urban wind energy regime in Cape Town, South Africa. This was done by meeting the following research objectives:

- To quantify the urban wind regime in Cape Town
- To identify locations where there is sufficient wind resource potential
- To determine which type of small-scale wind turbine generates the highest AEP values in a given local wind regime
- To determine at what times during the day a typical small scale turbine will generate electricity
- To calculate whether it is cost effective to install a small scale wind turbine in Cape Town

1.5 THESIS OUTLINE

Chapter 1 presents an introduction to the research. In it, the background, the problem statement, the scope of the study as well as the aims and objectives of the study are discussed.

Chapter 2 provides a theoretical framework of the urban wind resource and the technologies used to harness it. This is accomplished through a detailed review of available literature surrounding the urban wind regime, including research on the types of wind turbines used worldwide, physical parameters which influence the performance of wind turbines, methods that are used in order to conduct a wind energy resource assessment as well as the diverse applications of wind energy in an urban environment.

Chapter 3 presents and defines the research methodology applied to the study. This includes the outline of the study's research design,

followed by a section detailing the procedure undertaken during the data analysis. The procedure followed in order to validate the model is specified in this chapter, as well as the procedure followed to conduct a sensitivity analysis based on varying the hub height of the turbine at each location. The final section illustrates the method used to calculate the Levelized Cost of Electricity (LCOE) for a small scale turbine.

Chapter 4 introduces the results of the model followed by a detailed discussion of these results. The results from the wind resource assessment of all six locations are measured against each other. A turbine assessment is presented, including a comparison of the various chosen wind turbines and the results of the hub height sensitivity analysis. The results of the daily electricity generation analysis are presented in detail in this Chapter. The results of the LCOE analysis are discussed.

Conclusions drawn from the results are presented in Chapter 5 as well as suggestions for future research in the field of urban wind energy.

Additional results from the wind resource assessment carried out at the selected sites are shown in Chapter 7.

2

LITERATURE REVIEW

This chapter presents the theoretical framework of the study. In this chapter, the growing use of wind energy for electricity generation, both globally and in South Africa, is discussed. The physical parameters identified from the literature as the most significant in their effects on the urban wind environment are presented and discussed. This chapter also illustrates the different types of wind turbines that are used in the urban wind environment as well as the various applications of these urban wind turbines.

2.1 THE GROWING USE OF WIND ENERGY

As countries become ever more aware of the threats of climate change and the impacts associated with the burning fossil fuels, the drive towards using sustainable energy resources grows. The two leading means of electricity generation in this sustainable energy revolution are solar energy and wind energy. Theoretically, a combination of both these resources would hold far more energy than the human population could consume. In a more local context, South Africa has abundant resources of both solar and wind energy. As the cost of the technologies associated with both resources has decreased, so the availability and attractiveness of these technologies have increased, leading to their establishment as serious competitors to the traditional fossil fuelled means of electricity generation in the energy landscape.

South Africa is one of the countries globally to have seen considerable growth in the use of wind energy in the last few years (Energy Blog, 2017). This can be attributed to the success of the South African government's electricity capacity expansion programme, Renewable Energy Independent Power Producer Procurement Program (REIPPPP), which resulted in the procurement of a total of 2422 MW of wind energy since 2011(Energy Blog, 2017; Eberhard et al., 2014). The initiative consisted of a number of bidding rounds which saw prospective buyers bid against each other for the rights to set amounts of generation capacity at a fixed cost per kWh over the 20-year lifetime of the Power Purchase Agreement (PPA). This bidding process saw the cost of wind-generated electricity go down by almost 60% (Energy Blog, 2017; Eberhard et al., 2014). The projects chosen under the REIPPPP are, almost without exception, large-scale wind farms, identified by the project developers through detailed wind resource mapping. The mapping of South Africa's wind resource was originally carried out by researcher Roseanne Diab for the Department of

Mineral and Energy Affairs and then subsequently improved upon by Kilian Hagemann , who developed a mesoscale map of the available wind resources in South Africa for his PhD thesis entitled ' Mesoscale Wind Atlas of SA' (Fant et al., 2016). Hagemann estimated that South Africa could produce just over 80 TWh of electricity from its wind resource, i.e. approximately 35% of current electricity usage in the country (Fant et al., 2016). The South African National Energy Development Institute (SANEDI) also commissioned a Wind Atlas for South Africa (WASA). These three studies have identified the regions in South Africa with the highest potential for wind energy and these areas are generally located along the southern coast lines of South Africa, away from any urban development.

2.2 BASIC FLUID MECHANICS

This section introduces basic concepts of fluid mechanics as they relate to the context of the wind regime around a wind turbine. A fluid is defined as a substance that exists in either a liquid or gaseous form (Çengel & Cimbala, 2006). These two phases are two of the four phases of matter with the other phases being the solid phase and plasma. The defining difference between a solid and fluid is its ability to resist applied shear (or tangential) stresses (Çengel & Cimbala, 2006). A solid can resist these stresses by deforming while a fluid cannot resist these stresses and deforms continuously. In fluids stress is proportional to strain rate while in solids the stress is proportional to strain (Çengel & Cimbala, 2006). If a constant shear force is applied to a solid, the solid will eventually cease deforming at a certain fixed strain angle while a fluid never ceases deforming and reaches a certain rate of strain (Çengel & Cimbala, 2006).

When dealing with flowing fluids, the concept of a streamline is useful to visualise the flow of the fluid. A streamline is defined by Çengel & Cimbala (2006) as 'a curve that is everywhere tangent to the instantaneous local velocity vector' or in other words a streamline shows the direction in which a fluid element with no mass will travel at any instant in time. A collections of streamline is termed a streamtube (Çengel & Cimbala, 2006). A pathline is similarly defined as the path that a particle will follows in a fluid over a time period (Çengel & Cimbala, 2006).

2.3 WIND RESOURCE

2.3.1 *Origin of wind*

Global wind patterns are caused by pressure differentials created by the irregular heating of the earth's surface due to solar radiation (Manwell et al., 2010). The surface of the earth nearer to the equator

absorbs more solar irradiation than the areas closer to the poles. This uneven incoming solar radiation causes convective cells to emerge in the troposphere (the lower levels of the atmosphere) subsequently causing air to rise at the equator and sink at the poles (Manwell et al., 2010). The convective cells are also influenced by the Coriolis force which is caused by the rotation of the earth, inertial forces of global wind energy patterns and the frictional force of the earth's surface (Brower, 2012).

2.3.2 *Temporal characteristics of wind*

Wind speed can vary with time and these variations are divided into the following categories (Manwell et al., 2010):

- Inter-annual
- Annual
- Diurnal
- Short term

Inter-annual variations in wind speed occur over periods that are longer than one year (Manwell et al., 2010). These variations can be caused by regional, hemispheric, and global climate variances such as the El Niño events (New York State Energy Research Development Authority (NYSERDA), 2010). Annual variations denote the seasonal or monthly fluctuations that affect the wind resource during the year as various locations are subjected to local weather patterns which change during the course of the year (Manwell et al., 2010).

Diurnal variations in wind speed concern changes in wind speed which occur daily, caused by fluctuations in the heating of the earth's surface due to solar radiation (Brower, 2012). Short term wind speed denotes fluctuations in wind speed which occur over a period of hours or minutes (Brower, 2012). Wind speed variations at this time interval include a stochastic variable that is generally known as turbulence (Manwell et al., 2010). Turbulence is defined as the random fluctuations in wind speeds which are imposed on the average wind speed (Manwell et al., 2010). Fluctuations of wind speed in this temporal interval may also be caused by gusts. A gust is defined as a distinct event which occurs in a turbulent wind regime (Manwell et al., 2010). Gusts are classified according to amplitude, rise time, maximum gust variation, and apse time (Manwell et al., 2010).

2.3.3 *Spatial characteristics of wind*

Wind speeds may also vary between locations. These variations may be down to topographical or ground cover differences between the

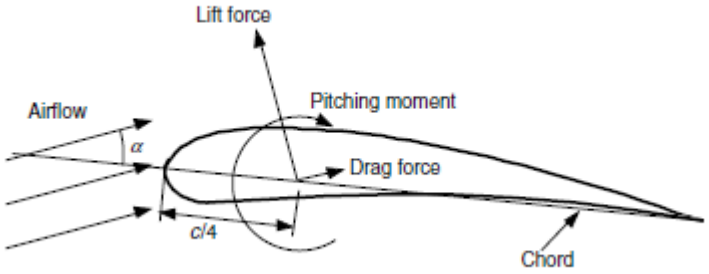

Figure 2.1: Forces acting on an aerofoil (Manwell et al., 2010)

locations (Manwell et al., 2010). Additionally the wind speed may vary due to a location's proximity to mountains or bodies of water, especially the ocean (Brower, 2012)

2.4 WIND TURBINES

A turbine is a class of turbomachine which extracts energy from a fluid (such as wind) (Dick, 2015). This energy is then used to turn a rotating component (usually known as a rotor) and this rotation is used to drive an external load (Dick, 2015). According to Dick (2015), a turbomachine is a type of machine that 'exchanges energy between the continuous flow of a fluid and a continuously rotating blade system, with the energy exchange based on flow-generated forces.' In the case of a wind turbine, the fluid that is used is the wind.

The blades of a wind turbine resemble the wings of an aircraft, otherwise known as aerofoils (Dick, 2015). According to Manwell et al. (2010) 'aerofoils are structures with specific geometric shapes that are used to generate mechanical forces due to the relative motion of the aerofoils and a surrounding fluid.' As air flows over the surface of the aerofoil, it creates a variety of forces which act on the aerofoil. The collection of these forces are generally resolved into two forces and one moment which act on the aerofoil. These forces are shown in Figure 2.1.

The lift force is perpendicular to the direction of the airflow and is a result of the unequal pressures which act on the upper and lower surfaces of the aerofoil. The drag force is mainly due to the fiction forces which act along the surface of the aerofoil and is also due to the shape of the aerofoil's surfaces. The pitching moment acts in a direction that is perpendicular to the cross section of the aerofoil. Bernoulli's principle governs the pressure variations that are caused by the airflow which acts on the surface of an aerofoil and the principle states that the sum of the pressures (both static and dynamic) are constant provided frictionless flow is assumed(Manwell et al., 2010).

Bernoulli's principle can be expressed as:

$$p + \frac{1}{2}pU^2 = constant$$

Where p is the static pressure

U is the local velocity along the aerofoil's surface.

A negative pressure gradient forms as the air flow encounters and has to accelerate around the leading top edge of the aerofoil. The design of the shape of an aerofoil is such that a positive pressure gradient is formed along the bottom edge of the aerofoil. If the design of the aerofoil allows the airflow speed on the upper surface of the aerofoil to be larger than the airflow speed along the lower surface, the two pressure gradients combine to create a net lift force which acts on the aerofoil (Manwell et al., 2010). In the case of a Horizontal Axis Wind Turbine and a Darrieus wind turbine, this lift force causes the blades to turn and thus generate power.

Apart from exploiting the lift forces created by aerofoils, wind turbines may also make use of drag forces in order to rotate (Manwell et al., 2010). These turbines that use drag forces are termed Savonius turbines and are discussed later.

2.4.1 *Small-scale wind turbines*

The International Electrotechnical Commission (IEC) has developed the IEC 61400-2 standard which sets out requirements of various types of wind turbines (International Electrotechnical Commission, 2013) The IEC 61400-2 defines small wind turbines as any turbine whose rotor swept area is smaller than 200m^2 and with a rated power of below 50kW (Bukala et al., 2015a).There is, however, some variation in the definition with other sources stating that the rated power should be between 1.4kW and 16kW (Tummala et al., 2015).For the purpose of this study, the chosen wind turbines have a rated power that ranges between 800 W and 2500 W.

2.4.2 *Types of wind turbines*

Wind turbines are divided into two categories depending on their axis of rotation: Vertical Axis Wind Turbines (VAWT) and Horizontal Axis Wind Turbines (HAWT) (Manwell et al., 2010). The VAWT are generally used less frequently and are discussed first.

2.4.2.1 *Vertical Axis Wind Turbines (VAWT)*

Vertical Axis Wind Turbines (VAWT) are composed of a vertical shaft around which the blades rotate. VAWTs have several advantages over Horizontal Axis Wind Turbines (HAWT): chief among these advantages is that VAWTs do not depend on the direction of the wind in or-

der to generate electricity, unlike HAWTs which have to yaw into the wind. In addition, the mechanical components in VAWTs are located close to the ground, which can allow easier access for maintenance. (Ishugah et al., 2014).

VAWTs are again split into two major types, the Darrieus turbine and the Savonius turbine (Tummala et al., 2015).

Darrieus turbines

Darrieus turbines rely on lift forces in order to generate electricity. They generally consist of a vertical axis surrounded by numerous blades (straight or curved) (Tummala et al., 2015). An examples of a Darrieus turbine is shown in Figure 2.2 . The Darrieus turbine was invented by George Darrieus in 1931 in the United States of America (Lack, 2010). While these turbines do not have a self-starting mechanism and generally require more maintenance, they have higher efficiencies compared to the Savonius turbines (Lack, 2010).

Figure 2.2: Darrieus type VAWT (Schelmetic, 2013)

Savonius turbines

The other type of VAWT is the Savonius turbine. Patented by Sigurd Savonius in 1922, these turbines are based on wind drag and generally consist of two or three 'scoops' which give the turbine an 'S' like appearance when viewed from above (Tummala et al., 2015). A Savonius type wind turbine is pictured in Figure 2.3 and Figure 2.4. Figure 2.3 shows the side view of the turbine while Figure 2.4 shows

the top view of the turbine. Note the shape of the scoops in Figure 2.4. The curved nature of these scoops allows them to experience less drag when moving against the wind than when they are moving with the wind, causing a drag force differential which rotates the turbine (Lack, 2010). While this drag differential causes the turbine to spin, it is also responsible for the lower efficiencies of the Savonius turbine compared to those of the Darrieus turbine. This is because of the force that the wind exerts on the scoop as it moves against the wind, which causes the rotation of the turbine to slow. Nevertheless, Savonius turbines are generally cheaper and are more reliable than Darrieus type turbines (Tummala et al., 2015).

Figure 2.3: Side view of Savonius type VAWT (Markham, 2014)

2.4.2.2 *Horizontal Axis Wind Turbines (HAWT)*

Horizontal Axis Wind Turbines (HAWT) are the most frequently used type of wind turbine (Ishugah et al., 2014). As the wind flows past the blades, it generates a lift force on the blades which then turn and this then causes the horizontal shaft to rotate (Tummala et al. 2015). The number of blades used in HAWT designs may vary but the most common design features a three blade arrangement around a central hub. A three-bladed large-scale HAWT is shown in Figure 2.5. HAWTs have the ability to self-start, however, their performance is dependent on the direction of the wind unless they are fitted with a yaw-

Figure 2.4: Top view of Savonius VAWT (Green Ideas, 2010)

ing mechanism which allows them to change direction in accordance with the wind direction.

2.5 PHYSICAL PARAMETERS AFFECTING WIND ENERGY CONSERVATION

The function of a wind turbine is to convert energy from one form to another. It harnesses the kinetic energy from the wind flow and converts it into mechanical energy which moves the blades. This mechanical energy is then transformed into electrical energy which can be used to power electrical devices. Like all physical processes, these conversions between the various forms of energy entail losses. These losses can be noise, heat, or the remaining energy in the original wind stream. The theoretical efficiency of a wind turbine is governed by what is known as the Betz law.

2.5.1 *Betz Law*

Between 1922 and 1925, Albert Betz, a German scientist specialising in aerodynamics, proposed an upper bound of 16/27 (or approximately 0.593) to the maximum potential efficiency of a wind turbine (Lack, 2010). This upper efficiency limit accounts for the fact that it is impossible to extract all of the kinetic energy from a wind stream (Bukala et al., 2015b). If all the kinetic energy were to be extracted from a wind stream by a wind turbine, the velocity of the wind on the downwind side of the turbine blades would be zero. According to the flow continuity principle, this cannot occur and thus some kinetic energy must remain in the wind stream (Bukala et al., 2015b).

Figure 2.5: Large scale HAWT (Turbinesinfo, 2010)

The equation for the available power in a wind stream of cross sectional area (A) is given by:

$$P = \frac{1}{2} * \rho * v^3 * A \tag{2.1}$$

With ρ being the air density and v being the velocity of the air flow.

The turbine transforms kinetic energy into mechanical energy. The velocity of the air flow exiting the turbine must thus be lower than the velocity of the flow entering the turbine (provided that the mass flow rate remains constant) (Lack, 2010). However, a lower velocity necessitates a widening of the cross sectional area, as it must accommodate the same mass flow rate (Lack, 2010). Consider Figure 2.6, which depicts the flow conditions upstream and downstream of an energy converter (such as a wind turbine).

The mechanical energy that the converter is able to extract from the air flow is given by the difference existing between the upstream power at point 1 in Figure 2.6 and the downstream power at point 2. This relationship can be described according to the following formula:

$$P = \frac{1}{2}\rho A_1 v_1^3 - \frac{1}{2}\rho A_2 v_2^3 = \frac{1}{2}\rho(A_1 v_1^3 - A_2 v_2^3) \tag{2.2}$$

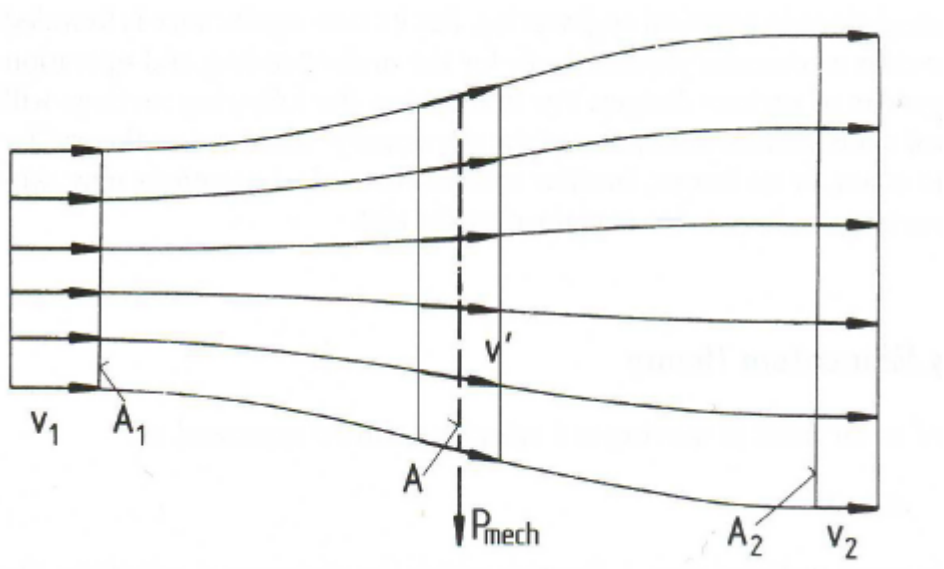

Figure 2.6: Flow conditions through an energy extractor (Lack, 2010)

In order for the mass flow continuity to be valid:

$$\rho A_1 V_1 = \rho A_2 V_2 \tag{2.3}$$

Therefore

$$P = \frac{1}{2}\rho A_1 V_1 (v_1^2 - v_2^2) \tag{2.4}$$

Or alternatively

$$P = \frac{1}{2} m (v_1^2 - v_2^2) \tag{2.5}$$

According Lack (2010), in order to find the ratio of $v_2$to v_1 that maximises the power output, another way of expressing the mechanical power is needed. This is done by using the law of conservation of momentum which is expressed as Newton's first law which states that the force acting on an object (F) is calculated as:

$$F = m(v_1 - v_2) \tag{2.6}$$

Following on from Newton's first law, Newton's third law dictates that 'for every action there is an equal and opposite reaction' and therefore there needs to be a complimentary force acting on the force described in equation 9. This force is the force exerted by the energy

converter onto the air flow (Lack, 2010). The power required by this reactionary force is given by:

$$P = Fv' = m(v_1 - v_2)v' \tag{2.7}$$

Equating equations (8) and (10) and solving for v' gives:

$$\frac{1}{2}m(v_1^2 - v_2^2) = m(v_1 - v_2)v' \tag{2.8}$$

$$v' = \frac{1}{2}(v_1 + v_2) \tag{2.9}$$

Therefore the velocity of the air stream at the point of the energy converter in Figure 2.6 is simply the arithmetic mean of the velocities at point 1 and point 2 (Lack, 2010).

With the velocity at the energy converter known, the mass flow at the point is given by:

$$m = \rho * v^{'} * A = \frac{1}{2}\rho * A * (v_1 + v_2) \tag{2.10}$$

Therefore the mechanical power output of the energy converter becomes:

$$P = \frac{1}{4}\rho * A * (v_1 + v_2)(v_1^2 - v_2^2) \tag{2.11}$$

Without any mechanical power being extracted from the air stream and with a constant cross sectional diameter, the theoretical available power available is given by:

$$P_0 = \frac{1}{2}\rho * A * v_1^3 \tag{2.12}$$

The power coefficient (Cp) of the converter is given by the ratio of the theoretical power (Po) and that power that is extracted by the converter (P):

$$C_P = \frac{P}{P_0} = \frac{(\frac{1}{4}\rho * A * (v_1 + v_2)(v_1^2 - v_2^2))}{(\frac{1}{2}\rho * A * v_1^3)} \tag{2.13}$$

$$C_P = \frac{P}{P_0} = \frac{1}{2}|1 - (\frac{v_2}{v_1})^2||1 + (\frac{v_2}{v_1})| \tag{2.14}$$

Therefore, the ratio between the velocities before and after the converter is all that is needed in order to calculate the power coefficient

(Lack, 2010). Solving for the maximum CP, which occurs with $v_2/v_1 = 1/3$, the following CP value is obtained:

$$C_P = \frac{16}{27} = 0.593 \tag{2.15}$$

This is the fraction known as the Betz factor. Deriving this factor from first principles reveals numerous important findings: firstly,, that the mechanical power available in the wind stream will increase by the cube of the wind velocity; that the available power will increase proportionally with the cross sectional area of the energy converter; and finally, even with ideal airflow and lossless conversion, the maximum mechanical energy that can be extracted is limited to 59.3% (Lack, 2010). The Betz law is represents a balance between the effectiveness of the air flow capture of a turbine and the turbines ability to convert the kinetic energy from the wind into mechanical energy.

Because of the difference in the way HAWTs and VAWTs extract energy from the wind stream, the application of the Betz law to VAWTs may not be valid (Th¨nnißen et al., 2016; Chen et al., 2011). Th¨nnißen et al. (2016) find that the maximum power output of a VAWT is approximately 65% or 6% higher than the Betz limit suggests.

2.5.2 *Turbulence*

The preceding section demonstrates the upper limit of the efficiency of a theoretical wind energy converter. However, this upper limit is not reached in practice as there are other factors which negatively affect the efficiency of wind turbines. This is especially true in an urban environment where the wind stream is notably turbulent.

Turbulence can be defined as the dissipation of the kinetic energy of the wind into thermal energy through the formation and destruction of eddies (or gusts) (Manwell et al., 2010).

For a wind turbine to perform optimally, the wind resource should be as smooth and laminar as possible (Bukala et al., 2015b). The presence of various obstacles in an urban environment (such as trees and buildings) disrupt the wind flow and create turbulence. This means that some of the kinetic energy that was originally available has now been irreversibly lost to phenomena such as chaotic flow and macro or micro vortices (Bukala et al., 2015b). Various authors (Rafety at al. 2004, Chiras et al. 2009) estimate this loss of kinetic energy to turbulence to be anywhere from 15% to 35%.

A turbulent bubble, as described by Chiras et al. (2009) is an example of obstacles reducing the available energy in a wind stream Figure 2.7 shows an example of a turbulence bubble occurring (after (Chiras et al. 2009). The Figure shows a building with a height of H can create a turbulence bubble that has a height of twice the building height and a width of twenty times the building height. This shows

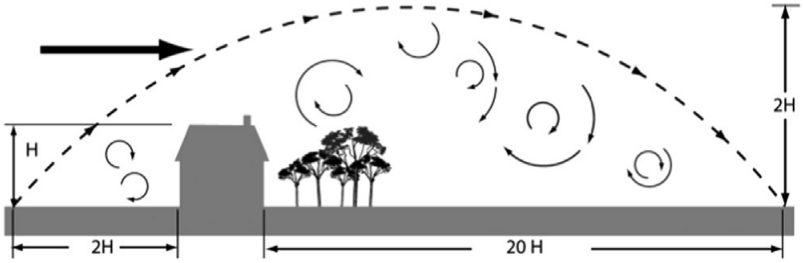

Figure 2.7: Example of a turbulence bubble occurring behind a building (Chiras et al. 2009)

that a building can have a significant impact on the surrounding wind regime. This effect may grow substantially in an urban environment where there are numerous buildings each with a varying height.

The wind regime located inside of a turbulence bubble similar to the one in Figure 2.7 will be characterised by increased turbulence compared with the wind regime outside of the bubble. Thus iInstalling a wind turbine anywhere inside the bubble (indicated by the dashed lines in Figure 2.7) will severely reduce the power that can be generated by the turbine. This phenomenon is intensified in the case of a dense urban area where the various buildings each have their own turbulence bubble and these bubbles intermingle and create a highly unstable wind regime . This means that installing wind turbines in heavily built-up urban areas is seldom economical or feasible from an energy production point of view (Bukala et al., 2015b, Fields at al. 2016).

In order to measure the turbulence of the wind, a simple ratio called Turbulence Intensity (TI) has been developed (Elliot and Infield, 2014). The TI ratio requires precise wind data and is thus sometimes difficult to accurately estimate for a location. It expressed as a percentage and is given by the following formula:

$$I_z = \frac{\sigma_z}{V(z)} \tag{2.16}$$

With σ_z being the standard deviation of the wind speed and V(z) being the mean wind speed at a specified interval (z).

The interval between wind speed measurements can have a significant effect on the TI of a location. Elliot and Infield (2014) found that the TI can change by up to 22% when the measurement interval is changed from 1 minute to 10 minutes. While Elliot and Infield (2014) find significant variation due to changes in the data measurement interval, Pagnini et al. (2015) do not find any evidence of this effect on their experiment. This contradiction between the two studies further highlights the uncertainty associated with urban wind data.

In order to quantify the turbulence of a specific site, the IEC 61400-2 standard has introduced the Normal Turbulence Model (NTM) (Carp-

man, 2011). The NTM is used to help estimate the wind power potential of small-scale wind turbines but the NTM seems to underestimate the true level of turbulence at an area compared to in-situ recording of turbulence data. Some areas showed a turbulence level that was twice as high as what was predicted by the NTM (Carpman, 2011).

2.5.3 *Tip speed ratio*

Yet another important parameter concerning the efficiency of wind turbines is the Tip Speed Ratio (TSP) (Bukala, 2015; Manwell et al., 2010). The TSR is defined as the ratio between the rotating tip speed of the rotating blade and the undisturbed wind velocity at the hub height and is commonly noted as λ (Bukala, 2015). TSR is expressed as:

$$\lambda = \frac{\omega r}{V_w} \tag{2.17}$$

WITH

ω the rotational speed (rad/s)

R the rotor diameter (m)

V_w the wind speed (m/s)

A higher TSR means that the axis of rotation and the aerodynamic forces that are generated are nearly parallel which is not conducive to high turbine efficiency (Bukala, 2015). However there are two negative aspects to having a low TSR. The first concerns wake turbulence behind the turbine, which is defined as the area behind the turbine which suffers from decreased wind speeds and increased vortices caused by the wind flowing around the rotor blades (Manwell et al., 2010) A slower rotational speed (and thus a lower tip speed) requires a higher amount of torque to produce the same amount of power, and this higher torque causes larger wake turbulence. This wake turbulence represents unrecovered kinetic energy meaning that the larger the wake turbulence the lower the efficiency of the turbine (Bukala, 2015). This means that a lw tip speed ratio will require a larger deflection of the wind flow and thus there will be a higher rotational energy associated with the wind stream in the downwind side of the rotor.

The second negative consequence of having low tip speed is an increase in tip losses. Tip losses and the mass of the blade increase with an increase in the width of the blade however, wider blades create more lift and thus more force. In addition, higher lift also places extra stain on the turbine bearing which increases the need for maintenance (Bukala, 2015).

2.5.4 *Wind Shear*

Wind speeds at ground level are negligible and increase with increasing height above the ground (Bukala et al., 2015). This phenomenon is called the vertical wind shear or vertical profile of the wind speed and it is a central design constraint due to two reasons: the first is that the wind shear influences the wind resource potential at a specific height; secondly, the wind shear impacts on the lifetime of wind turbine components (Manwell et al., 2010). The Hellmann power equation is used to account for the variation of wind speed with height and is given by:

$$v_z = v_{z_o} * (\frac{z}{z_o})^{\alpha} \tag{2.18}$$

WITH

z being the height above the a reference point on the Earth's surface

z_0 being the known height of the reference point

v_{z_0} being the known wind speed at the reference point

α being the wind shear coefficient

A standard coefficient of a= 1/7 is used by numerous studies (Bukala et al., 2014; Ray et al., 2006; Khalfa et al, 2014.) This study has used this power law with an a coefficient of 1/7. Khalfa et al., (2014) find that the 1/7th power law is a highly effective law that can be used to extrapolate the wind speeds in rough locations. For the purposes of this study, a reference height of 15m was used to ensure that the data sets from the six locations could be compared against each other (this is further explained in the methodology Chapter 3). In addition, the difference between the recorded height of the data at each of the six locations and the reference height were very small (in the range of 1 to 3 m). This means that the variation in wind speed as calculated by the 1/7th law is very small for each of the locations and any errors caused by the use of the 1/7t power law are thought to be negligible. Figure 2.8 shows the effect that increasing height has on the wind speed. This relationship is one that is characterised by decreasing returns to height as the rate of change of wind speed relative to height decreases with increasing height above ground level.

2.6 METHODS USED TO ASSESS WIND ENERGY POTENTIAL

While sections 2.1 to 2.5 have focus on the wind turbines and issues affecting the data available for wind energy assessment, this section describes how to use the information on the wind turbines and the data that has been collected in order to estimate the potential energy

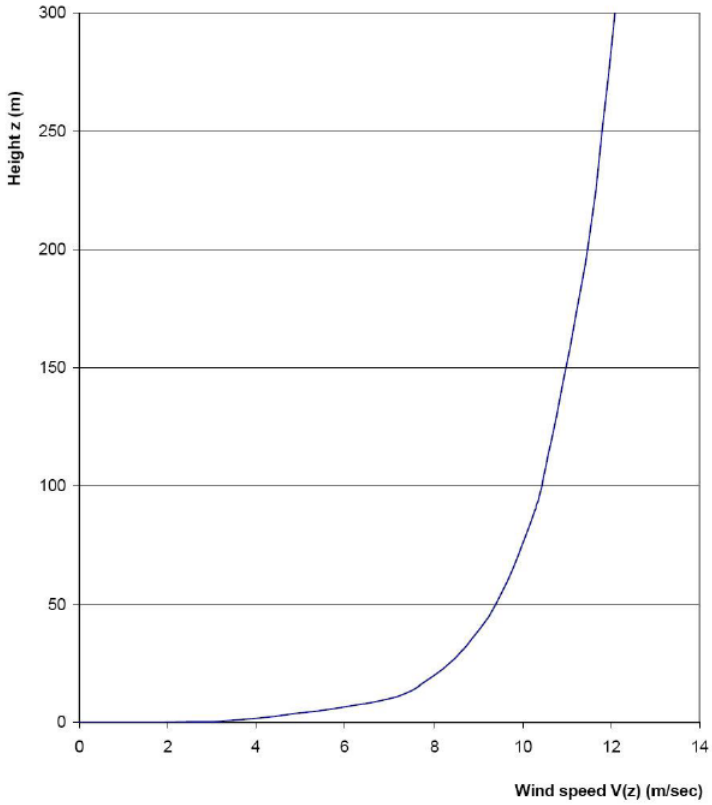

Figure 2.8: Wind speed as a function of height (Ragheb, 2017)

output of a specific wind turbine at a specific location. As wind turbines can last for many years (the Kestrel e230i used in this study has a rated lifespan of 20 years) and cannot be easily moved once installed, it is imperative that the estimation of predicted energy output be as accurate as possible. However, the costs associated with gathering reliable wind energy measurements mean that a trade-off is required between accuracy and cost. Two main methods exist: the statistical use of probability distribution functions or the use of Computational Fluid Dynamics (CFD) software.

The use of probability density distribution functions aids in reducing the need for exhaustive physical recording of the wind speed. As a result, the use of such probability density functions, especially the Weibull and Rayleigh distributions, is standard practice when it comes to estimating the potential energy output of a chosen location (Celik, 2002; Ayodele et al., 2012; Usta, 2016). Other probability density functions such as the lognormal function, gamma function and the beta function are also often used, however this section will focus on the Weibull and Rayleigh distributions as they are the most common distributions used (Celik, 2002). The use of probability density functions does not eliminate the need for long term, accurate wind speed measurements but it does help to reduce the amount of data required (Wais, 2017).

2.6.1 *The use of the Weibull distribution in wind energy assessments*

The Weibull distribution is a continuous probability distribution that has been frequently used for wind resource assessments (Usta, 2016). Within the Weibull function there are two subsets of the distribution, the two-parameter Weibull and the three-parameter Weibull. Wais (2017) shows that the three-parameter Weibull distribution may provide more accurate results for urban wind energy applications because it takes into account the frequency of null wind speeds.

In order to account for the variance within the wind speed distribution the equation for the available power at a location is given by:

$$P = \frac{1}{2} * \rho * A * \sum p_{vi} * v_i^3 \tag{2.19}$$

With p_{vi} being the probability of wind speed v occurring. It is simply the expected value of wind power across all time periods i.

2.6.1.1 *2.3.1.1 Two parameter Weibull distribution*

According to Wais (2017) a two parameter Weibull Distribution is given the probability density function:

$$p(v) = (\frac{k}{c})(\frac{v}{c})^{k-1} \exp^{-(\frac{v}{c})^k}) \tag{2.20}$$

With v being the wind speed and v > 0, k > 0, c > 0.

A cumulative distribution function is given by:

$$F(v) = 1 - \exp^{-(\frac{v}{c})^k} \tag{2.21}$$

With v being the wind speed and v > 0, k > 0, c > 0.

The Parameter k is a dimensionless shape factor (A Rayleigh distribution is identical to a Weibull distribution with a shape factor of 2).While c is a scale parameter measured in m/s. Both these factors affect the shape of the Weibull distribution.

Numerous methods have been suggested to calculate the parameters of the Weibull distribution (Usta, 2016). This current study will use the Probability Weighted Moments Based on Power density method (PWMBP) proposed by Usta (2016). Despite all of these methods that are used to determine the Weibull parameters, there is no consensus amongst practitioners as to which method provides the most reliable estimation of the parameters.

The use of probability weighted moments (PWM) have infrequently applied to wind energy studies but have been used extensively elsewhere (Usta, 2016). The PWMs of a random variable X with a cumulative distribution function F(x) are defined by the following:

$$PWM_{i,r,s} = E[X^i(F(X))^r(1 - F(X))^s] \tag{2.22}$$

With i,r and s being real numbers.

In order to calculate the PWM for the Weibull distribution the following form is used:

$$PWM_{1,0,s} = \frac{c\Gamma(1 + 1/k)}{(1 + s)^{1+1/k}} \tag{2.23}$$

With s bring a positive integer and Γ( ) is a gamma function.

The PWMBP method uses the following equations to determine the Weibull parameters (Usta, 2016)

$$k = \frac{ln(2)}{ln(\bar{C})} \tag{2.24}$$

$$\bar{C} = \frac{\bar{v}}{\frac{2}{n(n-1)} \sum v_i(n - i)} \tag{2.25}$$

WITH

$\bar{v}$ the sample mean of the wind speed,

v_i is the ith ascending ordered wind speed data

N is the total number of wind speed data points recorded.

The scale parameter c is then given by:

$$c = \frac{\bar{v^3}}{\Gamma(1+\frac{3}{k})^{1/3}} \tag{2.26}$$

With $\bar{v^3}$ being the sample mean of the wind speed cubes (Usta, 2016).

2.6.1.2 *2.3.1.2 Three parameter Weibull distribution*

According to Wais (2017), the three-parameter Weibull distribution produces more accurate results when the wind data has a significant proportion of null wind speeds occurring. This may make it better suited to small-scale urban wind energy applications. The three-parameter Weibull probability density function is expressed as:

$$p(v) = (\frac{k}{c})(\frac{v-u}{c})^{k-1} \exp^{-(\frac{(v-u)}{c})^k} \tag{2.27}$$

Thus the three-parameter Weibull distribution is equivalent to the two-parameter distribution with the addition of u, which is the location parameter with values less than zero. The Weibull location parameter has the same value as the scale parameter c (Wais, 2017). The same method can be used to derive the Weibull parameters for the three-parameter distribution as was used for the two-parameter model in the previous section.

2.6.2 *The use of the Rayleigh distribution*

As indicated in the introduction to this section, the Rayleigh distribution is identical to a Weibull distribution with a shape parameter (k) of 2 (Grieser et al., 2015). The Rayleigh distribution is also equivalent to a chi distribution with two degrees of freedom (Pishgar-Komleh et al., 2015). The Rayleigh probability distribution may outperform the Weibull distribution if the wind data contains a significant amount of very low wind speeds (including zero wind speeds) (Pishgar-Komleh et al., 2015). The effectiveness of the Rayleigh distribution may be limited because the shape factor is set at 2 and does not vary. Owing to this fact, the Rayleigh distribution was not used in this current study and only the Weibull distribution was used.

2.6.3 *Computational Fluid Dynamics models*

Apart from the use of statistical distributions (such as the Weibull distribution that was discussed in the previous section) the other

main method of conducting wind energy resource assessments is to use Computational Fluid Dynamics (CFD) models (Simões & Estanqueiro, 2015; Yang et al., 2016). The use of CFD models may provide a more accurate estimate of the wind flow around obstacles which is highly important in urban areas. However, these models are very intensive (both in time spent setting up the model as well as the computational requirements needed to analyse the model) and they are therefore rarely used for resource assessments of large areas as they are better suited to small-scale applications (Simões & Estanqueiro, 2015).

Generally these CFD models solve the Reynolds Averaged Navier-Stokes (RANS) equations with turbulence closure (Kalmikov et al., 2010; Ledo et al., 2011). Yang et al. (2016) provide an in-depth overview of recent application of CFD models in urban wind resource assessments

In the past few years these methods to estimate the wind resource potential have been used to develop numerous urban wind turbine projects. The following section provides examples of urban wind energy developments and highlights the various lessons that have been learned through the implementation of these projects. s.

2.7 APPLICATIONS OF WIND ENERGY IN AN URBAN ENVIRONMENT

The 2016 World Wind Energy Association (WWEA) report on small-scale wind turbines notes that, as of the end of 2013, a cumulative total of at least 870,000 SWTs were installed all over the world with the sector having grown significantly over years 2005-2013, especially in the Chinese and American markets (Pitteloud & Gsänger, 2016). Processes and methods have been streamlined as the urban wind energy sector has grown and matured in these markets. While the urban wind energy market has grown in other countries, very little information on the potential market exists in South Africa, apart from an initial feasibility study on the installation of a wind turbine in Cape Town (conducted by Brosius (2009)). This section provides examples of wind energy installations across the globe, including building-mounted wind turbines as well as building-integrated wind turbines. In addition, issues concerning the installation of wind turbines in urban environments are discussed.

2.7.1 *Examples of urban wind turbines*

There are several examples of wind turbines being installed in urban environments (Fields et al, 2016; Li et al., 2016). These installations can either be classified as building-mounted wind turbines or building-integrated turbines. Building-mounted turbines are those that have

been retrofitted onto existing buildings while building-integrated turbines are those that have been included in the design process of the building. The most well-known example of a building-integrated wind turbine may well be the set of turbines installed in the Bahrain World Trade Centre (Ishugah et al., 2014). (shown in Figure 2.9) Note the positioning of the three turbines in the middle of the building. Due to their fixed nature, they are unable to yaw in order to face the prevailing wind direction.

Figure 2.9: Bahrain World Trade Centre (Skyscraper City, 2015)

The Bahrain World trade Centre makes use of three 29m diameter HAWTs and it is estimated that the turbines could produce between 1100 and 1300 MWh per annum which represents 11-15% of the building's annual energy use (Ishugah et al., 2014). An example of a building-integrated system which further integrates wind turbine technology is the Pearl River Tower in Guangzhou, China (Figure 2.10). This building uses four wind tunnel-like openings in its façade in order to channel the wind towards four VAWTs. The four wind turbines are expected to generate approximately 10 100 kWh per annum (Li et al., 2016). The completed Pearl River Tower is shown in Figure 2.10 below. From Figure 2.10, the four wind tunnel-like openings on the façade are easily seen. Similar to the Bahrain Would Trade Centre in 2.9, the Perl river tower cannot take advantage of any yawing mechanism should the wind change direction.

Examples of building-mounted wind turbines are more frequent due to the size of the existing building stock and the fact that small-scale wind turbines have only recently become economically viable to install (Fields et al., 2016). A common example of building-mounted wind turbines is the installation at Logan Airport in Boston, Massachusetts, USA (Ishugah et al., 2014). This project uses 20 small-scale wind turbines from AerVironment located on the parapet of the main building. It is estimated that the project will produce approximately 6000 kWh per annum (Gipe, 2008). Another prominent example of building-mounted wind turbines is the National Aero-

Figure 2.10: Pearl River Tower (Ling, 2012)

nautics and Space Administration's (NASA) Building 12 in Houston, Texas, which consist of four VAWT-type wind turbines each with a rating of 1kW (Fields et al, 2016).

The previous examples have all concerned urban wind energy projects outside of South Africa. For the purposes of this study, a thorough investigation into South African urban wind energy projects was carried out. The only example of research that was identified was an initial feasibility study which looked at placing a wind turbine on the roof of the South African Breweries (SAB) plant in Newlands, Cape Town (Brosius, 2009). The study found that, due to the variability of the wind resource at the plant, the payback period of the turbine would be over 30 years (Brosius, 2009). Although this result should be approached with discretion as the study used data recorded over a period of only two months. Consequently, this data set may not account for seasonal or yearly fluctuations and should not be seen as representative of the wind regime at the SAB plant in Newlands.

2.7.2 *Issues associated with urban wind turbines*

Although many studies clearly describe the potential benefits of urban wind turbines (Tummala et al. 2015; Karthikeya et al., 2015 and Yang et al., 2016), there has been some research indicating the shortcom-

ings of urban wind energy (Fields at al., 2016; Energy Savings Trust, 2009).

In the way of obstacles faced by potential urban wind energy resources, Fields et al. (2016) cite poor project planning, unexpectedly high project costs and poor plant performance. Additionally, the installation of an urban wind turbine may have motives other than energy production, including the recognition of 'green building' credentials, increased marketing and public relations prospects or the utilisation of various incentive mechanisms that are aimed at the use of renewable energy (Fields at al., 2016). Fields at al. (2016) found that in many cases the position on the building that offered the best wind resource was overlooked for positions which had poorer wind resource capabilities but were more visible to the general public. This is not a major concern if the project embraces a multi-objective framework when choosing which location to install the turbine. However, it becomes an issue when the turbine's energy production is the sole criteria on which it is judged. Fields at al. (2016) conducted case studies on six urban wind installations in the United States of America and in all of the examples, the actual electricity production of the turbines was much lower than what was predicted by the project developers. This points to the need to conduct high quality wind resource assessments during the design phase of the project which take various parameters into account that affect wind turbine performance (such as turbulence). Risks associated with wind turbine function should also be considered, including the risk of failure of turbine parts or the safety risk should ice be thrown off turbine blades, for instance. This is particularly pertinent as current international standards for wind turbines have been developed according to applications in non-urban areas, thus rendering these standards potentially inappropriate for urban applications (Fields at al., 2016).

Between March 2008 and March 2009, the Energy Savings Trust conducted in-situ measurement of 57 domestic wind turbines throughout the United Kingdom (Energy Savings Trust, 2009). Results from this study show that the building-mounted turbines failed to reach load factors of 3% and, in a few cases, the wind turbines were a net user of electricity due to the electricity usage of the inverter (Energy Savings Trust, 2009). The best performing building-mounted wind turbine produced just 975kWh over the year. Compared to the building-mounted turbines, free-standing turbines performed significantly better. Free-standing turbines had an average load factor of 19% and the best site had a load factor of 30% (Energy Savings Trust, 2009).It can thus be concluded that, where possible, free-standing wind turbines should be favoured over building-mounted turbines.

2.8 SUMMARY

Chapter 2 provided the necessary theoretical background in order to carry out the investigation into Cape Town's urban wind regime potential. Chapter 3 details the research methodology that is followed in order to investigate the outlined research objectives.

3

RESEARCH METHODOLOGY

3.1 INTRODUCTION

Owing to the surge in use of wind as a resource to generate electricity in recent decades, several studies have been conducted to analyse the wind resource potential in various urban environments (key studies are discussed in Chapter 2). The results from these studies have been contradictory at times, sparking off considerable debate regarding the realisable resource potential of urban wind energy. In addition, the urban wind resource potential studies have mostly focused on Europe, South East Asia and the United States of America. During the compilation of the literature review, only one other study on urban wind energy with focus on South Africa was found. That study was a project report for the Masters of Engineering from the Faculty of Engineering at the University of Stellenbosch and it examined the feasibility of installing a small-scale wind turbine at the South African Breweries (SAB) Newlands facility (Brosius, 2009). This study only collected the data over a period of two months and it is thus unable to draw any long-term recommendations or conclusions.

The methodology consisted broadly of the following steps:

1. Obtaining wind data from the South African Weather Service
2. Using Excel to transform the data into the necessary format
3. Running a programming script which analysed the wind resource potential using the *R* programming language
4. Combining the wind resource availability results with a power curve from a small scale wind turbine to determine the potential annual energy production.

The results from the different locations and the various power curves from the different small-scale wind turbines were compared with each other to identify which combination of factors produces the highest theoretical resource potential. This chapter is divided as follows: Section 3.2 describes the research approach and includes the rationale for the selection of the six locations and the four small-scale wind turbines used in this study. Section 3.2 also details any limitations to the research and outlines the assumptions that were made in the process of the study. Section 3.3 provides details of the data analysis procedure that is used to analyse and interpret the data. Section 3.4 explains how the validation of the model was carried out and Section 3.5 details the process followed in order to carry out the hub

height sensitivity analysis. The final section, Section 3.6 presents the method followed to calculate the Levelized Cost of Electricity (LCOE) for a given wind turbine.

3.2 RESEARCH DESIGN

3.2.1 *Selected Locations*

The six locations in Cape Town that are chosen for the study are: The Royal Cape Yacht Club located in the Table Bay harbour; the Astronomical Observatory located in Observatory; the Kirstenbosch Botanical Gardens located in Kirstenbosch; the Molteno reservoir located in Oranjezicht; the Automatic Weather station located near the Cape Town International Airport; and the Cape Town Weather Office (WO) station which is located at the Cape Town International Airport. The latitude and longitude of the six stations are shown in Table 3.1 .The location of the six stations around the Cape Town are is shown on the map in Figure 3.1.

Station Name	Latitude (°S)	Longitude (°E)
Kirstenbosch	-33.9860	18.4307
Astronomical Observatory	-33.9336	18.4775
Cape Town Royal Yacht Club	-33.9206	18.4430
Molteno Reservoir	-33.9385	18.412
Automatic Weather Station	-33.9789	18.600
Cape Town Weather Office	-33.963	18.602

Table 3.1: Latitude and longitude for the chosen stations

3.2.1.1 *Royal Cape Yacht Club*

The initial set of data for this study was recorded at the Royal Cape Yacht Club (RCY) located in Duncan Road at the Table Bay Harbour in Cape Town. The coordinates for this station are 33.92° S and 18.44° E and the height of the station is 11m above sea level. This site was chosen for this study due its close proximity to the ocean and thus strong on-shore and off-shore breezes. There has been a weather station located there since 2001 and the current set up of the weather station has been in operation since 2011. This particular station makes use of a RM Young wind sensor to measure the wind data (Mkhwanazi, personal communication 2017, May 25).

Out of the 731 days between the 1st of January 2015 and the 31st of December 2016, data is available for 729.4 days. The data recorded at the RCY club is believed to be very reliable and robust as the availab-

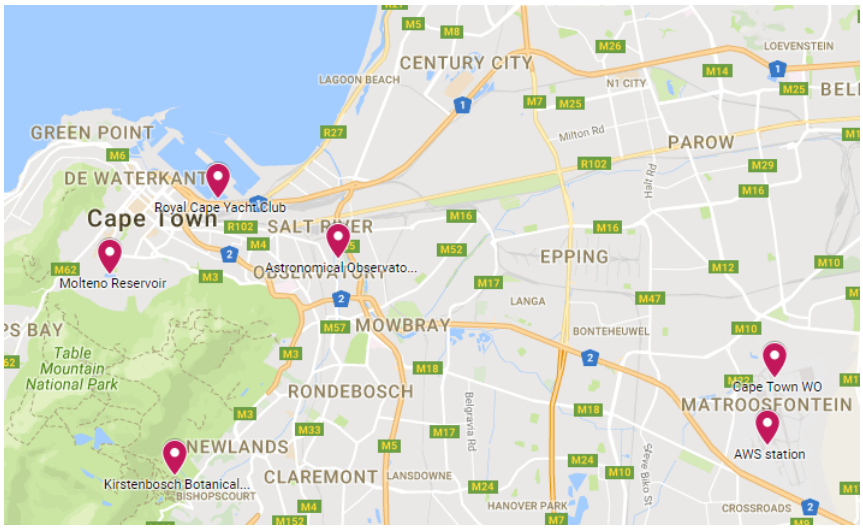

Figure 3.1: Locations of the six wind data measuring stations (Source: author's own)

ility of the weather station is 99.8% over the duration of the two-year recording period. This shows that the data that is used in this analysis is reliable and it gives a representation of the wind regime at the Royal Cape Yacht Club.

3.2.1.2 *Kirstenbosch Botanical Gardens*

The second station that was analysed was located in the Kirstenbosch Botanical Gardens in Kirstenbosch, Cape Town. Weather data has been recorded at this location since 1999 and the current set up of the weather station was installed in 2010. This location was chosen as it is one of the only recording stations on the southern side of Table Mountain and there are numerous residential suburbs in the surrounding areas. This location should therefore give a good indication of the resource potential for residential-scale wind turbines in the immediate area. The coordinates of the station are 33.99° S and 18.43° E and the height of the station is 156m above sea level. This weather station also makes use of a RM Young wind sensor (Mkhwanazi, personal communication 2017, May 25).

Out of 731 recording days, data from the Kirstenbosch station is available for 731 days. This means that the availability of data is 100% which shows that this weather-data recording station is reliable. In addition the weather recording station comfortably passed the South African Weather Service's verification, conformance, and maintenance report in March 2017 which shows that the data recorded by the station is accurate and robust. This report conforms to the standards laid out by the World Meteorological Organization's (WMO) Commission for Instrument and Methods of Observations Guide (CIMO) (South African Weather Service (SAWS), 2017).

3.2.1.3 *Automatic Weather Station*

The next station to be analysed was the Cape Town Automatic Weather Station (AWS) located at 33.9789° S and 18.6° E near the Cape Town International Airport. This station also makes use of a wind data recorder manufactured by RM Young.

Out of 731 recording days, data from the AWS station is available for 729.8 days. This means that the availability of data is 99.8% which shows that this weather-data recording station is reliable. In addition the AWS station comfortably passed the South African Weather Service's verification, conformance, and maintenance report in February 2017 which shows that the data recorded by the station is accurate and robust. This report conforms to the standards laid out by the World Meteorological Organization's (WMO) Commission for Instrument and Methods of Observations Guide (CIMO) (South African Weather Service (SAWS), 2017).

3.2.1.4 *Molteno Reservoir*

The next set of data that was analysed come from the weather-recording station located at the Molteno reservoir in Cape Town. The site is located in the suburb of Oranjezicht and the coordinates for the station are 33.9385° S and 18.412° E. This site was chosen because of its location in a residential suburb on the slopes of Table Mountain, thus providing an accurate prediction of the urban wind regime in the suburb of Oranjezicht. This station also makes use of a wind data recorder manufactured by RM Young.

The availability of the data from the Molteno reservoir is approximately 100% as there are only 88 intervals of five (5) minutes each of wind data recording that are missing for the entire two year period which is a total of 210 528 recording periods. This data thus provides a robust and accurate description of the wind regime at the Molteno reservoir.

3.2.1.5 *South African Astronomical Observatory*

The next station analysed was the South African Astronomical Observatory located in Observatory, Cape Town. The coordinates for this station are 33.9336°S and 18.4775° E. The station is located at a height of 15m above sea level and makes use of a wind data logger manufactured by RM Young. There has been a weather recording station at the Observatory since 1841 and the most recent upgrade of the station occurred in 2009 (SAWS, 2017). The recording station passed the most recent verification, maintenance, and conformance report in February 2017 (SAWS, 2017).

3.2.1.6 *Cape Town Weather Office*

The final data set used in this study was obtained from the Cape Town Weather Office (WO) station located at the Cape Town International Airport. The coordinates for this station are 33.963° S and 18.602° E. This station was chosen as it is 1.92km away from the Cape Town AWS station. These two stations were chosen to highlight how the wind regime may change over short distances in the urban environment. Like all other wind-data recording stations in this study, the WO station makes use of a RM Young manufactured wind sensor. Data was available for this station for a total of 729.4 days out of a possible 731 days. This gives the recording station an availability of 99.8% which shows that this data a good representation of the wind regime at the Cape Town International Airport.

3.2.2 *Selected small-scale wind turbines*

Four potential small-scale wind turbines were identified after consultation with various manufacturers and a careful review of similar small-scale urban wind power studies (Grieser et al., 2015; Karthikeya et al, 2015; and Sunderland et al., 2016). The four wind turbines were: the SkyStream 3.7 manufactured by Xzeres; the Kestrel e230i manufactured by Kestrel; the eddyGT manufactured by Urban Green Energy; and the Turby turbine manufactured by Core International with research assistance from the Delft University of Technology.

The first two turbines of the group, the SkyStream and the Kestrel, are Horizontal Axis Wind Turbines (HAWTs) and the remaining two are Vertical Axis Wind Turbines (VAWTs). Two HAWTs and two VAWTs were chosen in order to assess which of the two turbine types was best suited to the specific wind regime at the chosen locations. The SkyStream and the Turby were larger and had a higher-rated output compared to the Kestrel and the eddyGT, respectively. This comparison was done to assess whether a small-scale turbine with a higher-rated capacity is better suited to the urban environment compared with a very small-scale turbine.

Even though four different wind turbines were chosen for this study, the study did not seek to identify the best small-scale wind turbine for all locations. This study attempted to identify which types of wind turbine tended to give the best results at specific locations based on the data that had been recorded at that location. Each of the four turbines had its own advantages and possible disadvantages and therefore differed in their suitability to different locations and wind regimes.

The specifications of all four wind turbines are given in Table 3.2 which illustrates the differences between the four chosen wind turbines. All of the wind turbines that have been selected are well known and have a proven track record in small-scale applications.

Specification	Kestrel e230i	SkyStream 3.7	eddyGT	Turby
Turbine type	HAWT	HAWT	VAWT	VAWT
Rated output (W)	800	2400	1000	2500
Rated wind speed (m/s)	12.5	13	12	14
Cut in wind speed (m/s)	2.5	3.5	3	4
Rotor diameter (m)	2.3	3.7	1.8	2
Number of blades	3	3	3	3

Table 3.2: Wind turbine specifications

The power curves for each of the four turbines were obtained from the Wind Power Program Wind Turbine Database (Wind Power Program, 2017). As these power curves have been derived from the manufacturer's data, it would be prudent to presume that these power curves overestimate the real world performance of the wind turbine. This is because the real-world power output of a turbine is dependent on numerous factors which may not be fully accounted for in a laboratory setting normally used by manufacturers to calculate power curves. Figures 3.2-3.5 show the power curve for the eddyGT, the Kestrel, the SkyStream, and the Turby turbines respectively.

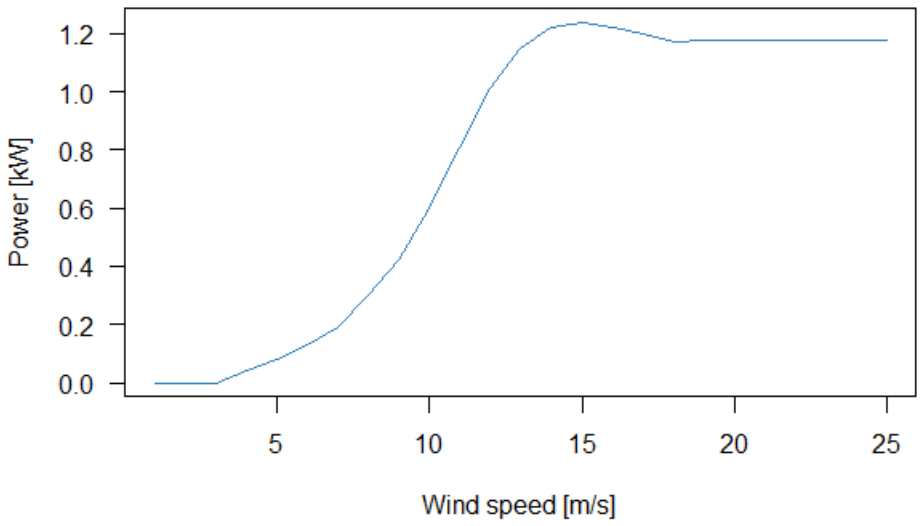

Figure 3.2: eddyGT power curve (Wind Power Program, 2017)

Figure 3.6 shows a plot of all of the power curves for the chosen turbines. From Figure 3.6 the two larger turbines (SkyStream and Turby) and the two smaller turbines (Kestrel and eddyGT) are easy to see.

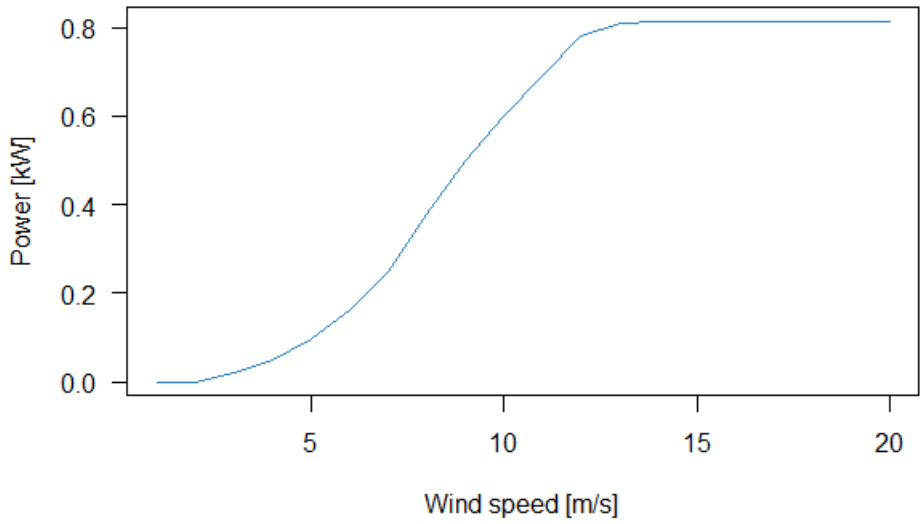

Figure 3.3: Kestrel power curve (Wind Power Program, 2017)

3.3 DATA ANALYSIS PROCEDURE

The method used to analyse the wind data from the six different locations is a combination of a Microsoft Excel spreadsheet and a script compiled in the R programming language. The spreadsheet component of the model sorts the data from the South African Weather Service into a data structure that can be recognised by the *R* script. The *R* script then uses this sorted data and interprets it in the *R* environment to produce various results related to the wind resource potential.

R is an open-source programming language and software environment which makes use of a freely-available General Public Licence (R Development Core Team, 2008). *R* was developed in 1992 by Ross Ihaka and Robert Gentleman and is currently managed by the *R* Development Core Team with a stable beta version released in 2000 (Development Core Team, 2008). The *R* Development Core Team also provides information regarding the capabilities and structure of *R*.

In recent years, *R* has become one of the main programming languages for data analysis and statistical modelling (Tippmann, 2014). The *R* script that was written is largely based on the *R* package 'bReeze' which was developed by Christian Graul and Carsten Poppinga (Graul & Poppinga, 2015). In the *R* environment, a package is a self-contained set of functions that are grouped together to meet a given objective. The bReeze package applies a set number of functions to wind data in order to calculate the wind energy resource potential of a specific location.

For the purposes of this study, the original bReeze package is combined with the *R* Stats package (one of the main statistical analysis packages in *R*) in order to produce comparative statistical outputs

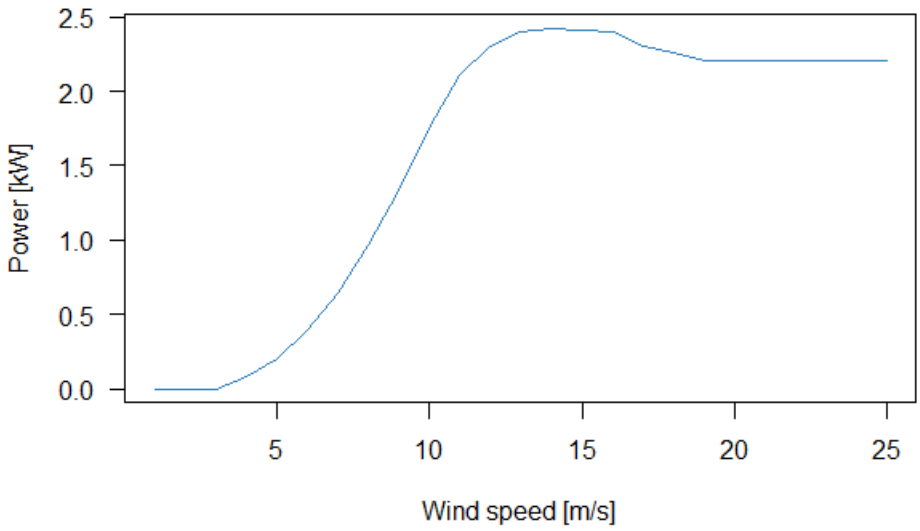

Figure 3.4: SkyStream power curve (Wind Power Program, 2017)

alongside the wind resource potential calculated by bReeze alone. The functions of bReeze that are used in the calculations of this study include: the total wind energy content, calculation of the Weibull probability density function, frequency of the wind speed, and turbulence intensity. Samples of the *R* script that was used in the calcualtion of the weibull parameters, the energy content, and the Annual Energy Pproduction values are shown in Appendix C.

3.3.1 *Total wind energy content*

The package bReeze is used to calculate the theoretical wind energy content from the calculated Weibull parameters. This is similar to the wind energy potential of a chosen site discussed in Chapter 2; only a brief discussion of the method that bReeze uses to calculate the total wind energy content is provided here. The wind power density function is described by bReeze using the following expression:

$$E(v) = \frac{1}{2}\rho v^3 f(v) \tag{3.1}$$

With ρ being the air density, v the wind speed and f(v) is the chosen probability density function.

Splitting the wind speeds up into various wind speed bins (v_b) gives the following formula:

$$E(v) = \frac{1}{2}\rho H \sum v_b^3 W(v_b) \tag{3.2}$$

With H being the time period under consideration (this would be 8760 hours for an annual assessment), and W(v_b) being the probab-

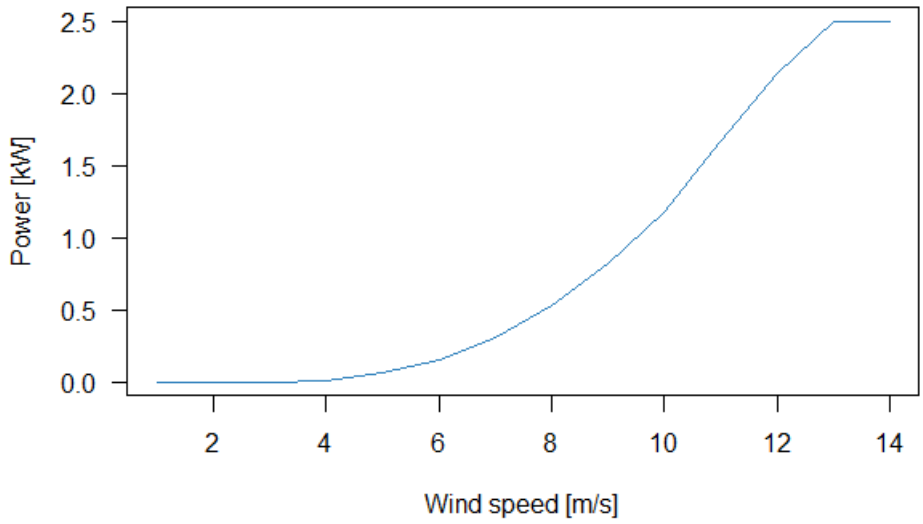

Figure 3.5: Turby power curve (Wind Power Program, 2017)

ility of the specific wind speed bin occurring which is determined by the chosen probability density function.

3.3.2 *Wind speed correction*

The data from each of the six locations was recorded at various heights specific to that location. Therefore, in order to compare the wind energy content of the various sites, the wind speed data was corrected to reflect the wind speeds that occur at each location but at a constant height of 15m above ground level. This is done to account for the wind shear phenomenon and to ensure a fair comparison between the six locations.

As discussed in Chapter 2, there are several laws that can be used for the extrapolation of wind speeds to various heights. In this study, the wind profile power law with an exponent of $1/7$ was used. Therefore, using this standard exponent, the power law expression becomes

$$v_1 = v_2 * (\frac{z_2}{z_1})^{\frac{1}{7}} \tag{3.3}$$

This expression was applied to all six data sets in order to provide a standard height at which the wind resource potential of the six sites could be compared against each other.

3.3.3 *Annual energy production*

The bReeze package can calculate the average annual energy production by a specified wind turbine in a specified location (Graul & Pop-

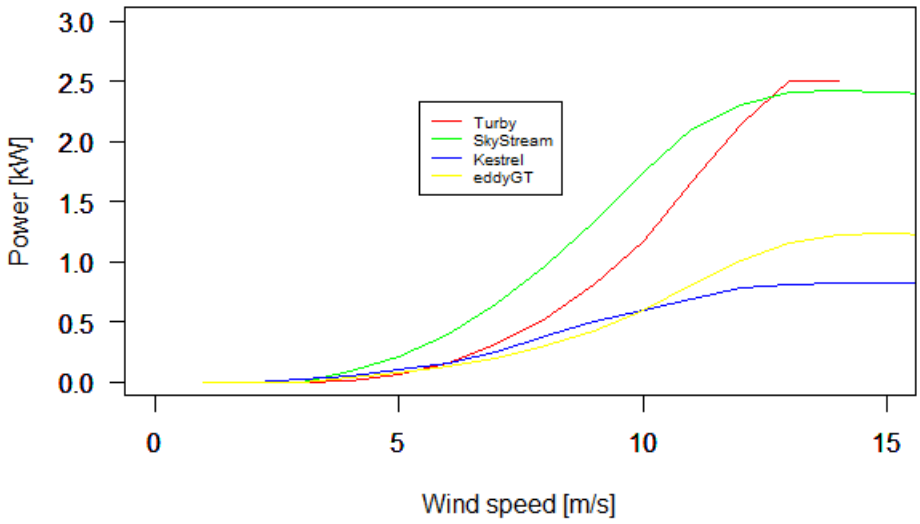

Figure 3.6: Power curves for all turbines (Wind Power Program, 2017)

pinga, 2015). This average energy production can be expressed by the following equation:

$$E = T \int f_v p_v \tag{3.4}$$

With f_v being the probability density function of the chosen site's wind speed v, the power curve of the chosen wind turbine is represented by p_v and finally T is the time period for which the energy production must be calculated. The two speeds, v_{out} and v_{in}, are the cut out and cut in wind speeds for the chosen wind turbine. Cut in wind speed is the minimum wind speed necessary for the wind turbine to begin to operate and cut out wind speed is the maximum wind speed at which the wind speed can operate safely.

The bReeze package takes Equation 3.4 and uses it to calculate the Annual Energy Production (AEP) for a chosen wind turbine at a specific location. The AEP is given by the following:

$$AEP = A_{turb} \frac{\rho}{\rho_{pc}} H \sum W(v_b) P(v_b) \tag{3.5}$$

With A_{turb} being the average availability of the chosen turbine, ρ_{pc} being the air density that the turbine's power curve was developed for, H is the number of hours (for AEP, the number of hours is 8760), Wv_b is the probability density function for the wind speed bin v_b, and $P(v_b)$ is the power output of the wind turbine at the specific wind speed bin (Graul & Poppinga, 2015).

The AEP is then used to determine the Capacity Factor (CF) of the wind turbine at a specific site by the use of the following formula:

$$CF = \frac{AEP}{P_{rated} * 8760} \tag{3.6}$$

With P_{rated} being the rated power of the turbine.

3.3.4 *Turbulence intensity*

One of the key parameters for understanding the output from urban wind turbines is the turbulence intensity. Turbulence is defined as the range of wind velocity variations experienced at a location in a specified time perio (Graul & Poppinga, 2015). Some of the parameters that affect turbulence are surface roughness, topography, and thermal effects. All three of these parameters vary significantly in an urban environment. The surface roughness will vary depending on the type of construction materials used, the topography will vary as new buildings are constructed, and the thermal properties of urban areas vary widely depending on the time of day, the season of the year or the type of buildings nearby. Therefore, one can expect urban wind flows to be characterised by high levels of turbulence which can lead to increased loads on the wind turbine, which in turn may exacerbate fatigue and necessitate more frequent maintenance. High turbulence may also reduce the energy production of the wind turbine. A good measure of the turbulence of a site is given by the Turbulence Intensity (I). The bReeze package calculates the Turbulence Intensity by the following simple equation:

$$I = \frac{\sigma}{v_{avg}} \tag{3.7}$$

With σ being the standard deviation of the wind speed for a specific period and v_{avg} being the average wind speed measured in the same period. In the data sets obtained from the SAWS, the standard deviation for each five minute interval was not available. Therefore, a moving average standard deviation per hour was calculated and used to determine the TI in each five minute interval

3.4 EXPECTED DAILY ELECTRICITY GENERATION

In addition, the daily electricity generation profiles for two locations over two separate days were analysed. This was done in order to investigate at what period of the day a small scale turbine would be producing electricity. These generation curves are useful to investigate as they show how closely the amount of electricity generated from

a small-scale wind turbine matches the typical demand profile at any period of time during the day. The closer the two curves resemble each other, the better electricity can be utilised immediately and the lesser the need there is for electricity storage systems.

The Molteno and Cape Town WO sites were chosen to produce these electricity generation curves, and the Kestrel e230i turbine power curve was chosen as the representative small-scale power turbine. The five minute wind speed data for the two sites for two different days (21st June 2016 and 21st December 2016) were used to calculate the expected electricity generation of the turbine at each location.

The power curve from the Kestrel e230i turbine was then applied to the average five minute wind speeds from the two sites and the estimated amount of electricity generated was recorded. The electricity produced per five minute interval by the turbine was then compared against a typical South African load profile curve.

3.5 HUB HEIGHT SENSITIVITY ANALYSIS

A sensitivity analysis was done in order to examine the effect of changing the hub heights of the various turbines at each of the chosen locations. This exercise involved varying the hub heights for each turbine at each location and recording the change in the Annual Energy Production (AEP) values. The hub heights chosen for this exercise were 15m, 20m, 25m, and 30m. These different hub heights were used as inputs into the bReeze package and the AEP results were recorded and compared against each other for each of the different heights.

3.6 COST OF ELECTRICITY

In order to evaluate the costs associated with the generation of electricity from small scale wind turbines in this study, the Levelized Cost of Electricity (LCOE) was calculated for the Kestrel e230i wind turbine at each of the six locations. These LCOE costs were then compared against the City of Cape Town's domestic electricity tariff to assess the viability of a small-scale wind turbine in Cape Town.

The LCOE metric is a well-known and often-used method of evaluating the costs of generating electricity from different technologies (Energy Information Administration (EIA), 2017). The LCOE metric returns the cost of generating electricity over the lifetime of the turbine per kilowatt hour (kWh) and for this study it includes the costs of the capital costs of the Kestrel e230i turbine, the installation costs (including transport and site preparation costs, and the maintenance costs associated with operating the turbine over its 20 year lifetime. These costs were obtained directly from the manufacturer of the Kestrel turbine (Gouws, personal communication, August 23 2017). These costs are then discounted back to present value using

a discount rate of 8.4%. This rate is the same rate that was used by the South African Department of Energy during the process of developing the 2016 version of the Integrated Resource plan for electricity (Department of Energy, 2016). The discounted costs are then summed over the 20 year lifetime of the turbine and divided by the total amount of electricity that the turbine is expected to produce over its lifetime. The LCOE formula is given by the following equation (United States Department of Energy, 2013):

$$LCOE = \frac{\sum \frac{I_t + M_t + F_t}{(1+r)^t}}{\sum \frac{E_t}{(1+r)^t}} \tag{3.8}$$

WITH

I_t being the investment expenditure in year t,

M_t being the maintenance costs in year t,

F_t is the fuel costs in year t (for this study there are no fuel costs),

r is the discount rate, and n is the total life of the wind turbine.

The Kestrel e230i turbine was selected for this LCOE analysis because it is made in South Africa and reliable cost data for it could be sourced. The other three turbines are not manufactured in South Africa and thus accurate cost data could not be sourced and in addition the costs associated with importing the turbine may inflate the overall project cost.

According to the manufacturer of the Kestrel e230i turbine, the costs associated with purchasing, installing, and maintaining the turbine over its 20 year life time are detailed in Table 3.3 (Gouws, personal communication, August 23 2017)

Item	Cost (including VAT)	Frequency
Turbine cost	R 85 337	Once off
Installation costs	R 29 526	Once off
Civil costs and site preparation	R 17 670	Once off
Dismount the turbine and check the turbine	R 7 068	Every 5 years
Dismount and replace all bearings	R 12 387	Every 10 years

Table 3.3: Cost information for the Kestrel e230i turbine

3.7 MODEL VALIDATION

The bReeze model was validated in two ways. Firstly, the bReeze package was run using the example data provided in the original

package documentation in order to confirm that the amended package still operated in the same manner as the original bReeze package.

The second part of the validation was to take the data from one of the locations (Royal Cape Yacht Club) and use Microsoft Excel alone to compute the necessary outputs such as the Weibull parameters, turbulence intensity and the total wind energy content.

The results from the validation model run in Excel and the results obtained from bReeze were similar down to at least two decimal places. This confirms that the bReeze model is accurate and that it produces results that are representative of the wind regime at the specified location.

Two statistical methods were chosen to evaluate the goodness-of-fit measurements between the recorded data and the results from the bReeze package. These two methods were the Root Mean Square Error (RMSE) and the Coefficient of Determination (R^2). The RMSE is often used to test the accuracy of predicted values of a model versus the actual recorded data (Pishgar-Komleh et al, 2015). The RMSE measures the standard deviation of the residuals (Barnston, 1992). RMSE can be given by:

$$RMSE = \sqrt{\frac{\sum(x_{obs} - x_{pre})^2}{N}} \tag{3.9}$$

WITH

x_{obs} being the observed data point

x_{pre} being the predicted data point

N being the number of observations in the sample

The coefficient of determination or goodness-of-fit is given by:

$$R^2 = \frac{(\sum(x_{obs} - \bar{x_{obs}})(x_{pre} - \bar{x_{pre}}))^2}{\sum(x_{obs} - \bar{x_{obs}})^2 \sum(x_{pre} - \bar{x_{pre}})^2} \tag{3.10}$$

The lowest value of the RMSE together with the highest value for the R^2 will help show if the fitted model is an adequate representation of the recorded data at the specific recording station (Pishgar-Komleh et al, 2015).

3.8 LIMITATIONS

One of the initial limitations encountered during the data collection is that the study uses data that has been exclusively obtained from the South African Weather Service (SAWS). No additional measurements or verification on the data were carried out by the author. However, all

six locations meet the SAWS MetCap framework which sets out rules and procedures for the collection and analysis of wind data obtained from weather measurement stations (De Jager, personal communication 2017, August 18). The MetCap framework is based on standards issued by the World Meteorological Organisation (WMO) (De Jager, personal communication 2017, August 18). This quality control framework operates on two levels, with level one quality control conducted by the regional weather offices and level two quality control checks being conducted at the SAWS' head office (De Jager, personal communication 2017, August 18).

The data that is used in the study is obtained from six discrete wind measurement stations in and around Cape Town. Due to the variable nature of the urban wind resource the results of this study should not be used to infer the wind resource potential for any other location in Cape Town apart from the sites of the six measurement stations where the data were recorded.

The study makes use of data recorded over a period of 24 months, from the 1st of January 2015 until the 31st of December 2016. This period should be long enough to account for any seasonal fluctuations in the wind resource. However, over longer periods, the wind resource may shift consequently rendering the results of this study invalid. Any further studies should therefore make use of the most up to date wind data that can be obtained.

3.9 SUMMARY

This Chapter presented the methods that were followed in order to evaluate and investigate the data which was done meet the various research objectives. The following Chapter presents the various results that were obtained using the various research methods that are presented in Chapter 3.

4

RESULTS AND DISCUSSION

This chapter presents and analyses the results of the urban wind energy model discussed in the previous chapter. Section 4.2 presents the main results from each of the six chosen locations in the Cape Town area; Section 4.3 lays the groundwork for a comparison of the locations' data with one another; Section 4.4 sees the addition of power curves of the selected wind turbines to these results in order to calculate the Annual Energy Production (AEP) and then compares the various AEP values for the turbines against each other; Section 4.5 concludes the chapter with a discussion on the combined results and a summary of the model.

4.1 CAPE TOWN'S URBAN WIND REGIME

This section presents the main results of the wind energy resource assessment for each of the six locations. Additional results from each of the six locations are presented in Appendix 7.1.

4.1.1 *Royal Cape Yacht Club*

The wind rose for the Royal Cape Yacht Club is shown in Figure 4.1. The wind rose combines the wind speed and wind direction into one graph to show how they are distributed at the chosen location. From the wind rose it is clear that the majority of the wind at the RCY comes from both a southerly direction and a northerly direction.

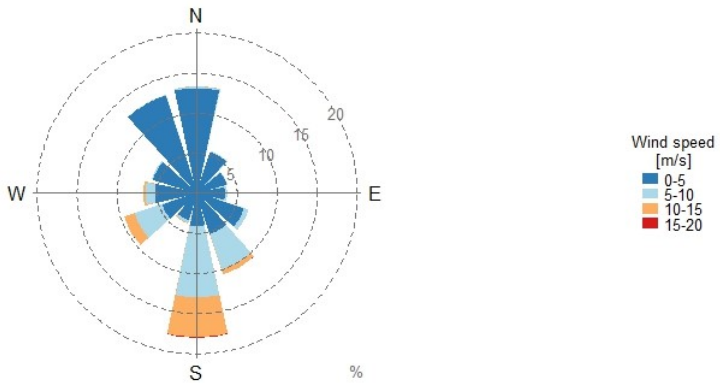

Figure 4.1: Wind rose for the Royal Cape Yacht Club

Figure 4.2 highlights the mean monthly wind speed at the Royal Cape Yacht Club over the two recorded years, namely 2015 and 2016.

Again the pattern of higher summer wind speeds and lower wind speeds during the winter months is visible from the two lines. The mean wind speed over the two years for the RCY is 3.61 m/s.

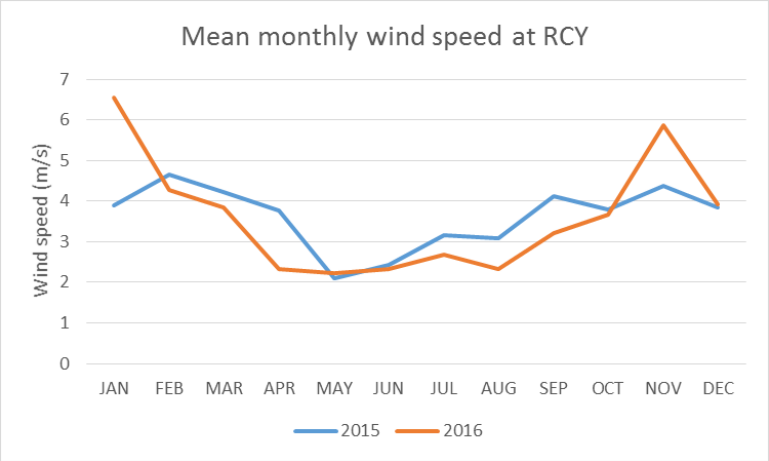

Figure 4.2: Mean wind speeds at the Royal Cape Yacht Club

The Weibull parameters were calculated for the wind data from the RCY. A shape parameter (A) of 3.7 and a scale parameter (k) of 1.1 were calculated by the bReeze package. These parameters were then used to plot the Weibull distribution. The Weibull distribution is plotted as the red line in Figure 4.3 against the wind speed distribution which is shown as the blue histogram bars. The coefficient of determination for the Weibull plot is calculated to be 0.85. This shows that the Weibull distribution is a good fit for the recorded data from the Royal Yacht Club. Further proof of the good fit between the Weibull probability density function and the observed data is given by the Root Mean Square Error (RMSE) which has a value of 0.03 m/s for the data at the Cape Royal Yacht Club.

For the RCY club, the total energy available per meter square of rotor area per year was calculated to be 1181 kWh/m²/a. Splitting this figure up into the various wind speed bins, 433 kWh/m²/a was provided by the 0-5 m/s wind speed bin, 507 kWh/m²/a from the 5-10 m/s wind speed bin, 234 kWh/m²/a from the 10-15 m/s bin and 4 kWh/m²/a from the 15-20 m/s speed bin. Splitting the data up in this manner shows the influence of the wind speed on the amount of energy available. Due to the cubic relationship between wind speed and energy available, the wind speed bin of 5-10m/s provides 42.93% of the energy at the location while only accounting for 18% of the wind speed data.

The wind energy content is split up in a different manner in Figure 4.4 which shows the wind energy distribution according to the wind direction. From Figure 4.4 it is clear to see that a large majority of the wind energy occurs from a southerly direction.

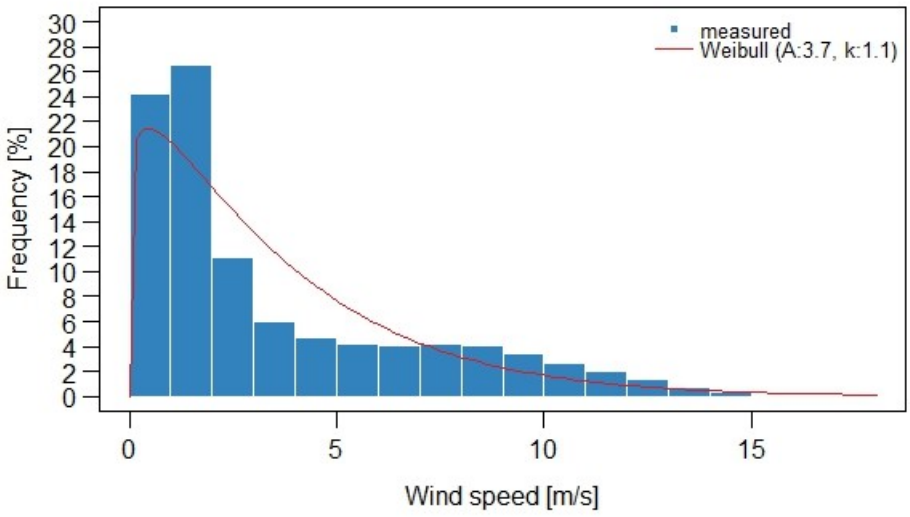

Figure 4.3: Weibull distribution for the Royal Cape Yacht Club.

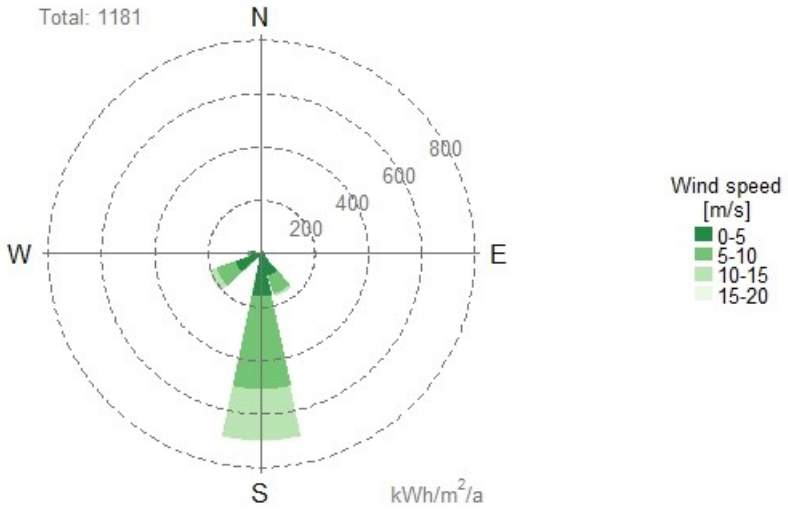

Figure 4.4: Wind energy distribution for the Royal Cape Yacht Club

4.1.2 *Kirstenbosch*

Figure 4.5 shows the wind rose that has been calculated for the Kirstenbosch station. From the wind rose, it is clear to see that the majority of data falls in the 0-5m/s wind speed bin and the prevailing wind direction is West North West and then West.

Figure 4.6 shows the mean monthly wind speeds for the two years recorded at the Kirstenbosch station. From the figure, it can be seen that there are no significant seasonal effects of the wind speeds at the station. The monthly mean wind speeds for the station are low

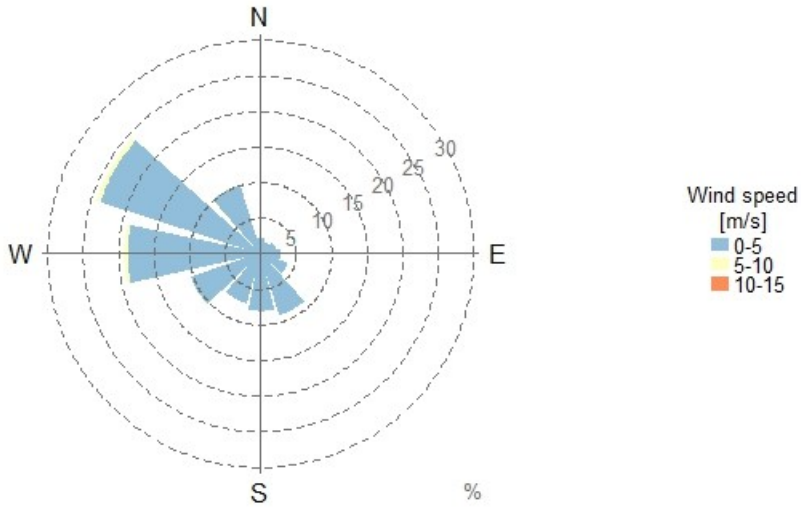

Figure 4.5: Wind rose for the Kirstenbosch station

and this will have an impact on the available wind energy at the Kirstenbosch site. The average wind speed over the two years is 2.04 m/s.

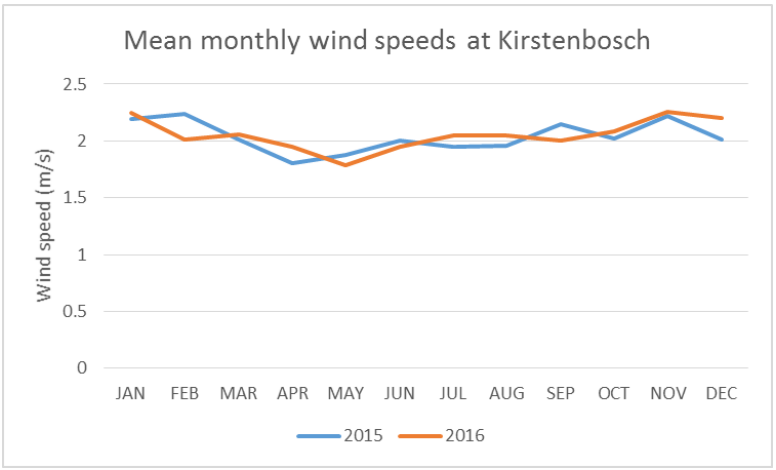

Figure 4.6: Mean monthly wind speeds for Kirstenbosch

From the wind speed distribution, the Weibull parameters were calculated for the Kirstenbosch station. A shape parameter (A) of 2.3 and a scale parameter (k) of 2.22 were calculated from the Kirstenbosch data set. These parameters were then used to plot the Weibull distribution. The Weibull distribution is plotted as the red line in 4.7 against the wind speed distribution which is shown as the blue histogram bars. From Figure 4.7 it can be seen that approximately 12% of the wind data fell in the wind speed bin of 0-1m/s, 43% fell in the 1-2m/s category and 34% fell into the 2-3m/s category with the remaining data in the higher wind speed categories. This again shows

the low wind speeds at this location. The coefficient of determination for this data set was calculated to be 0.82 which shows that the fitted Weibull distribution is a sound representation of the wind data recorded at the Kirstenbosch station. The RMSE value for the data at the Kirstenbosch site was calculated to be 0.0674 m/s which again indicates that the recorded values and the values predicted by the Weibull function are a good fit.

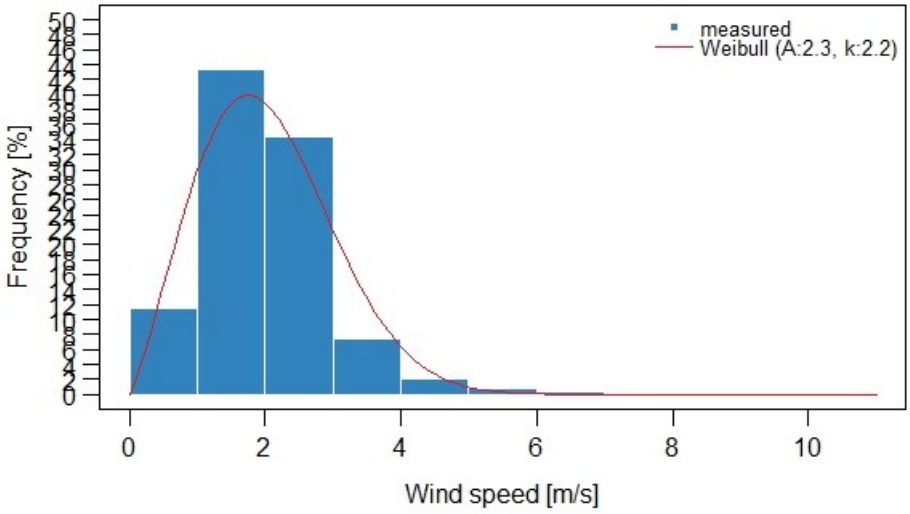

Figure 4.7: Weibull distribution for the Kirstenbosch station

The Weibull distribution was used in order to calculate the theoretically available wind energy resource potential for the Kirstenbosch site. For this site, due to the low wind speeds recorded, the total energy available per meter square of rotor area per year was calculated to be 80 kWh/m²/a. 79 kWh/m²/a was derived from the 0-5m/s wind speed bin and the remaining 1 kWh/m²/a was from the 5-10m/s wind speed bin. The amount of wind energy available at the Kirstenbosch station is shown in Figure 4.8 which splits the wind energy into the various direction whom which the wind blows. As was seen before at this station, the majority of wind, and hence energy, comes from a Western direction.

The results from the Kirstenbosch station are the lowest in terms of wind speed and therefore resource potential. A site visit was carried out to attempt to identify the reasons why the wind speeds were so low at this station. This station is located in the Kirstenbosch National Botanical gardens. In the immediate vicinity of the measurement station there are numerous small trees and shrubs however, these plants are not thought to be the main reason for the low wind speeds as the measurement system is located on a metal pole which is comfortably above the surrounding vegetation. This is evident in n Figure 4.9 which pictures the wind speed recorder mounted on the metal

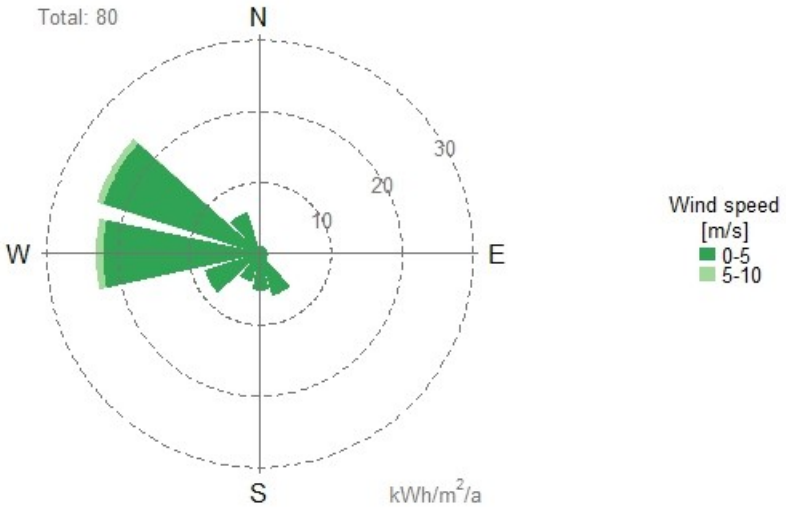

Figure 4.8: Wind energy available at the Kirstenbosch station

pole which is comfortably taller than the surrounding vegetation. The slopes of table Mountain are also visible on the right-hand side of the picture.

The Kirstenbosch Botanical gardens are located on the south-east slopes of Table Mountain. Table Mountain may therefore shelter the site from the wind and this could account for the low wind speeds recorded at the Kirstenbosch site.

4.1.3 *Automatic Weather Station*

The wind rose for the AWS station is plotted in Figure 4.10 below. It is evident that the vast majority of the wind speed data recorded fell below 10m/s. The prevailing wind direction is from the south.

Figure 4.9: Kirstenbosch gardens site

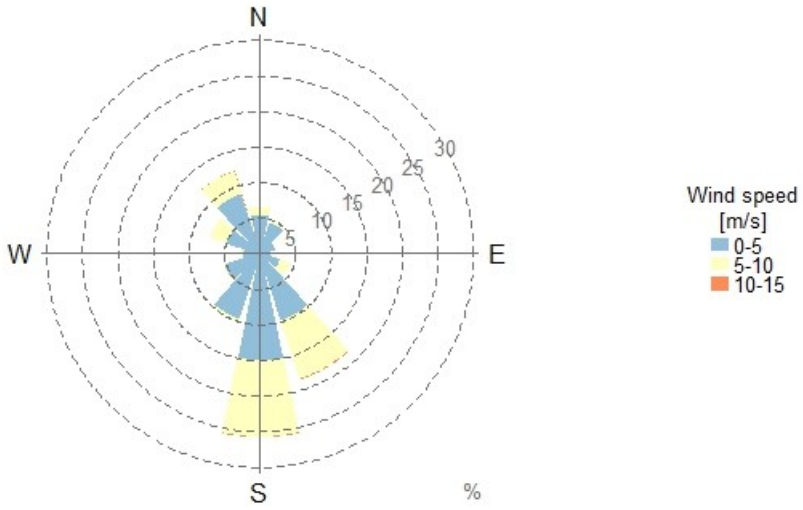

Figure 4.10: Wind rose for the AWS station

The average wind speed for the AWS station over the two years was 3.83 m/s. The mean monthly wind speeds for the station are shown in Figure 4.11. From the figure the seasonal fluctuations in wind speed are clear to see with a pronounced dip in the wind speeds occurring in the months from May to July.

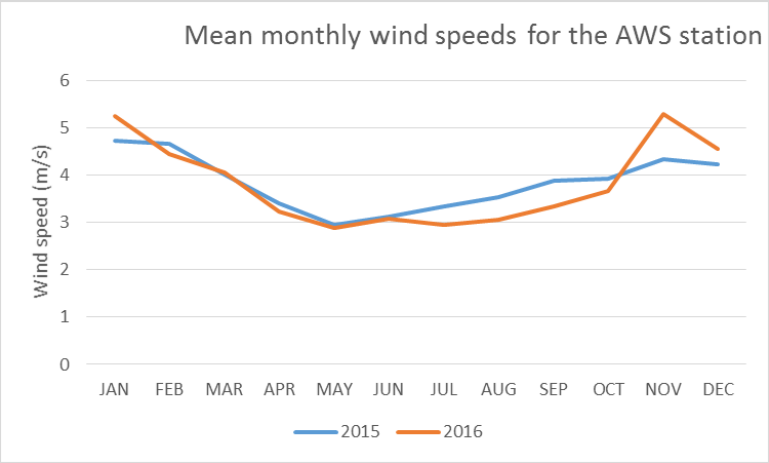

Figure 4.11: Mean monthly wind speeds for the AWS station

Using the wind speed data from the AWS station, the Weibull parameters were derived for the station. The shape factor (A) was determined to be 4.3 and the scale parameter (k) was found to be 1.9. The Weibull probability density function was plotted using these parameters and it is represented by the red line in Figure 4.12 while the recorded data wind speed distribution is shown in the same figure as the blue bars. A coefficient of determination of 0.95 was calculated for the AWS data set. This shows that the Weibull probability distribution provides a very good estimation of the wind regime experienced at the AWS station. This site had an RMSE value of 0.0165 m/s which highlights the good fit between the recorded data and the values predicted by the Weibull curve.

Using the Weibull probability density function, the potential wind energy resource for the AWS station was calculated. For this station the total energy available per meter square of rotor area per year was calculated to be 610 kWh/m²/a. Splitting this total energy value up into the wind speed bins reveals that 379 kWh/m²/a came from the 0-5m/s bin while 231 kWh/m²/a came from the 5-10m/s bin. Again, the majority of the wind energy comes from winds with a southerly direction and this is expected as the majority of the wind data recorded shows that the prevailing wind at the AWS is from the South. This can be seen in Figure 4.13.

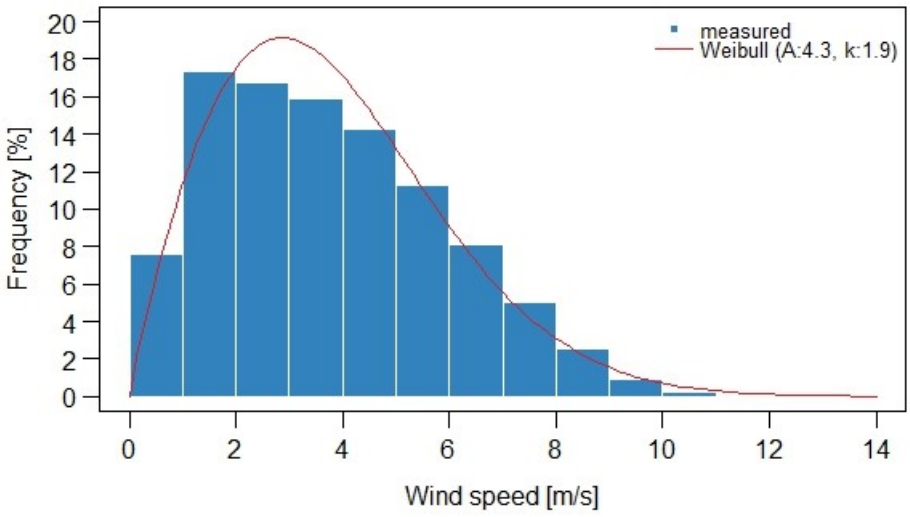

Figure 4.12: Weibull distribution for the AWS station

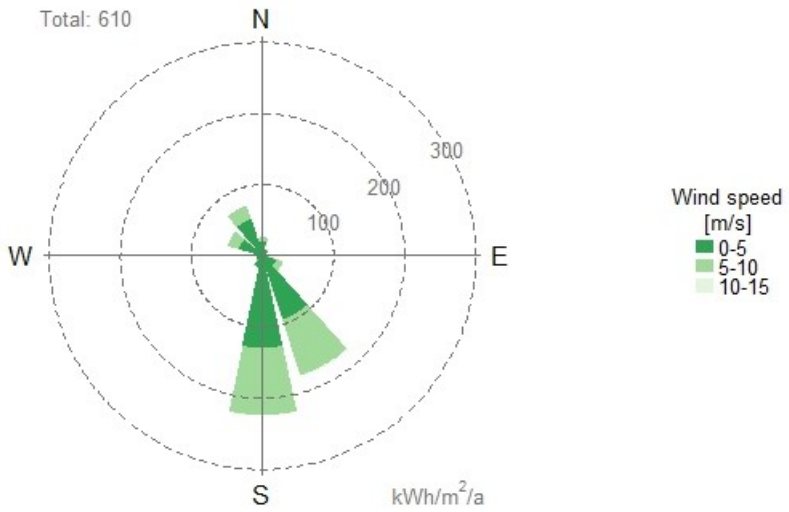

Figure 4.13: Wind energy distribution for the AWS station

4.1.4 *Molteno Reservoir*

The wind rose for the Molteno reservoir is shown in Figure 4.14. From the wind rose, it is clear to see that the site experiences wind from a wide range of directions with a slight majority coming from a southerly direction. The wind rose gives further evidence that the significant majority of wind speed recordings are below the 5m/s threshold.

Figure 4.15 shows the mean monthly wind speeds recorded at the Molteno reservoir for the years 2015 and 2016. The figure shows the lower wind speeds that are experienced at the site during the autumn

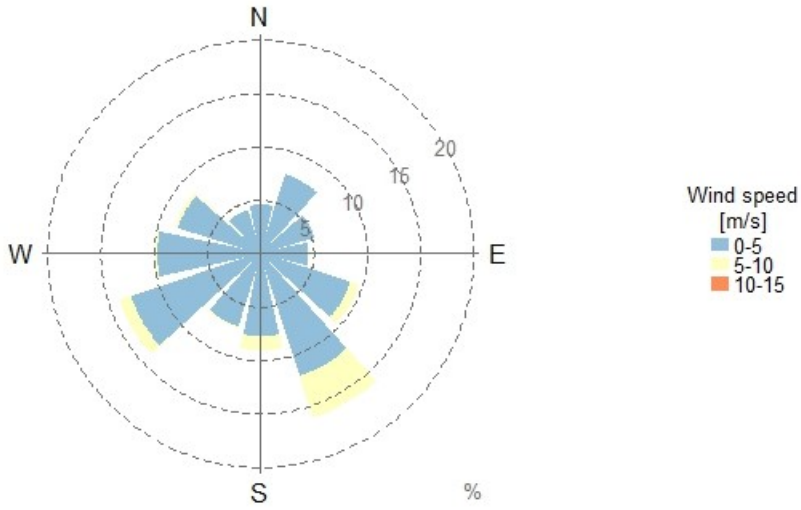

Figure 4.14: Wind rose for the Molteno reservoir

and winter seasons. The average wind speed over the two year period was 2.35 m/s.

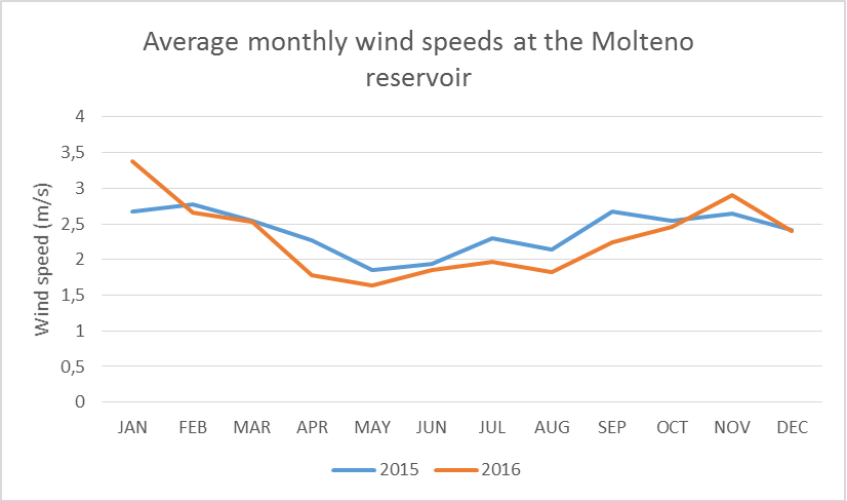

Figure 4.15: Mean monthly wind speeds for the Molteno reservoir

The Weibull parameters for the Molteno reservoir were calculated from the data recorded over the two year period. A shape factor (A) of 2.6 and a scale factor (k) of 1.5 were calculated. From these parameters, the Weibull probability distribution was plotted as the red line in Figure 4.16 while the histogram of the recorded data is shown by the blue columns. The value of the coefficient of determination between the Weibull distribution and the recorded values was 0.95, which highlights that this Weibull was a good fit for the data recorded at the Molteno reservoir. A RMSE value of 0.0194 m/s was calculated for the Molteno reservoir site.

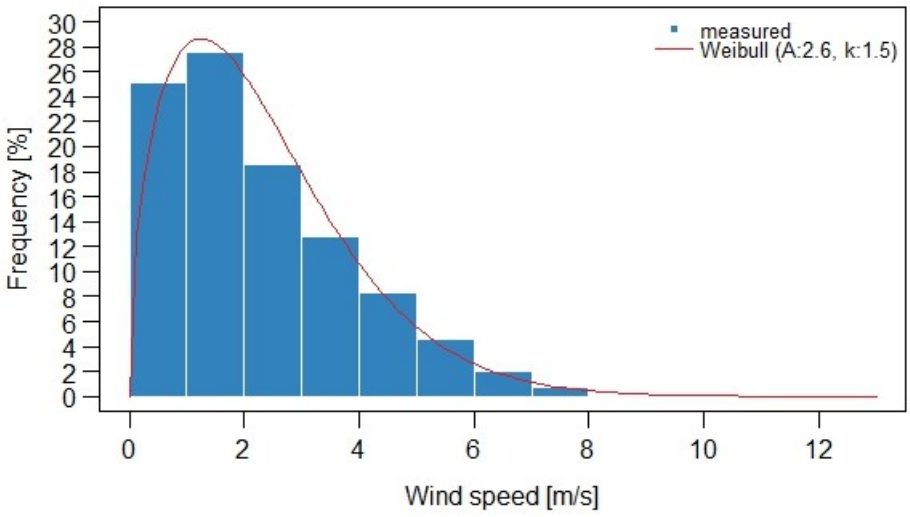

Figure 4.16: Weibull distribution for the Molteno reservoir

Using the Weibull distribution that was derived in the preceding section, the wind energy resource potential was calculated for the Molteno reservoir site. For the site, the total energy available per meter square of rotor area per year was calculated to be 189 kWh/m²/a. 160 kWh/m²/a of that figure came from the 0-5m/s wind speed bin and the remaining 29 kWh/m²/a came from the 5-10m/s wind speed bin. Figure 4.17 plots these resource potential values for the site and it shows that the majority of the energy is derived from wind with a southerly direction.

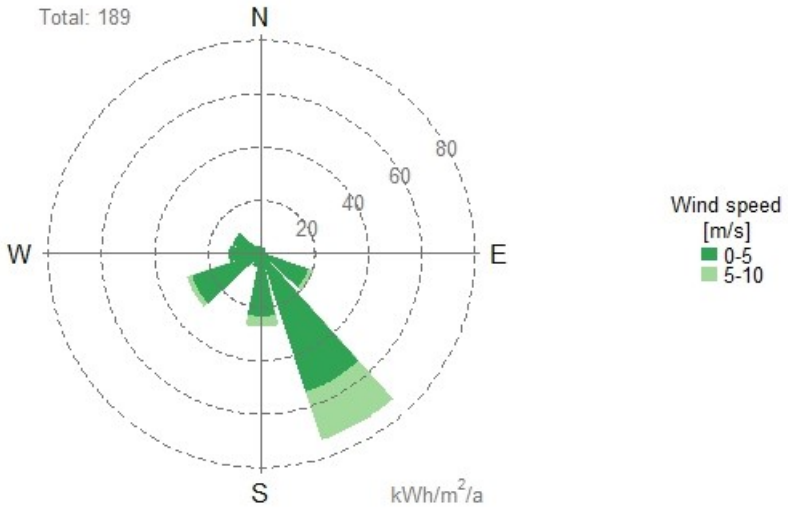

Figure 4.17: Wind energy resource potential for the Molteno site

4.1.5 *South African Astronomical Observatory*

Figure 4.18 shows the wind rose for the Observatory data set. The prevailing wind is from a southerly direction and the majority of the wind speeds are below 5m/s.

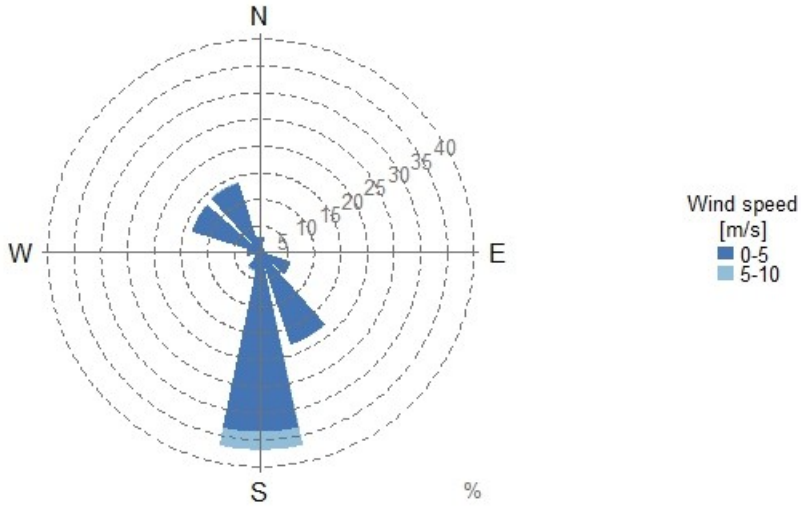

Figure 4.18: Wind rose for the Observatory station

The mean monthly wind speeds for the Observatory station also show evidence of the low wind speeds associated with the location and are shown in Figure 4.19. Again there is a slight decrease in wind speeds during the winter months. Over the two year period, the average wind speed for this station was 2.33m/s.

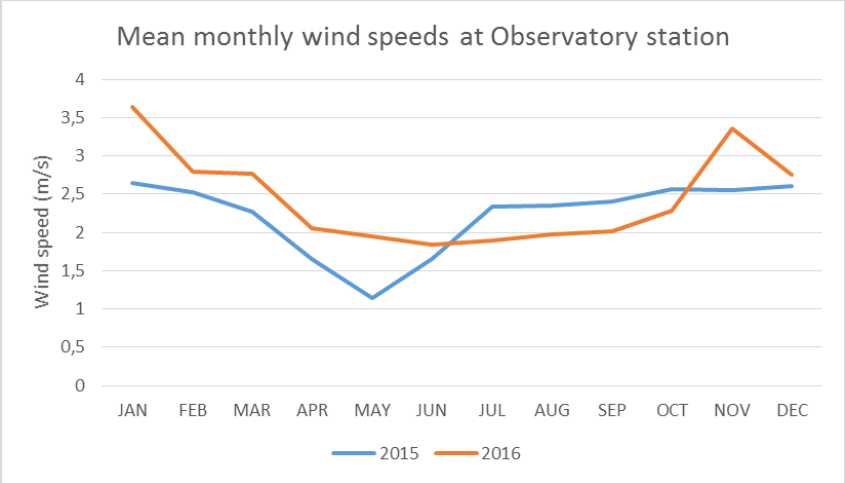

Figure 4.19: Mean monthly wind speeds recorded at the Observatory station

The Weibull parameters were calculated using the wind speeds data from the Observatory station and are shown in Figure 4.20. The

shape factor (A) was calculated as 2.6 while the scale factor (k) was 1.8. The fitted Weibull curve had a coefficient of determination value of 0.972 which shows that the fitted Weibull distribution is an excellent representation of the data from the Observatory station. The Weibull distribution is shown in Figure 4.20 as the red line and the blue columns represent the wind speed distribution of the recorded data. For the Observatory station a RMSE value of 0.0179 m/s was calculated.

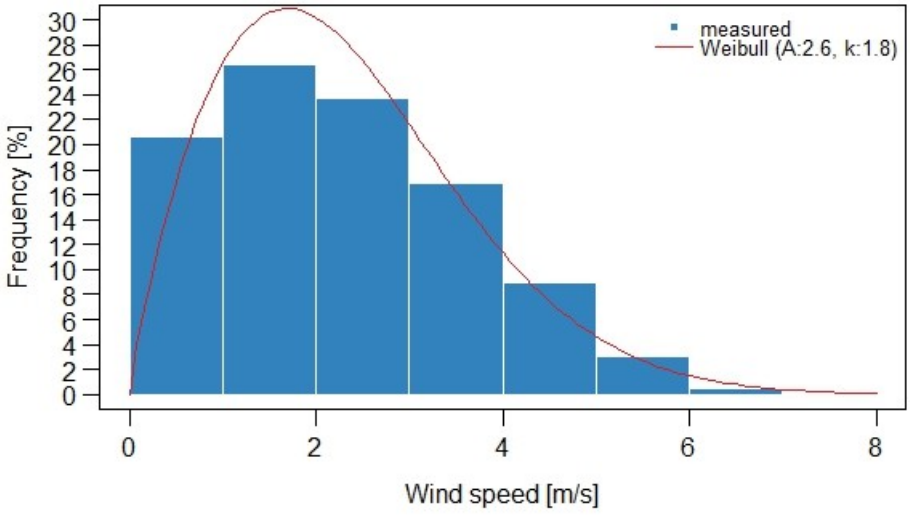

Figure 4.20: Weibull distribution for the Observatory station

The theoretical wind resource potential was calculated using the Weibull distribution that was plotted in Figure 4.20. The wind energy potential was calculated to be 145 kWh/m²/a. This value is one of the lowest energy potentials in this study. The wind energy resource for this site is illustrated in Figure 4.21. This figure shows that a significant portion of the energy resource is derived from winds with a southerly direction and that most of the energy is available from winds with speeds of less than 5m/s.

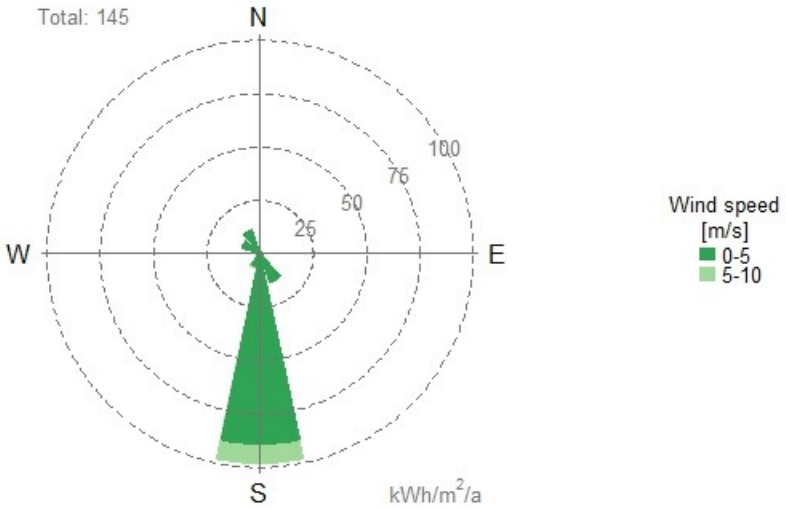

Figure 4.21: Wind energy resource for the Observatory station

4.1.6 *Cape Town Weather Office*

The wind rose for the Cape Town WO station is shown in Figure 4.22. From Figure 4.22 it can be seen that the majority of wind speeds recorded at this station are between 5-10 m/s and the prevailing wind direction is from the South.

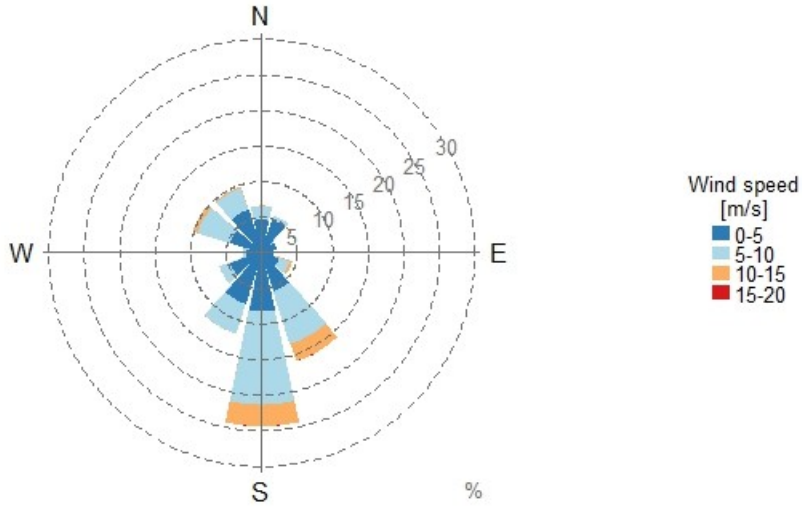

Figure 4.22: Wind rose for the WO station

Figure 4.23 shows the average monthly wind speeds that were recorded at the WO station. The decrease in average wind speeds during the autumn and winter months is evident from the figure. The

average wind speeds for the entire two year recording period is 5.06 m/s. .

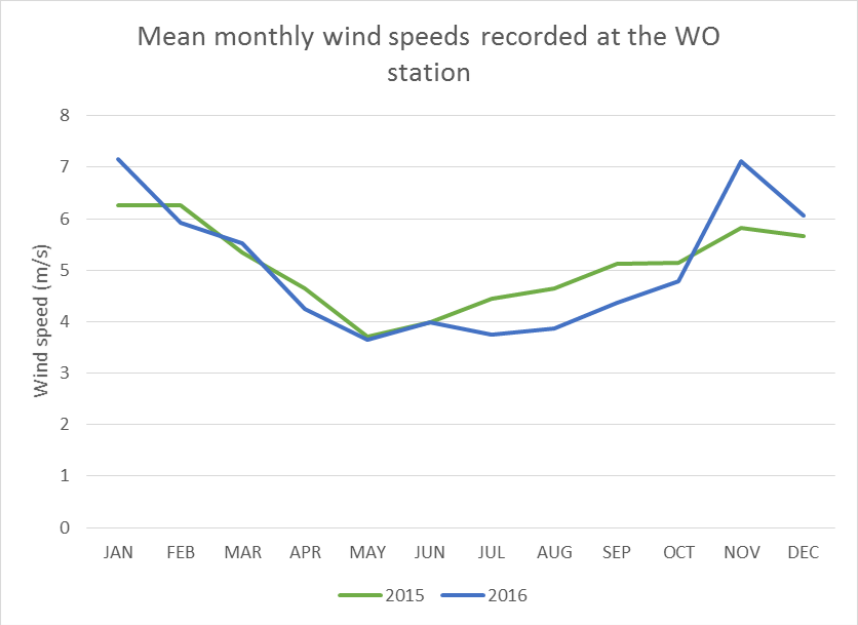

Figure 4.23: Mean monthly wind speeds for the WO station

The next step in the analysis of the wind data was to calculate the Weibull parameters for the WO station. A shape parameter (A) of 5.7 and a scale parameter (k) of 1.8 were determined as a result. These values were then used to plot the Weibull probability density function, illustrated by the red line in Figure 4.24. The blue columns in Figure 4.24 show the wind speed distribution of the recorded data. The Weibull curve has a coefficient of determination of 0.97 which indicates that the Weibull curve is an accurate fit of the recorded data. Further evidence of the good fit between the recorded data at the WO station and the station's predicted Weibull curve is the station's RMSE value which was calculated at 0.0088 m/s.

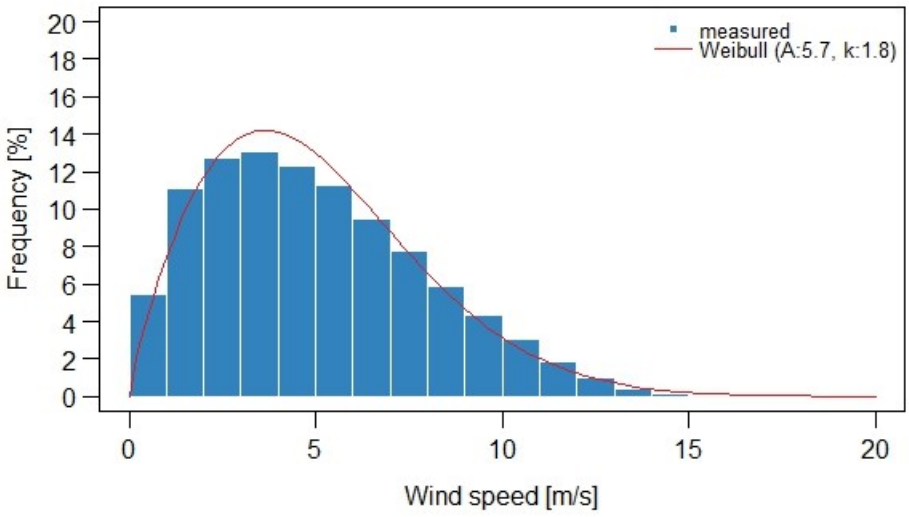

Figure 4.24: Weibull distribution for the WO station

Using the Weibull curve that was developed in the preceding paragraph, the theoretical wind energy resource potential was estimated for the WO site. This is shown in Figure 4.25. The total energy available at the site was calculated to be 1474 kWh/m²/a. Again, the predominate direction is South and the majority of the wind energy comes from wind speeds between 5-10 m/s.

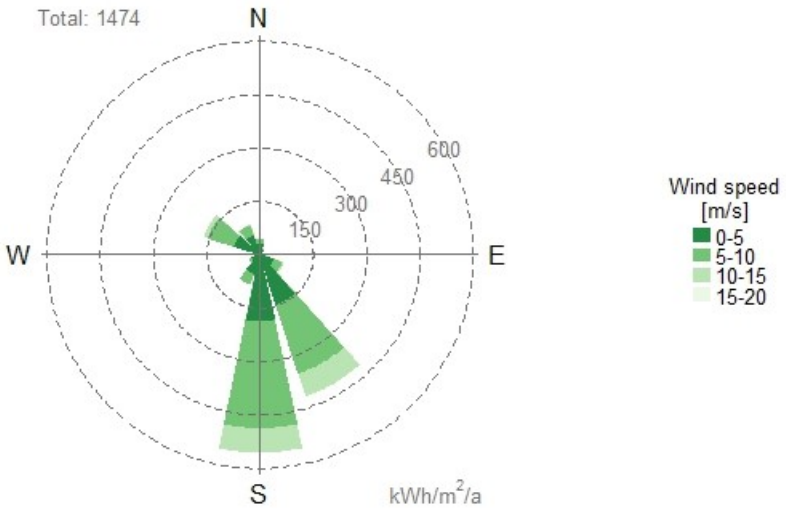

Figure 4.25: Wind energy resource potential for the WO station

4.2 QUANTIFICATION OF THE URBAN WIND REGIME

Where the previous section presents the individual results from all six of the wind data recording stations used in this study, this section quantifies the urban wind resource potential of Cape Town. These stations are all located in Cape Town within an area that is roughly square in shape and that has dimensions of approximately 11.5km in the North-South direction and 19.9km in the East-West direction. Despite this relatively tight spatial grouping of the chosen sites, the main finding of this study is the extreme variation that was found between the sites.

This section quantifies the urban wind resource potential of Cape Town by presenting the wind speed distribution results as well as the results from the wind energy resource assessment. Following the assessment of the urban wind energy resource as a whole, an in-depth comparison of two locations (selected according to their location and wind resource potential), AWS and the Cape Town WO station, is included. A comparison of the results of the more 'suburban' or residential locations (Molteno, Observatory, and Kirstenbosch) with the non-residential locations (Royal Cape Yacht Club, AWS, and the WO station) is also included. The criteria for this grouping is the fact that the three 'residential' locations are surrounded by residential areas with many buildings in the nearby vicinity while the 'non-residential' areas are located in more open areas without being surrounded by residential buildings. In the case of the WO and AWS stations, they are located in the relatively open area near the Cape Town International Airport while the RCYC is located adjacent to the Atlantic ocean and there are few surrounding buildings nearby.

4.2.1 *Wind speeds*

The average wind speeds recorded varied significantly from station to station. The station with the highest average wind speed for the whole two-year recording period was the WO station with a wind speed of 5.056m/s. The lowest average wind speed was 2.044m/s, recorded at the Kirstenbosch recording station. The average of all six stations for the two year period was 3.24m/s. Of the six recording stations, five of them experienced seasonal fluctuations in their average monthly wind speeds with only the Kirstenbosch station showing no signs of higher wind speeds in the summer period. The seasonal fluctuations as well as the monthly average wind speeds for all six stations are shown in Figure 4.26. The figure shows that the WO station consistently has the highest average monthly wind speeds and the Kirstenbosch station has the lowest recorded average wind speeds for majority of the year.

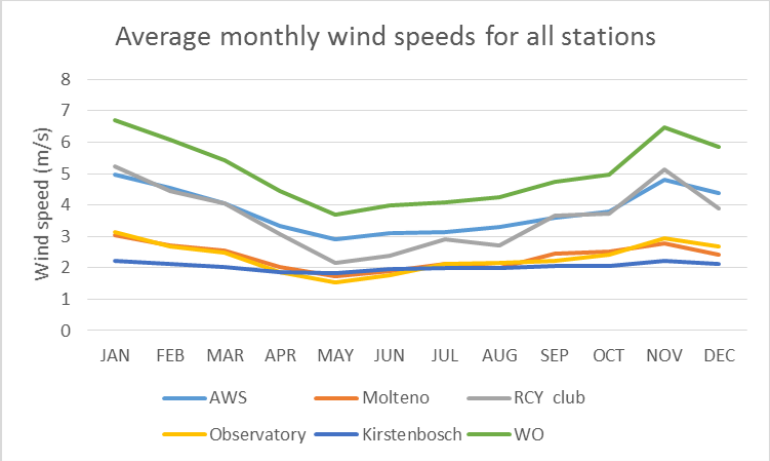

Figure 4.26: Average monthly wind speeds for all stations

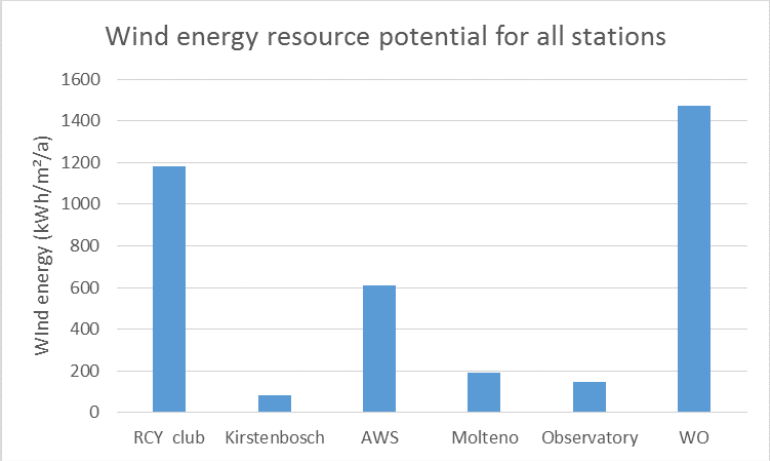

Figure 4.27: Wind energy resource potential for all stations

4.2.2 *Energy potential*

Using the wind speed data for all of the stations, the theoretical wind energy resource potential was calculated (shown in Figure 4.27). It is clear to see from the figure that the annual energy resource potential varies between the stations included in the study. It can also be seen that the WO station has the highest energy potential with a value of 1474 kWh/m²/a, while the Kirstenbosch station has the lowest energy potential with a value of 80 kWh/m²/a. These results are expected as these two stations also have the highest and lowest average wind speeds respectively. Comparing the Kirstenbosch station to the WO station, the Kirstenbosch station only has approximately 5% of the wind energy potential of the WO station. This again highlights the variability of the wind resource depending on the location.

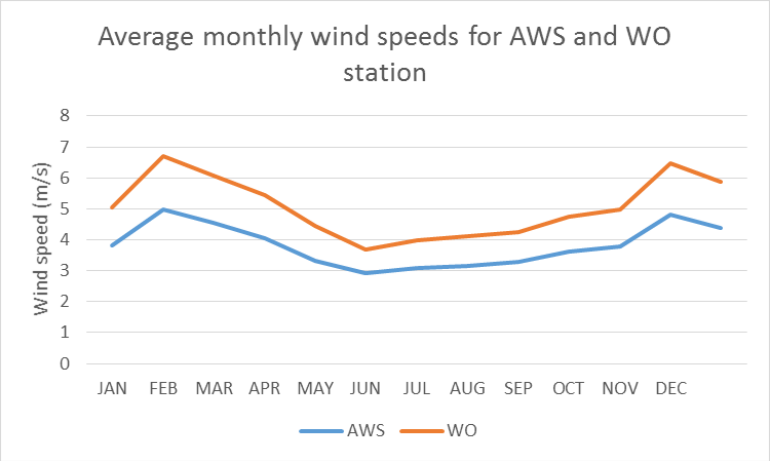

Figure 4.28: Monthly wind speeds for the AWS and WO station

4.2.3 *Comparison between the WO station and the AWS station*

A further comparison of the results from the AWS and WO stations proves illuminating for the purposes of this study. These stations are both located near the Cape Town International Airport and are only separated by a distance of 1.9km, however, the energy resource potential results from the two stations differ significantly. The two-year average wind speeds for the AWS and WO station are 3.83m/s and 5.056m/s respectively. This means that the two-year wind speed for the AWS station is only approximately 24% lower than that of the WO station. The mean monthly wind speeds for the two stations are shown in Figure 4.28. From the figure it can be seen that both stations have similar wind regimes with roughly the same pattern of wind speed fluctuations playing out at both stations. However, the major differences between the two stations begin to emerge when the wind speed distributions of the two stations are analysed.

The variance in the wind speed distributions is plotted in Figure 44. From Figure 4.29, it can be seen that the AWS station experiences lower wind speeds at a significantly higher frequency than the WO station, which experiences a much wider distribution of wind speeds. This variation in the wind regimes between the two stations leads to a significant difference in the potential wind energy resource of the two stations. The AWS station has a wind energy resource potential of 610 kWh/m²/a while the WO station has a potential of 1474 kWh/m²/a. This translates into a 58% difference in the energy potential between the two sites. This finding points to the need for accurate long term on-site wind measurement and it highlights the pitfalls that could be experienced if data from a nearby wind recording station is used to decide whether or not to install a small scale wind turbine. The exact reason why there is such a variation between the two stations is

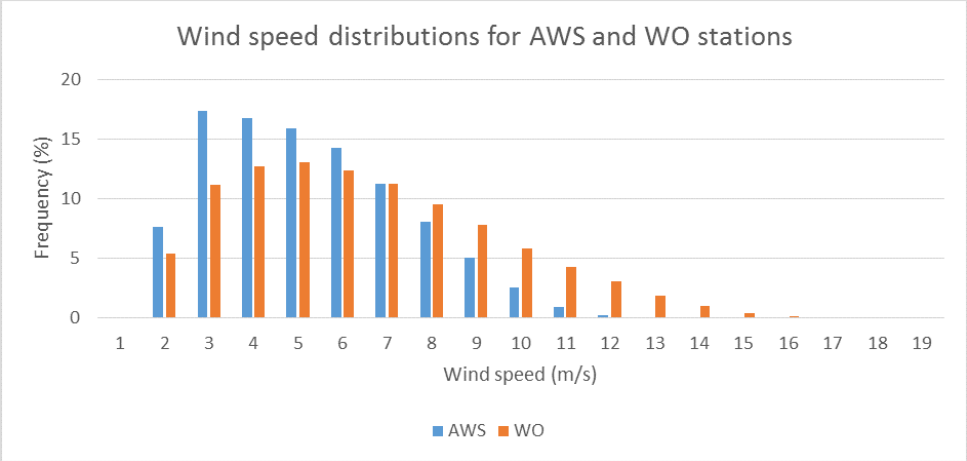

Figure 4.29: Wind speed distributions for the AWS and WO stations

Area type	Station	Wind speed (m/s)	Available energy (kWh/m²/a)
Residential	Kirstenbosch	2.04	80
Residential	Observatory	2.33	145
Residential	Molteno	2.35	189
Non-residential	RCYC	3.83	1181
Non-residential	AWS	3.83	610
Non-residential	WO	5.06	1474

Table 4.1: Residential vs non-residential areas

outside the scope of this study but some possible reasons may be the effects of surrounding buildings or variations in local topography.

4.2.4 *Residential wind resources vs. non-residential wind resources*

A comparison between the recording stations located in residential suburbs (Kirstenbosch, Observatory, and Molteno) and those located in non-residential areas (Royal Cape Yacht club, AWS, and the Cape Town WO station) yields interesting results. Both the AWS and WO stations are located at the Cape Town International Airport while the Royal Cape Yacht club is located in the Table Bay harbour. All three of these locations are thus classified as non–residential for the purposes of this study, having taken into account the larger concentration of industrial and/or commercial activity when compared with the Observatory, Kirstenbosch, or Molteno sites. The resutls from the residential and non-residential areas are shown in 4.1

The three residential areas have the lowest average wind speeds and hence the smallest potential wind energy resources of the sites in this study. The average wind speeds for the Kirstenbosch, Molteno, and Observatory sites are 2.044 m/s, 2.35 m/s, and 2.33 m/s re-

Station	RMSE (m/s)	R^2
Royal Cape Yacht Club	0.03	0.85
Kirstenbosch Botanical Gardens	0.07	0.82
Automatic Weather Station	0.02	0.95
Molteno Reservoir	0.02	0.95
Astronomical Observatory	0.02	0.97
Cape Town Weather Office	0.01	0.97

Table 4.2: Results of the model validation

spectively while the three non-residential locations had average wind speeds of 3.83 m/s for the AWS station, 3.826 m/s for the Royal Cape Yacht club, and 5.056m/s for the Cape Town WO station .

These low average wind speeds translate into the residential areas having the lowest wind energy resource potential as well. The three residential sites have wind energy potentials of: 189 kWh/m²/a for the Molteno site; 145 kWh/m²/a for the Observatory site; and 80 kWh/m²/a for the Kirstenbosch site. In comparison, the lowest non-residential site, the AWS site, had a wind energy potential of 610 kWh/m²/a. These results may therefore potentially indicate that industrial and commercial spaces offer better wind energy resources compared with residential areas. This difference could possibly be due to the increased turbulence around residential areas which contain many more obstructions for the wind to flow around. However, further and detailed research is required to confirm if a similar result if found for other non-residential and residential areas.

4.3 RESULTS OF THE MODEL VALIDATION

The bReeze package produces an accurate representation of the wind regime at each of the six locations in this study. This was shown via the results of the model validation exercise, RMSE and R², calculations. These results are shown in the Table 4.2 below. The RMSE values had a maximum of 0.07 m/s for the Kirstenbosch station and a minimum of 0.01 m/s for the Cape Town WO station. The Coefficient of Determination (R²) values also show a similar result with the R² values ranging from a minimum of 0.82 at the Kirstenbosch site to 0.97 at the Cape Town WO site.

4.4 COMPARISON OF THE VARIOUS WIND TURBINES

Following the assessment of the wind resource potential at the locations studied, the power curves collected from the four small-scale wind turbines were applied to the wind energy resource potential of

each site in order to simulate the energy output of a turbine installed at the location.

In order to compare the results from the turbines, a constant hub height of 20m was selected for all locations and all turbines. As stated previously in this report, the wind speeds recorded at each station were corrected to a constant height of 15m. These speeds were corrected again to the 20m hub height for the Annual Energy Production calculation. This simplification of the analysis is necessary in order to evaluate the wind turbines in relation to one another. In practice, however, the hub heights of installed wind turbines are carefully determined using wind profile calculations at the specific locations. Numerous other factors would influence the hub height decision including the heights of surrounding trees and buildings, the structural limits of the wind turbine tower and various planning permission processes for the specific location. It is not believed that having a constant hub height for all turbines unfairly prejudices any one turbine.

Due to the range of wind speeds experienced at the stations and therefore the variations in the wind energy resource potential, values for the Annual Energy Production (AEP) also varied significantly. The AEP values range between the lowest value of 0.659 kWh/a for the Turby turbine at the Kirstenbosch site and 4304.71 kWh/a for the SkyStream turbine at the Cape Town WO location. Over the six-station data set the wind turbine with the highest capacity factor was the Kestrel e230I with an average capacity factor of 10.1%. Due to its larger size, the SkyStream was the turbine that had the highest AEP at all of the locations except the Kirstenbosch site where the Kestrel e230i had the highest AEP. On average the HAWTs wind turbines had higher AEP and capacity factor ratings than their VAWTs counterparts. This finding is in agreement with international experience (Fields et al., 2016; Energy Saving Trust, 2009).

The AEP for the various turbine choices at the Royal Cape Yacht Club is shown in Figure 4.30. Due to the relatively good wind regime experienced at the RCYC, all four turbines produce relatively good results. The SkyStream has the highest AEP at 3301.54 kWh/a, the Turby turbine follows with 2406.5 kWh/a, the Kestrel produces the third largest AEP with 1224.46 kWh/a and the eddyGT produces 784.74 kWh/a. However, despite its lower AEP value, the Kestrel has the highest capacity factor with 17.2%. This is followed by the SkyStream at 15.5%, the eddyGT with 13.8% and finally the Turby with 11%.

Figure 4.31, includes the AEP figures for Kirstenbosch, the station with the lowest wind energy resource potential. As this station has a low wind energy resource, the Kestrel's lower cut-in speed allows it to perform the best out of the four turbines. Nevertheless, the Kestrel is calculated to produce a relatively low energy output of 19.205 kWh/a. The SkyStream produces 13.734 kWh/a, the eddyGT produces 4.331

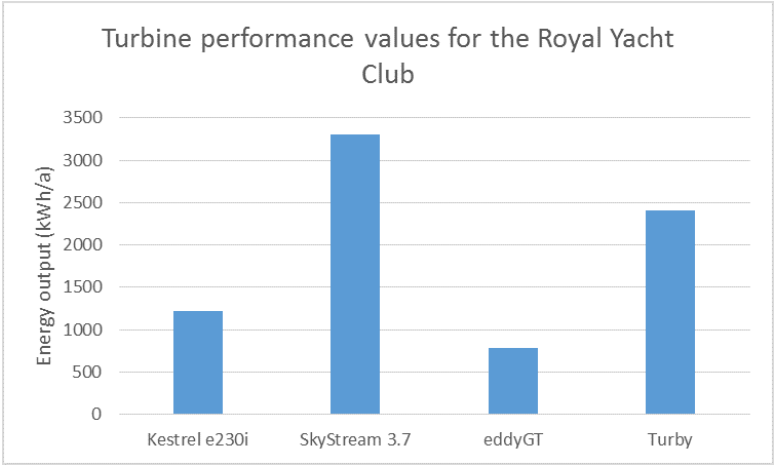

Figure 4.30: Turbine performance results at the RCY club

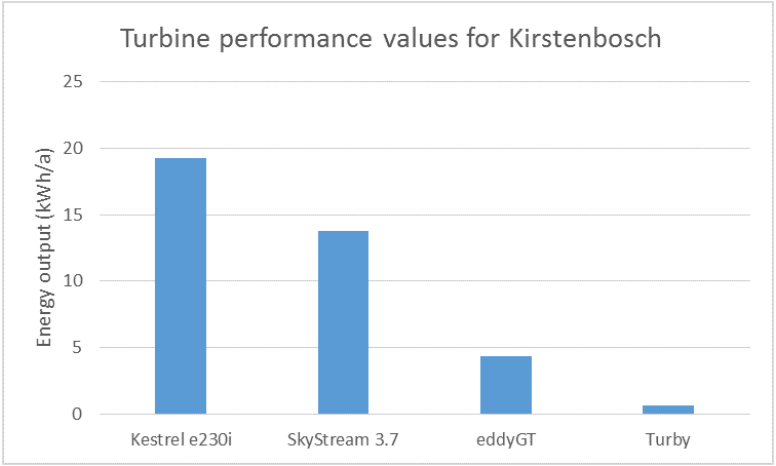

Figure 4.31: Turbine performance curves for Kirstenbosch

kWh/a and the Turby produces 0.659 kWh/a. The capacity factors for all four wind turbines is below 0.5%.

The four turbine power curves were then applied to the data from the AWS station to calculate the AEP values of the turbines at the station (represented in Figure 4.32). The higher wind resource at this station means that the AEP for all the turbines is larger than the AEP at the Kirstenbosch site. At the AWS site, the SkyStream again produces the most energy at 2402 kWh/a, the Turby turbine produces 1227 kWh/a, the Kestrel provides 982 kWh/a, and the eddyGT provides 524 kWh/a. The capacity factors for the various turbines at the AWS station are as follows: the Kestrel achieved a capacity factor of 14%; the SkyStream 11%; the eddyGT achieved 9%; and the Turby reached 6%.

The next station to be analysed was the Molteno station. At this station the highest AEP was again achieved by the SkyStream with 518.22 kWh/a. The Kestrel turbine produced 259.05 kWh/a, which is better than both the VAWTs at this station. The AEP for the Turby was

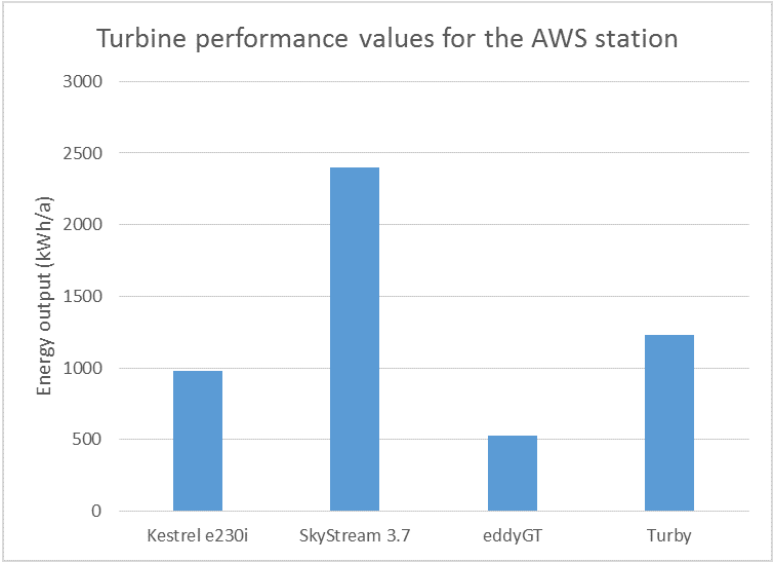

Figure 4.32: Turbine performance curves for the AWS station

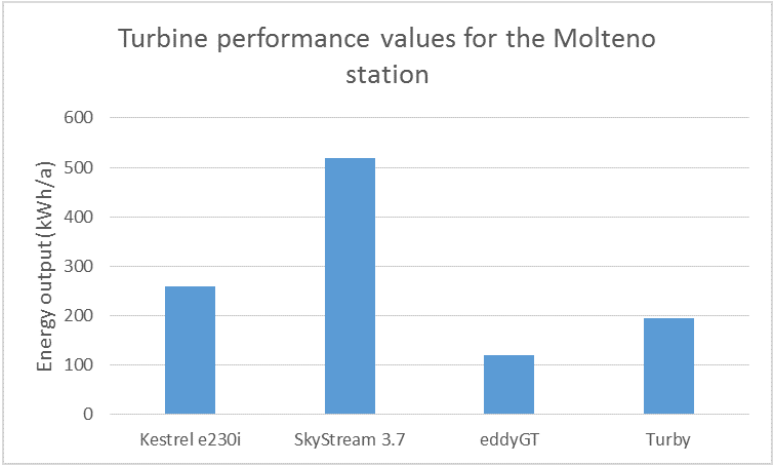

Figure 4.33: Turbine performance values for the Molteno station

calculated at 195.04 kWh/a while the eddyGT had the lowest value of 119.96 kWh/a (values are represented in Figure 4.33). The HAWTs once again performed better than their VAWT equivalent. The Kestrel turbine achieved a capacity factor off 3.6%, the SkyStream 2.4%, the eddyGT 2.1%, and the Turby 0.9%.

Figure 4.34shows the AEP figures for the four turbines at the Observatory station. The SkyStream again had the highest AEP with 339.5 kWh/a and the turbine had a capacity factor of 1.6%. The Kestrel had the second highest AEP with 199.5 kWh/a and a capacity factor of 2.8%. Both VAWTs achieved nearly identical AEP values with 85.89 kWh/a for the Turby and 85.27 kWh/a for the eddyGT. The capacity factors for the Turby and the eddyGT were 0.4% and 1.5% respectively.

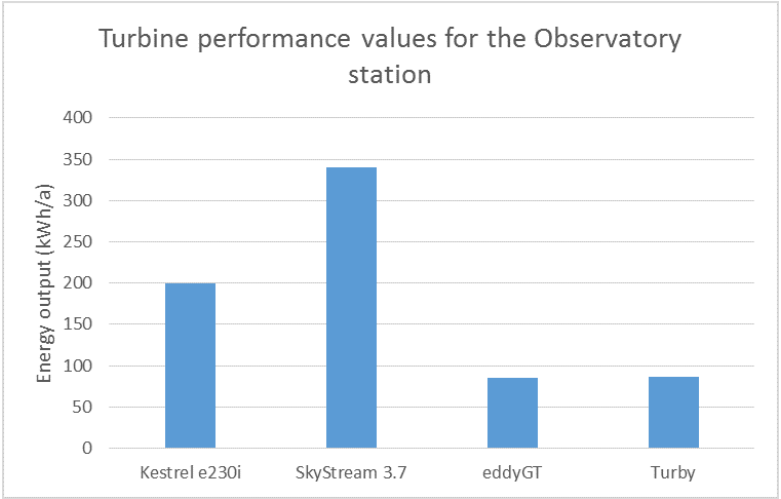

Figure 4.34: Turbine performance values for the Observatory station

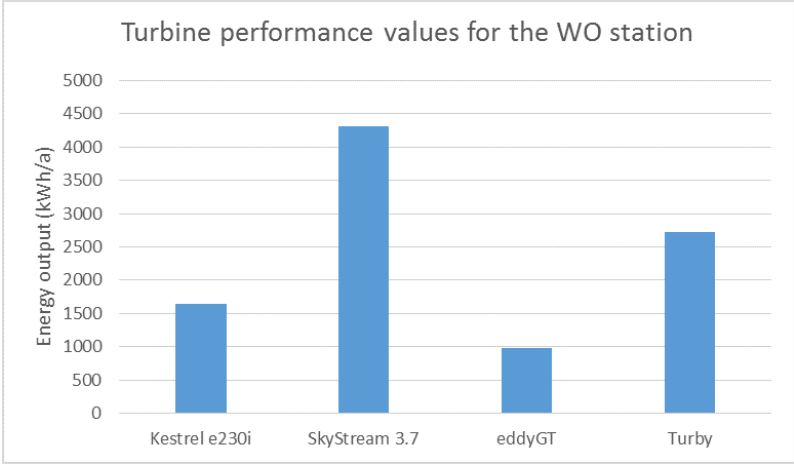

Figure 4.35: Turbine performance values for the WO station

The final AEP analysis was carried out on the Cape Town WO station data set. The AEP figures from this station are shown in Figure 4.35. This station had the highest AEP value of all the stations in this study with 4304.71 kWh/a achieved by the SkyStream turbine at this location. At this station the SkyStream had a capacity factor of 20.3%. The Turby had the second highest AEP values with 2730.34 kWh/a and it had a capacity factor of 12.5%. The Kestrel was next with 1636.82 kWh/a and it had a capacity factor of 22.9%. The eddyGT had an AEP at this station of 975.59 kWh/a being produced despite the favourable wind regime. The eddyGT had a capacity factor of 17.1%.

Turbine Type	Kestrel e230i	eddyGT	Turby	SkyStream
Change in AEP from 15-20m (%)	13.1	15.9	20.3	14.8
Change in AEP from 20-25m (%)	9.5	11.4	14.2	10.6
Change in AEP from 25-30m (%)	7.4	8.9	10.9	8.1

Table 4.3: Sensitivity analysis for the WO station

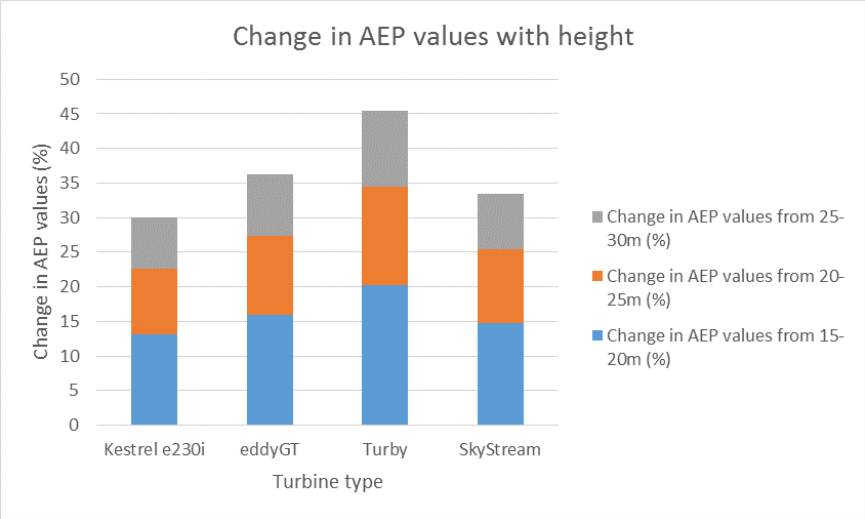

Figure 4.36: Results of the hub height sensitivity analysis for the WO station

4.5 HUB HEIGHT SENSITIVITY ANALYSIS

The results of the sensitivity analysis for the Cape Town Weather Office (WO) station was carried out by setting the hub height of the turbine in the bReeze Annual Energy Production calculation at 15m, 20m, 25m, and 30m. The results from this analysis for this station are shown in Table 4.3 and 4.36below.

Table 4.3 shows that for the Kestrel turbine, moving from a hub height of 15m to a height of 20m results in an increase in the AEP values of 13.1%. An increase in height from 20m to 25m results in an increase of 9.5% and increasing the height from 25m to 30m results in a 7.4% improvement in the AEP values. The sensitivity analysis results for the other stations are included in Appendix 7.2.

Figure 4.36 shows the impact of each successive increase in height for the turbines at the WO station. From the figure, it can be seen that the minimum increase in AEP values was 30% for the Kestrel while the maximum increase was just over 45% for the Turby turbine.

There is a positive relationship between hub height and wind resource potential and this relationship shows signs of diminishing improvements in resource potential with respect to height. This is to be expected (as discussed in Chapter 2). This means that the percentage increase in AEP values decreases as the hub height increases.

4.6 COMPARISON OF THE RESULTS FROM THE CURRENT STUDY TO INTERNATIONAL EXPERIENCES

Capacity factors for roof-mounted turbines in Europe, the United Kingdom, and the United States of America range between 4% and 6.4%, increasing to approximately 10.4% if the turbine is located in an open field with few surrounding obstacles (Mithraratne, 2009). The results obtained in this study for the residential sites (Kirstenbosch, Observatory, and Molteno), which have capacity factors ranging from 0%-3.6%, are lower than the results found by Mithraratne (2009) who analysed the potential for roof-mounted wind turbines in urban areas in New Zealand in his research, while the turbines located in the non-residential areas, (AWS, WO, and the RCY Club) which have capacity factors between 6%-22.9%, represent values higher than Mithraratne (2009) findings.

In their domestic small-scale wind field trial report of 2009, the Energy Savings Trust recorded the performance of 57 installed domestic small-scale wind turbines over a period of one year (Energy Savings Trust, 2009). The wind turbines involved in this study were in the range of 400 W and 6 kW, which is similar to the range of turbines analysed in this study. The Energy Savings Trust found that none of the building-mounted wind turbines had a capacity factor of more than 10% and that no urban building-mounted wind turbine generated more than 200 kWh/a (Energy Savings Trust, 2009). The best-performing building-mounted wind turbine reached a capacity factor of 7.4% and generated approximately 975 kWh during the course of the year (Energy Savings Trust, 2009).

The free-standing turbines, however, performed significantly better than the building-mounted turbines. The average capacity factor for all free-standing turbines was 19% and the highest capacity factors recorded were above 30% (Energy Savings Trust, 2009). These capacity factors for free-standing wind turbines are similar to the capacity factors calculated for the turbines in this study.

An example of a project which sees the effective use of building-mounted turbines is the Twelve West mixed-use development in Portland, Oregon (USA). In preparation, a thorough wind resource assessment was carried out in conjunction with Oregon State University's Aero Engineering Laboratory, which predicted an annual energy production of 9000 kWh (Fields et al., 2016). After the installation of four SkyStream 3.7 wind turbines, the project generates approximately 5500 kWh/a (Fields et al., 2016). Out of the twelve case studies that Fields et al. (2016) conducted, the Twelve West's actual energy production came closest to its estimated energy yield. The turbines are located at an elevation of 82m which is significantly higher than the proposed turbines in this study situated in Cape Town. At a total project cost of $240 000, it will take roughly 40 years to payback the

investment when taking into account the United States Government's 30% Investment Tax Credit (Fields et al., 2016).

Another one of the case studies investigated by Fields et al. (2016) was the NASA Building 12 in Houston, Texas. This project consisted of four eddyGT turbines manufactured by Urban Green Energy. These are the same turbines as the current Cape Town study. While the Twelve West project was the best performing project of the twelve case studies analysed by Fields et al. (2016), the Building 12 project was the worst. The project was estimated to produce 1250 kWh per year but, despite detailed pre-construction wind data recordings, the project only delivered 0.11692 kWh in March of 2015 (Fields et al., 2016). While more time is needed to gather actual annual energy-production data the project developers do not expect the project to yield any significant payback despite the project cost of US$100 000 (Fields et al., 2016). One reason given for the project's poor performance is the fact that the project developers purchased the turbines before any wind resource assessment was conducted (Fields et al., 2016).

These above-mentioned results show that the results from the current Cape Town study are in line with international experiences. They show that the urban wind resource varies drastically and therefore it is essential to conduct thorough wind resource assessments prior to project commencement.

4.7 EXPECTED DAILY ELECTRICITY GENERATION

The preceding sections of this thesis have dealt with the results for annual values of resource potential for the chosen sites or the annual energy production values of a given turbine at a specific site. This section provides information on the electricity production of a small-scale turbine with an interval of five minutes at two sites in the Cape Town area on two different days. These generation curves will then be compared against a typical daily demand profile so as to identify if there are periods of the day when the generation curve follows the same shape as the demand profile. The power curve from the Kestrel e230i is shown in Figure 4.37. The Kestrel turbine was selected because it is the turbine with the average highest capacity factor out of the four small-scale wind turbines chosen for this study and it is readily available in South Africa.

The Molteno site was chosen for this analysis as it is the site with the highest wind resource potential located in a residential area. The Cape Town WO station was chosen as it is the site with the highest wind energy resource potential of all of the six locations and it is located in an area with a high amount of surrounding commercial and industrial buildings.

For each of the two sites, two days were selected, one that represented the summer wind regime and the other representing the winter

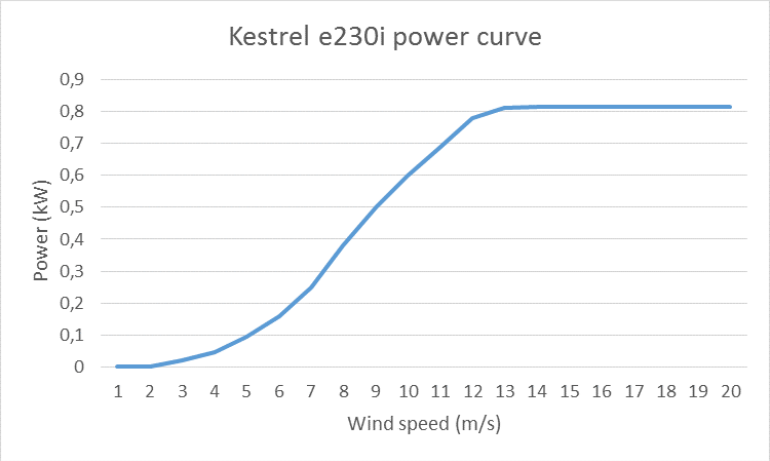

Figure 4.37: Kestrel e230i power curve

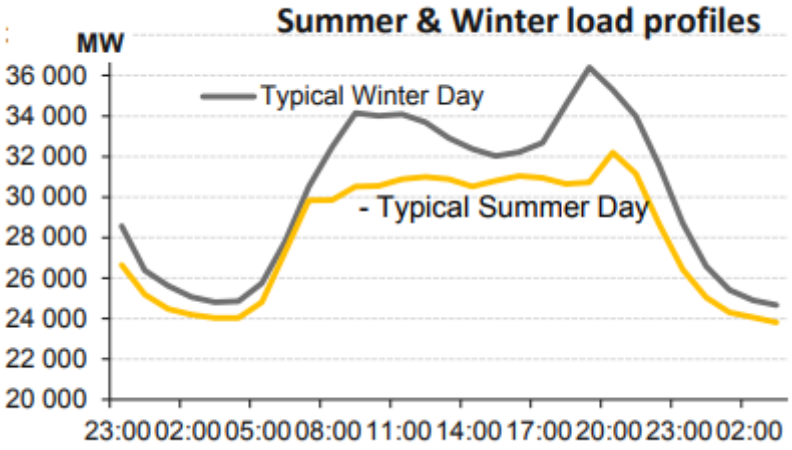

Figure 4.38: Typical daily Eskom load profiles (Matona, 2014)

wind regime. The 21st of December 2016 was chosen to be representative of the summer wind conditions as it is the summer solstice in the southern hemisphere and likewise the 21st of June 2016 was selected as being representative of the winter wind conditions as it is the winter solstice in the southern hemisphere. .

Figure 4.38 shows the typical daily load profile for Eskom, the South African public electrical utility. From Figure 4.38, , it can be seen that in winter there are two demand peaks, one representing the morning peak at approximately 09:00 and the later evening peak at approximately 20:00. In summer, the load is more constant during the day with only a slight peak in the evening.

The results for the daily generation analysis at the Molteno reservoir site from the 21st of December is shown in Figure 4.39. From Figure 4.39 it is clear that the majority of the electricity is produced during the day with a large peak around 12:00 and a smaller peak at

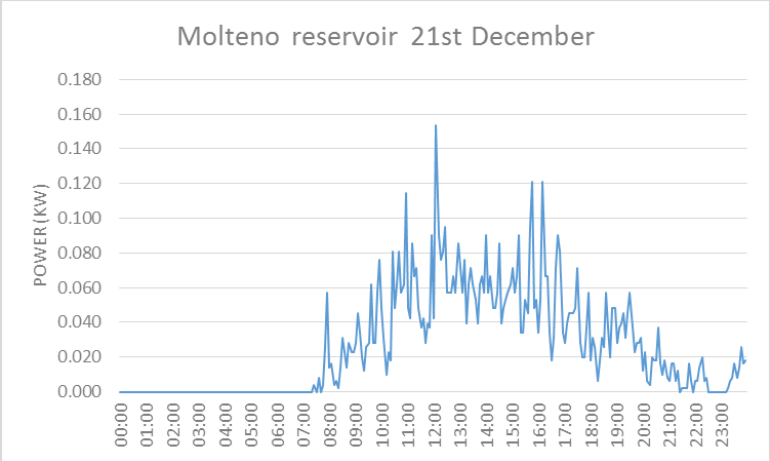

Figure 4.39: Molteno reservoir daily generation curve for the 21st of December

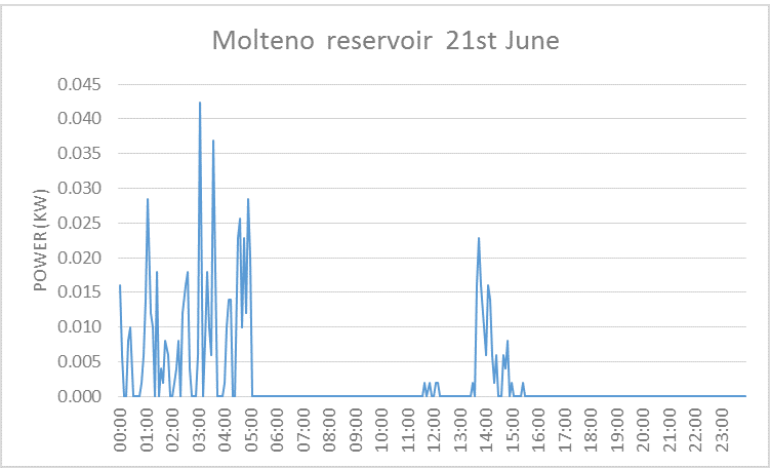

Figure 4.40: Molteno reservoir daily generation curve for the 21st of June

16:00. The total electricity generated at the Molteno site for the 21st of December was 0.63 kWh. Although the majority of the electricity generated at the Molteno site for the 21st of December occurs during the day, it is of a small magnitude.

Figure 4.40 represents the electricity generation on the 21st of June at the Molteno reservoir site. The electricity produced is negligible except for a small peak above 0.04 kW at approximately 03:00. The total electricity generated was 0.032 kWh for the 21st of June. The majority of the electricity produced at the site does not match the typical load profile as shown in Figure 4.38 and the amount of electricity produced during the day is almost negligible.

Figure 4.41 shows the electricity generated at the Cape Town WO site for the 21st of December. Again it can be seen that electricity is generated throughout the day on the 21st of December with peak generation occurring at 17:00. This resembles the typical load curve

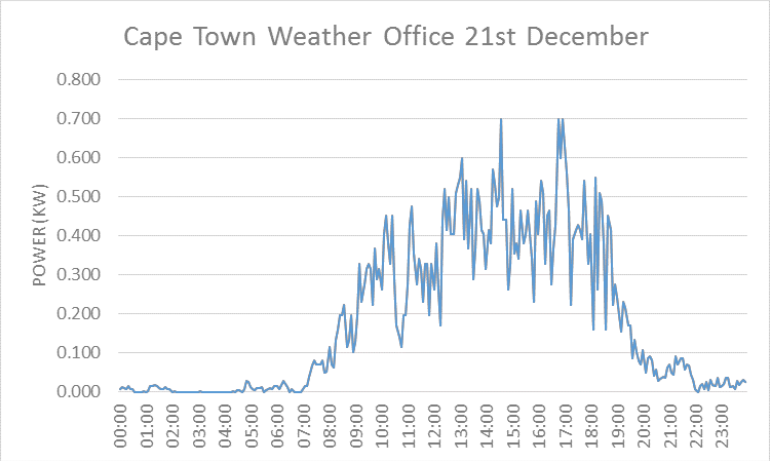

Figure 4.41: Cape Town WO daily generation curve for the 21st of December

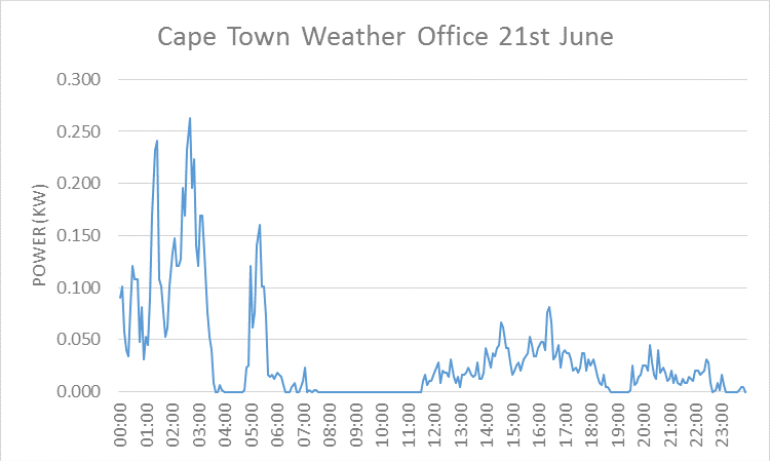

Figure 4.42: Cape Town WO daily generation curve for the 21st of June

from Eskom. The total electricity generated for the day was 4.401 kWh.

The results of the daily generation analysis for the Cape Town WO station during the 21st of June is shown in Figure 4.42. . Similarly to the Molteno reservoir site during the 21st of June, there is negligible electricity generation occurring during the day except for a small (less than 0.05 KW) portion of electricity generated between 12:00 and 19:00. There is also a spike in the early hours of the morning. The total electricity generated at the WO site was 0.768 kWh during the 21st of June.

The results from the daily generation curves from the two sites once again show the seasonal fluctuations that were evident in the monthly wind speeds of the various locations. These results also show that, during the 21st of December, the majority of the electricity is generated during the day which resembles the Eskom typical summer load profile shown in Figure 52. This result is of use as it shows that

Station	Electricity generated (kWh/year)
Royal Cape Yacht Club	1225
Kirstenbosch	19
Automatic Weather Station	982
Molteno reservoir	259
Observatory	200
Weather Office	1637

Table 4.4: Estimated amount of electricity generated at each station

Station	LCOE (R/kWh)
Royal Cape Yacht Club	5.49
Kirstenbosch	354.27
Automatic Weather Station	6.85
Molteno reservoir	25.98
Observatory	33.66
Weather Office	4.11

Table 4.5: LCOE values for the six locations

the majority of electricity generated during the 21st of December 2016 can be used directly and its use does not necessitate the installation of additional energy storage systems. However, at both sites during the 21st of June, there is negligible electricity generation occurring during the day with only a small spike during the early hours of the morning. It is unlikely that this small amount of electricity can be used when it is generated which may require the installation of additional energy storage systems to store this small amount of electricity.

4.8 LEVELIZED COST OF ELECTRICITY

Using the bReeze package the calculated amount of electricity generated by the Kestrel e230i turbine at each of the six locations is given by Table 4.4 below:

These values for the estimated amount of electricity produced at each of the six locations was then used in the LCOE calculation for each of the six locations. The results of the LCOE for Kestrel e230i turbine at a height of 20m at each of the six locations is given in Table 4.5 below:

From the results of the LCOE analysis it can be seen that the lowest value for the LCOE is at the Cape Town Weather Office with a value of R 4.11/kWh. This is significantly above Cape Town's domestic electricity tariff for households that consume more than 600

kWh per month which stands at R 2.34/kWh (City of Cape Town, 2017). The LCOE analysis was also done for the Kestrel turbine but at a height of 30m above the ground, the LCOE value at the WO station decreased to R 3.49. This is because the turbine will generate more electricity at the higher height. Even at this higher height of 30m the LCOE of electricity generated from the turbine is still R 1.15 more than the cost of using electricity provided by the City of Cape Town.

For comparison, Lazard's Levelized Cost of Energy Analysis shows that Solar PV on residential rooftops is expected to cost between $0.138/kWh to $0.222/kWh or equivalently R 1.86/kWh to R 3.08/kWh (using the December 2016 exchange rate of R 13.71 to $ 1 and then correcting the December 2016 values to August 2017 Rand) (Lazard, 2016). These results show that electricity from small scale wind turbines is not cost competitive in the current South African market.

4.9 RESULTS SUMMARY

The summary of the overall results for all six stations and all four of the chosen turbines is shown in Table 4.6. The table shows the significant variation in nearly all of the parameters calculated. Across the six locations, the Kestrel turbine produced an average of 681.89 kWh/a with an average capacity factor of 10.1%, the SkyStream produced an average of 1813.29 kWh/a with a capacity factor of 8.53 %, the eddyGT produced 415.63 kWh/a and its capacity factor was 7.3%, and finally the Turby produced 1107.63 kWh/a with a capacity factor of 5.06%. The HAWTs performed better than their VAWT counterparts at every location despite the HAWTs having a smaller-rated capacity (the Kestrel had a rated capacity of 800W vs. the eddyGT's capacity of 1000W and the SkyStream had a capacity of 2400W vs. the Turby's 2500W). The key to the HAWTs better performance is their lower cut-in wind speed relative to the VAWTs. This allows the HAWTs to take better advantage of the low average wind speeds generally experienced in urban areas.

4.10 CHAPTER SUMMARY

This chapter has presented the results from the wind energy resource assessment carried out at each of the six location in and around Cape Town. The average wind speed at the six locations was 3.24 m/s with the highest average wind speed being recorded at the Cape Town WO station with 5.06 m/s and the lowest of 2.04 m/s at the Kirstenbosch station.

The wind energy resource at the stations varied substantially, from just 80 kWh/m²/a for the Kirstenbosch station to a high of 1474 kWh/m²/a at the Cape Town WO station. The average wind en-

Result	RCYC	Kir	AWS	Mol	Obs	WO
Average wind speed (m/s)	3.61	2.04	3.83	2.35	2.33	5.06
Energy potential (kWh/m²/a)	1181	80	610	189	145	1474
Kestrel AEP (kWh/a)	1224.5	19.2	982.3	259	199.49	1636.8
Kestrel Capacity Factor	0.172	0.003	0.14	0.036	0.028	0.229
SkyStream AEP (kWh/a)	3301.5	13.73	2401.9	518.2	339.55	4304.7
SkyStream Capacity Factor	0.155	0.001	0.11	0.024	0.016	0.203
eddyGT AEP (kWh/a)	784.7	4.331	523.9	119.96	85.27	975.5
eddyGT Capacity Factor	0.138	0.001	0.09	0.021	0.015	0.171
Turby AEP (kWh/a)	2406.5	0.659	1227.4	195.04	85.897	2730.3
Turby Capacity Factor	0.11	0	0.06	0.009	0.004	0.125

Table 4.6: Summary of results for the six stations

ergy resource potential for all six locations in this study is 613.12 kWh/m²/a.

Using the calculated wind energy resource potential, the Annual Energy Production for four different turbines was calculated for each of the six locations. These AEP values also varied drastically with the high of 4304 kWh/a being calculated for the SkyStream turbine at the WO station and a low of just 0.66 kWh/a being calculated at the Kirstenbosch station with the Turby turbine. In addition to the variation of the AEP values, the capacity factors for the four turbines varied significantly. The highest capacity factor recorded was 22.9 % which was achieved by the Kestrel turbine at the WO site and the lowest capacity factor was recorded at the Kirstenbosch site when the Turby turbine achieved a 0% capacity factor. The average capacity factor across the six locations for the Kestrel was 10.1%, for the SkyStream 8.53 %, for the eddyGT 7.3%, and for the Turby 5.1%.

Owing to the lower cut in wind speeds of the HAWTs, they performed better than their VAWTs counterparts. A low cut-in wind speed is therefore key in maximising the energy extracted from the urban wind regime which is generally characterised by low average wind speeds.

5

CONCLUSIONS AND RECOMMENDATIONS

The need to transition the global energy system away from its reliance on fossil fuels and towards the use of renewable energy technologies is discussed in Chapter 1 and Chapter 2. To this end, two of the dominant technologies for generating electricity from renewable sources are the use of Solar Photovoltaic (PV) panels and wind turbines. Recently, the importance of small-scale or urban wind energy has been discussed with several authors suggesting that urban wind energy may play a large role in meeting a portion of the urban electricity demand in the future. However, the knowledge surrounding the realisable potential of small-scale urban wind energy is sparse, especially in South Africa where there only one short-term study has been conducted (Brosius, 2009). The aim of this study was therefore to assess the wind energy resource potential for Cape Town. In order to achieve this aim, an existing methodology that was used to conduct wind energy resource assessments for large-scale wind energy applications was modified to better suit the small-scale wind energy sector. This methodology was then applied to six wind energy data sets which were recorded by the South African Weather Service at six different locations in the Cape Town Area. This methodology is presented in Chapter 3 of this study. The data sets were then analysed and the results of the analysis are presented in Chapter 4. This chapter distils these results into a number of conclusions and recommendations.

5.1 CONCLUSIONS

5.1.1 *Quantification of the urban wind potential in Cape Town*

The wind energy resource potential of six locations in Cape Town was quantified. Out of the six chosen locations in the Cape Town area, three of the locations (Royal Cape Yacht Club, the Automatic Weather Station (AWS), and the Cape Town Weather Office (WO)) initially showed potential for the installation of a small scale wind turbine, with the HAWTs having higher AEP values at each of the six locations compared to their VAWT counterparts. The results of the wind resource assessment are summarised in the table below. These three locations were situated in non-residential areas. The three locations that were situated in residential areas had much lower wind resource potential. This may be due to the increased number of obstructions (houses and trees) in residential areas when compared to the non-residential locations that were selected for this study.

Station	RMSE (m/s)	R^2
Royal Cape Yacht Club	0.03	0.85
Kirstenbosch Botanical Gardens	0.07	0.82
Automatic Weather Station	0.02	0.95
Molteno Reservoir	0.02	0.95
Astronomical Observatory	0.02	0.97
Cape Town Weather Office	0.01	0.97

Table 5.1: Selected $R^2$and RMSE results

The significant variability in the wind resource between locations was one of the main findings of this study. The conclusion that can be drawn from this finding is that the variability of the wind resource at the various locations hinders the wide-spread uptake of small-scale wind power as the results from one area cannot be reliably used to infer the wind resource potential at another nearby site. This was shown by the comparison of the results between the AWS and Cape Town WO station. These two stations are only separated by a distance of 1.9km but their average wind speeds varied by 24% and their wind energy resource potential varied by 58%. This fact calls for in depth, on-site wind resource

5.1.2 *Applicability of the Weibull distribution to the recorded wind speed data sets*

The Weibull probability density function can be used as an accurate representation of the wind speed distribution at a chosen location. This is in line with other findings from international studies which show that the Weibull probability density function can be a good representation of the wind regime at a chosen site. Two measures of the accuracy of the Weibull function were calculated for this study. These two measures were the Residual Mean Square Error (RMSE) and the coefficient of determinations (R^2). The calculated values of these two metrics are briefly shown in the table below. The RMSE values had a maximum of 0.07 m/s for the Kirstenbosch station and a minimum of 0.01 m/s for the Cape Town WO station. The Coefficient of Determination (R^2) values also show a similar result with the R^2 values ranging from a minimum of 0.82 at the Kirstenbosch site to 0.97 at the Cape Town WO site. Both of these measures proved that the calculated Weibull function accurately represented the wind data recorded at the various stations. These results are shown in 5.1

5.1.3 *Comparison of the different wind turbine types*

The two Horizontal Axis Wind Turbines (HAWTs) used in this study had higher Annual Energy Production (AEP) values than their Vertical Axis Wind Turbine (VAWT) counterparts in both electricity produced and capacity factors. This is shown in the Table below which highlights the AEP values for each of the four turbines at each location. The Kestrel e230i and the eddyGT AEP values are comparable as they are the two smaller turbines with similar rated outputs. Likewise, the SkyStream 3.7 and the Turby are comparable as they are the two larger turbines. The difference in the AEP values is possibly due to the lower cut in wind speeds of the HAWTs compared to the cut in wind speeds for the VAWTs and these cut in wind speeds are shown in Table below which also highlight the specifications of the various turbines.

This finding does not conclusively show that HAWTs are better suited to extracting energy from the urban wind regime in all situations but there is a clear trend to be seen from the results of this study. A low cut-in wind speed allows a turbine to start generating electricity at lower wind speeds and the urban wind regime is characterised by low wind speeds. This study used a wind turbine's annual energy production (AEP) as the sole criterion when judging the turbine's performance.

5.1.4 *Daily electricity generation*

The daily generation profile curves were developed for two locations over two separate days. This was done in order to evaluate at what times during the day a typical turbine is expected to generate electricity. The results from the Molteno reservoir and the Cape Town Weather office combined with the power curve of the Kestrel e230i turbine show that during the 21st of December 2016 the majority of the electricity generated by the turbine occurred during the day which closely matched Eskom's typical summer load profile. While the shape of the generation curve matched the Eskom summer load curve, the magnitude of electricity generated was not sufficiently large to recommend the installation of a turbine at these locations. The Cape Town WO station generated 4.4 kWh and the Molteno reservoir site generated 0.63 kWh during the 21st of December 2016.

During the 21st of June 2016 however, the generation curve at both of the locations did not resemble the typical Eskom winter load profile. The majority of the electricity generated at both these sites was in the early hours of the morning and both sites generated less than 1 kWh each. This section of the analysis further highlighted the variability of the wind resource potential not only between the two sites,

but also showed the seasonal and inter-day fluctuations of electricity generation.

5.1.5 *Impact of hub height on the expected energy production of a certain location*

A summary of the results from the sensitivity analysis that was conducted on the hub heights of the turbines at the Cape Town WO station is shown in the Table below. These results showed that increasing the hub height of the turbine will increase the expected energy production of a certain location. The relationship is also characterised by decreasing returns of wind speed relative to height. This finding is expected as it has been proven in other studies that the relationship between the wind speed and height above ground is positive with decreasing returns to wind speed relative to height. Therefore, there will be a height at which the advantages associated with a higher hub height are cancelled out by the disadvantages of a higher hub height (increased installation costs or increased regulatory requirements). It can thus be concluded that it is beneficial to install the urban wind turbine only as high as the point at which the disadvantages would begin to outweigh the advantages and no higher.

5.1.6 *Cost effectiveness of a small scale wind turbine in Cape Town*

The results from the Levelized Cost of Electricity (LCOE) analysis using the Kestrel e230i wind turbine show that electricity generated from small-scale wind turbines in Cape Town is not currently cost competitive. The lowest LCOE value for the Kestrel turbine with a hub height of 20m was R 4.11/kWh which is higher than the current domestic electricity tariff in Cape Town for households who use more than 600kWh per month which stands at R 2.34. The LCOE analysis was also done for the Kestrel turbine but at a height of 30m above the ground, the LCOE value at the WO station decreased to R 3.49. This is because the turbine will generate more electricity at the greater height. Even at this greater height of 30m, the LCOE of electricity generated from the turbine is still R 1.15 more than the cost of using electricity provided by the City of Cape Town.

5.2 RECOMMENDATIONS

5.2.1 *The need for on-site measurement*

The main recommendation of this study is that while there are undoubtedly locations where there is sufficiently high wind resource potential to consider the installation of a small-scale wind turbine, these locations require high quality on-site wind data recordings and

an appropriate wind resource assessment before any commitments to small-scale wind power are made. While these measurements are essential if the project is to be a success, they are often expensive and time-consuming to carry out. Therefore, any future study concerning urban wind energy should make use of detailed wind measurements taken at the particular location.

5.2.2 *Investigate different wind turbines*

This study illustrates the benefits of considering numerous different wind turbines once the wind resource assessment has been carried out. The energy output of the various turbines varies significantly at each of the six locations in this study. Other than energy output, other factors may influence the eventual choice of the turbine. These other factors could be the noise levels of the turbines during operation, consideration of the surrounding buildings, and the cost and availability of the various turbines in South Africa.

This study only used the AEP values to evaluate the various wind turbines. However it is recommended that, when deciding between wind turbines in a real-world assessment, other criteria should be included in the decision making process. These criteria may include: the cost of the turbines, the availability of the turbine in the country, the maintenance requirements of the turbine, as well of the relevant policy and regulatory environment governing the installation of a turbine at the chosen location.

5.2.3 *Increase the number of locations*

While this study chose six locations in the Cape Town area, more locations should be analysed in order to formulate a more detailed description of the urban wind energy regime in South Africa. Ideally, a pilot wind turbine project should be set up at one of the locations and the energy production of the pilot project could be compared against the results of a wind resource assessment. This would be informative as it would show the applicability of this methodology to results from the field. Already, the topic of the intense variability of the urban wind regime has been discussed in this study and, therefore, it may be interesting to examine whether this variability could have any further effects on results from an urban wind turbine.

5.2.4 *Comparison between small scale wind turbines and embedded solar PV*

Two of the most dominant technologies for residential scale-electricity generation are the use of small-scale wind turbines or the use of solar photovoltaic panels. Future research may compare the electricity out-

put of these two technology choices at various locations and conduct a detailed economic analysis as to which of the two technologies is the better technology for households to invest in at the moment.

5.2.5 *Verification of wind turbine power curves*

Further research could focus on the verification of the manufactures wind turbine power curves. These power curves form a critical part of the wind energy resource assessment and therefore, it is essential that the wind turbine power curves accurately reflect the on-site performance of the wind turbine.

5.2.6 *Investigate the policy environment surrounding urban wind energy*

This study has shown that the technical potential for urban wind turbines exists at certain locations in the Cape Town area. The next stage of the research into the slow uptake of small-scale wind turbines should thus focus on the existence of governmental policies which may hinder or incentivise the uptake of small-scale wind power.

6

REFERENCES

Ayodele, T., Jimoh, A., Munda, J. & Agee, J. 2012. Statistical analysis of wind speed and wind power potential of Port Elizabeth using Weibull parameters. *Journal of Energy in Southern Africa*. 23(2) 30-39.

Barnston, A. 1992. *Correspondence among the correlation, RMSE, and Heidke Forecast Verification Measures; Refinement of the Heidke Score*. Climate Analysis Centre, Washington D.C, United States of America.

Brosius, W. 2009. *Feasibility study of wind power at SAB Newlands.* MEng Thesis. University of Stellenbosch, Stellenbosch, South Africa.

Brower, M. 2012. *Wind Resource Assessment: A Practical Guide to Developing a Wind Project*. New Jersey, United States of America: John Wiley & Sons.

Bukala, J., Damaziak, K., Kroszczynski, K., Krzeszowiec, M., Malachowski, J. 2015. Investigation of parameters influencing the efficiency of small wind turbines. *Journal of Wind Engineering and Industrial Aerodynamic*s. 146 29-38.

Carpman, N. 2011. *Turbulence Intensity in Complex Environments and its Influence on Small Wind Turbines*. Uppsala University, Uppsala, Sweden.

Celik, A. 2002. Energy output estimation for small-scale wind power generators using Weibull representative wind data. *Journal of Wind Engineering and Industrial Aerodynamics*. 91 (2003) 693-707.

Çengel, Y & Cimbala, J. 2006. *Fluid Mechanics: Fundamentals and Applications*. New York, United States of America: McGraw-Hill.

Centre for Scientific and Industrial Research. 2016. *Wind and Solar PV Resource Aggregation Study for South Africa*. Centre for Scientific and Industrial Research, Pretoria, South Africa

Chen, C., Kuo, C., & Miao, J. 2011. What Happens to the Betz Limit in VAWT System? National Chung Hsing University, Taiwan.

Chiras, D., Sagrillo, M., Woofenden, I. 2009. *Power from the Wind: Achieving Energy Independence*. New Society Publishers, Gabriola Island, Canada.

City of Cape Town, 2017. *The Cost of Residential Electricity*. Available: http://www.capetown.gov.za/Family%20and%20home/residential-utility-services/residential- electricity-services/the-cost-of-residential-electricity [August 24 2017]

Department of Energy, 2016. *Integrated Resource Plan Update- Assumptions, Base Case Results and Observations-Revision 1*. Department of Energy: Pretoria, South Africa.

Dick, E. 2015. *Fundamentals of Turbo Machines*. Dordrect, Netherlands: Springer.

Dorvlo, A. 2002. Estimating wind speed distribution. *Energy Conversion Management* (43) 2311-2318.

Eberhard, A., Kolker, J. & Leigland, J. 2014. *South Africa's Renewable Energy IPP Procurement program: Success Factors and Lessons*. Public-Private Infrastructure Advisory Facility: World Bank Group. Washington D.C, United States of America.

Elliott, D. & Infield, D. 2014. An assessment of the impact of reduced averaging time on small wind turbine power curves, energy capture predictions and turbulence intensity measurements. *Wind Energy* 17(2) 337–342.

Energy blog. 2017. *Project Database*. Available: http://www.energy.org.za/knowledge-tools/project- database/ [March 28 2017]

Energy Information Administration. 2017. *Levelized Cost and Levelized Avoided Cost of New Generation Resources in the Annual Energy Outlook 2017.* Energy Information Administration: Washington D.C, United States of America

Energy Savings Trust. 2009. *Location, location, location: Domestic small-scale wind field trial report*. Energy Savings Trust, London, United Kingdom.

Fant, C., Gunturu, B., & Schlosser, A. 2015. Characterising wind power resource in Southern Africa. *Applied Energy*. 161(2016) 565-573

Fields, J., Oteri, F., Preus, R. & Baring-Gould, I. 2016. *Deployment of Wind Turbines in the Built Environment: Risks, Lessons, and Recommended Practices*. National Renewable Energy Laboratory, Denver, United States of America.

Gipe, P. 2008. AeroVironment's AVX 1000 Rooftop Turbines at Logan Airport. Available: http://www.windworks.org/cms/index.php?id=64&tx_ttnews%5Btt_news%5D=122&cHash=cbb ca4dfeebd12cbeea51940331592d9 [2 April 2017].

Global Wind Energy Council. 2016. Global cumulative Installed Wind Capacity. Available: http://www.gwec.net/wp-content/uploads/vip/GWEC_PRstats2016_EN_WEB.pdf [March 28 2017]

Graul, C. & Poppinga, C. 2015. *bReeze: Functions for Wind Resource Assessment*. R package version 0.4. Avalable: http://cran.r-project.org/package=bReeze. [05 May 2017].

Green Ideas. 2010. *Horizontal Axis Wind Turbines*. Available: http://verticalaxiswindturbines.blogspot.co.za/2010/10/how-efficient-are-vertical-axis-wind.htmlhttp://www.turbinesinfo.com/horizontal-axis-wind-turbines-hawt/ [April 01 2017].

Grieser, B., Sunak, Y. & Madlener, R. 2015. Economics of small wind turbines in urban settings: An empirical investigation for Germany. *Renewable Energy*. 78(2015) 334-350.

Hagemann, K. 2008. *Mesoscale Wind Atlas of South Africa*. PhD thesis, University of Cape Town, South Africa.

International Electrotechnical Commission. 2013. IEC 61400-2 Part 2: Small Wind Turbines. Geneva, Switzerland.

Ishugah, T., Li, Y., Wang, R. & Kiplagat. J. 2014. Advances in wind energy resource exploitation in urban environment: A review. *Renewable and Sustainable Energy Reviews*. 37(2014) 613-626

Justus, C., Hargraves, W., Mikhail, A. & Graber, D. 1978. Methods for estimating wind speed frequency distributions. Journal of Applied Meteorology (17) 350-353.

Justus, C., Mikhail, A. 1976. Height variation of wind speed and wind distribution statistics. *Geophysics Research Letters*. (3) 261-264.

Kalmikov, A., DuPont, G., Dykes, K. & Chan, C. *Wind power resource assessment in complex urban environments. MIT campus case-study using CFD analysis.* American wind Energy Association 2010 Wind Power Conference, 2010, 1-28.

Karthikeya, B., Prabal, S. & Srikanth, N. 2015. Wind resource assessment for urban renewable energy application in Singapore. *Renewable Energy*. 87(2016) 403-414.

Khalfa, D., Benretem, A., Herous, L. & Meghlaoui, I. 2014. Evaluation of the adequacy of the Wind speed extrapolation laws for two different roughness meteorological sites. *American Journal of Applied Sciences*. 11(4) 570-583

Lack, C. 2010. *Urban Wind Turbines*. MSc Thesis. Universitat Politècnica de Catalunya, Spain.

Lazard. 2016. Lazard's Levelized Cost of Energy Analysis- Version 10. Lazard, Hamilton, Bermuda

Ledo, L. Kosasih, P. & Cooper, P. Roof mounting site analysis for micro-wind turbines. *Renewable Energy* 36(2011) 1379- 1391.

Li, Q., Shu, Z. & Chen, F. 2016. Performance assessment of tall building-integrated wind turbines for power generation. *Applied Energy.* 165(2016) 777-788.

Ling, M. 2012. Pearl River Tower. Available: http://wind.psu.edu/research /building-integrated-wind- energy/database [2 April 2017].

Manwell, J., McGowan, J. & Rogers, A. 2010. *Wind Energy Explained: Theory, Design and Application*. 2nd edition. John Wiley & Sons, Chichester, United Kingdom.

Markham, D. 2014. This tiny portable wind turbine fits in your bag and charges your gadgets. Available: http://www.treehugger.com/wind-technology/tiny-portable-vertical-wind-turbine.html [April 01 2017]

Matona, T. 2014. Power System Status Update. Eskom, Johannesburg, South Africa.

Mithraratne, N. 2009. Roof-top wind turbines for microgeneration in urban houses in New Zealand. *Energy and Buildings*. 41 1013-1018.

New York State Energy Research Development Authority. 2010. Wind Resource Assessment Handbook. New York State Energy Research Development Authority, Albany, New York, United States of America.

Pagnini, L., Burlando, M. & Repetto, M. 2015. Experimental power curve of small-size wind turbines in turbulent urban environment. *Applied Energy*. 154 112-121.

Pishgar-Komleh, S., Keyhani, A. & Sefeedpari, P. 2015. Wind speed and power density analysis based on Weibull and Rayleigh distributions (a case study: Firouzkooh county of Iran). *Renewable and Sustainable Energy Reviews*. 42. 313-322

Pitteloud, J. & Gsänger, S. 2016. 2016 Small Wind world Report. World Wind Energy Association, Bonn, Germany

R Development Core Team. 2008. R: A language and environment for statistical computing. R foundation for Statistical Computing, Vienna, Austria Available: http://www.R-project.org. [05 May 2017].

Raftery, P., LeBlanc, M., Manning, J., 2004. WASP Validation of Forestry Effects. Proceedings of British Wind Energy Association Workshop on the Influence of Trees on Wind Farm Energy Yields. Glasgow, United Kingdom

Ragheb, M. 2017. Wind Shear, Roughness Classes and Turbine Energy Production. University of Illinois at Urbana-Champaign, Illinois, United States of America.

Ray, M., Rogers, A., & McGowan, J. 2006. *Analysis of wind shear models and trends in different terrains*. University of Massachusetts, Massachusetts, United States of America.

Schelmetic, T. 2013. Manufacturers, Researchers Quest for a Workable, Large-Scale Vertical Axis Wind Turbine. Available: http://news.

thomasnet.com/imt/2013/02/12/the-quest-for-a-workable- large-scale-vertical-axis-wind-turbine

[April 01 2017]

Seguro, J. & Lambert, T. 2002 Modern estimation of the parameters of the Weibull wind speed distribution for wind energy analysis. *Journal of Wind Engineering and Industrial Aerodynamics* (85) 75-84.

Simões, T. & Estanqueiro, A. 2015. A new methodology for urban wind resource assessment. *Renewable Energy*. 89(2016) 598-605.

Skyscraper City. 2015. Bahrain World Trade Centre. Available: http://

www.skyscrapercity.com/ showthread.php?t=1551469&page=64 [2 April 2017].

South African National Energy Development Institute (SANEDI). 2015. WASA: The Wind Atlas for South Africa. Phase 1. South African National Energy Development Institute, Sandton, South Africa.

South African Weather Service. 2017. Verification, Conformance and Maintenance reports for various weather stations. South African Weather Service, Pretoria, South Africa.

Stevens, M. & Smulders, P. 1979. The estimation of the parameters of the Weibull wind speed distribution for wind energy utilization purposes. *Wind Engineering* (3) 132-145.

Tippmann, S. 2014. Programming tools: Adventures with R. *Nature* 517 (109-110).

Th¨nnißen, F., Marnett, M., Roidl, B., & Schr¨der, W. 2016. A numerical analysis to evaluate Betz's Law for vertical axis wind turbines. *Journal of Physics: Conference Series* 753 (2016) 022056

Tummala, A., Velamati, R., Sinha, D. & Krishna, V. 2015. A review on small-scale wind turbines. *Renewable and Sustainable Energy Reviews*. 56(2016) 1351-1371.

Turbinesinfo. 2010. Vertical Axis Wind Turbine Information. Available: http://www.turbinesinfo.com/horizontal-axis-wind-turbines-hawt/. [April 01 2017]

United States Department of Energy. 2013. Levelized Cost of Energy. Department of Energy, Washington D.C, United States of America.

Usta, I. 2016. An innovative estimation method regarding Weibull parameters for wind energy applications. *Energy*. 106(2016) 301-314

Wais, P. 2017. A review of Weibull functions in wind sector. *Renewable and Sustainable Energy Reviews*. 70 1099-1107.

Wind Power Program. 2017. Wind Turbine Database-May 2017. Available: http://www.wind-power- program.com/download.htm#database. [August 22 2017]

Yang, A., Su, Y., Wen, C., Juan, Y., Wand, W. & Cheng, C. Estimation of wind power generation in dense urban area. *Applied Energy* 171(2016) 213-230.

7 APPENDIX

7.1 APPENDIX A: ADDITIONAL RESULTS FROM THE WIND RESOURCE ASSESSMENT

The results presented here are additional results from the wind resource assessment carried out at each of the six locations using the bReeze package.

7.1.1 *Royal Cape Yacht Club*

Figure 7.1 shows the wind speed variation for the station located at the RCY for the entire two-year period. It can be clear to see the wide variation of the wind speed experienced at the station with values ranging from 0m/s to speeds of approximately 20m/s. The seasonal effects on the wind speed can also be seen from Figure 7.1 with the three peaks (far left, middle, and far right of the graph) reflecting the summer season in Cape Town and the two troughs represent the winter months in Cape Town. The average wind speed at this station is higher during the summer months.

Figure 7.2, shows the wind direction variation experienced at the station from January 2015 through to December 2016. Figure 7.2 highlights the variation in wind direction with the wind blowing from all directions throughout the period and there is no clear prevailing wind direction at this station.

Figure 7.3 continues to highlight the variability in the wind direction by presenting the Turbulence Intensity (TI) of the wind at the RCY. Once again the values range considerably from near 0% to the extreme values of near 1400% but the majority of the values lie between 50% and 400%.

Figure 7.4 shows the distribution of the wind speeds recorded at the RCY Club. From the figure it can be seen that 50% of the wind speeds are below 2m/s and 68% of the wind speeds are below 4m/s.

The final result from the data obtained at the Royal Cape Yacht Club is Figure 7.5 which is a polar plot of the wind data. This plot is similar to the wind rose which was depicted in Figure 4.1 however, while the wind rose plotted the frequencies of the wind speed and wind direction, the polar plot graphs each data point with its corresponding wind speed and wind direction. The darker clustering of the data points show which wind speed and wind direction are most likely to occur. Again the prevailing wind direction is south and the large majority of data points are between 0 and 15m/s.

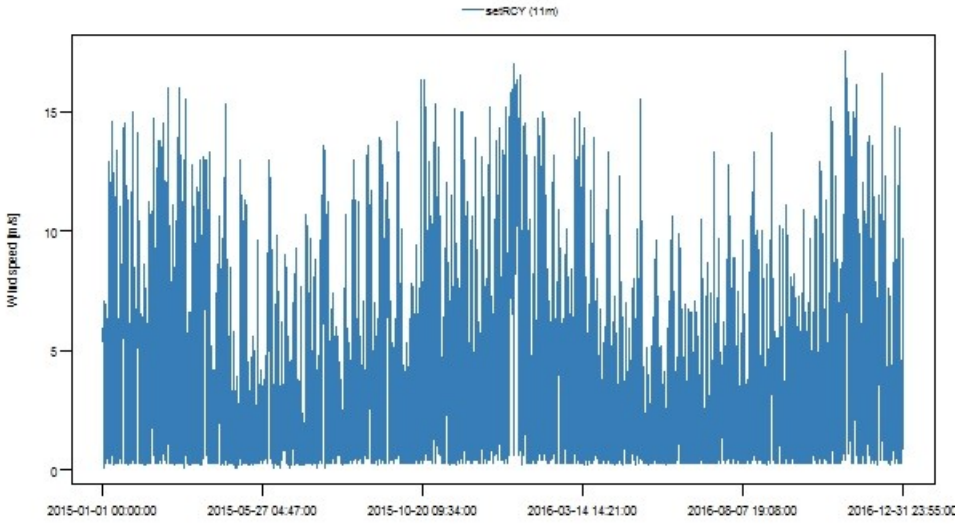

Figure 7.1: Wind speed variation for Royal Cape Yacht Club

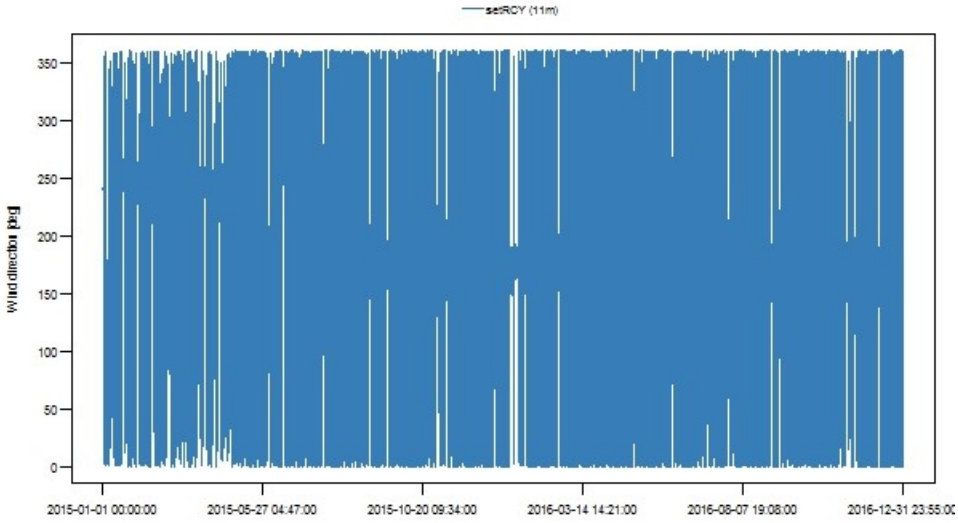

Figure 7.2: Wind direction variation at the Royal Cape Yacht Club

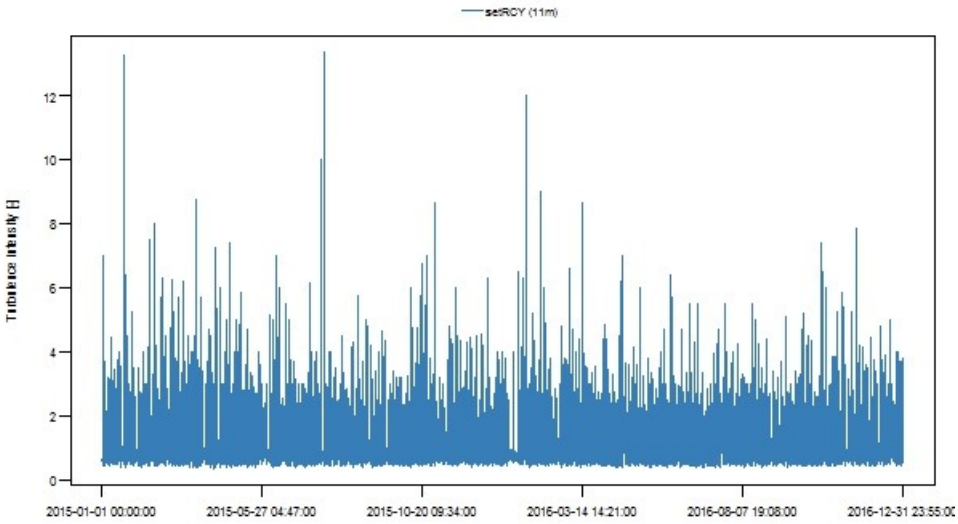

Figure 7.3: Turbulence intensity at the Royal Cape Yacht Club

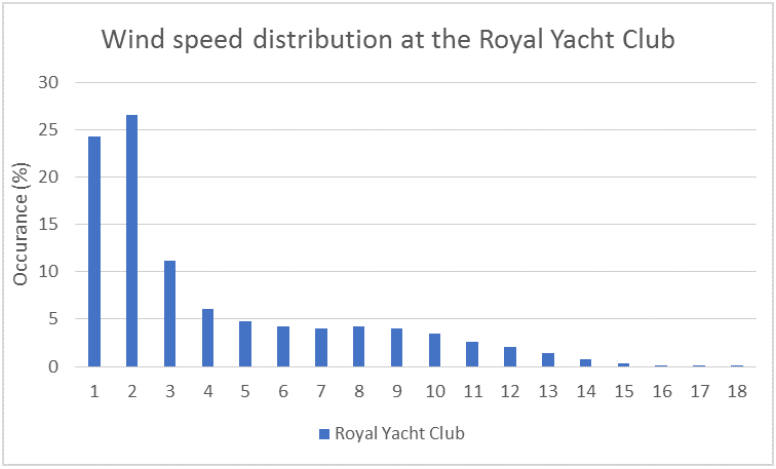

Figure 7.4: Royal Cape Yacht Club wind speed distribution

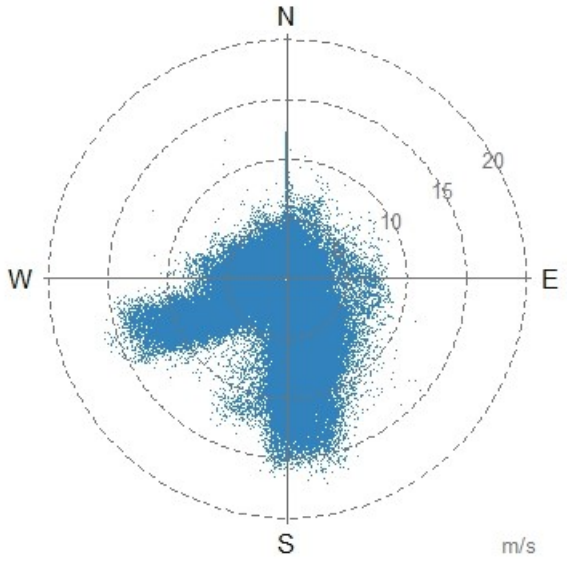

Figure 7.5: Polar plot for the Royal Cape Yacht Club

7.1.2 *Kirstenbosch*

The wind speed variation for the Kirstenbosch station is shown in Figure 7.6. This figure shows that the majority of the wind speeds recorded at this station lie within the 0-4m/s range with very few wind speeds over 8m/s being recorded over the two year period. There also does not seem to be any significant seasonal fluctuations occurring during the period.

The variations in the wind direction of the data from the Kirstenbosch station are shown in Figure 7.7. A large portion of the wind is coming from a range of 150°-300° measured clockwise from north. Again the wind direction varied significantly throughout the recording period.

The measure of the turbulence intensity at the Kirstenbosch station also reflects this variability of the wind direction as is shown in Figure 7.8. The values for the turbulence intensity lie mostly in the range of 50-300%.

At the Kirstenbosch station 98.68% of the recorded wind speed data was in the 0-5m/s wind speed bin, 1.3% of the data was in the 5-10m/s bin while the remaining 0.02% of the data fell in the 10-15m/s bin. Figure 7.9 shows the wind speed distribution for the Kirstenbosch site. From the figure it can be seen that just under 90% of all wind speeds recorded at this station are below 3m/s which is approximately the cut in wind speeds

The polar plot of the data from the Kirstenbosch station is shown in Figure 7.10. This figure plots each data point in terms of wind speed and wind direction for the entire two year period. From the figure, the low wind speeds recorded at the Kirstenbosch station are clear to

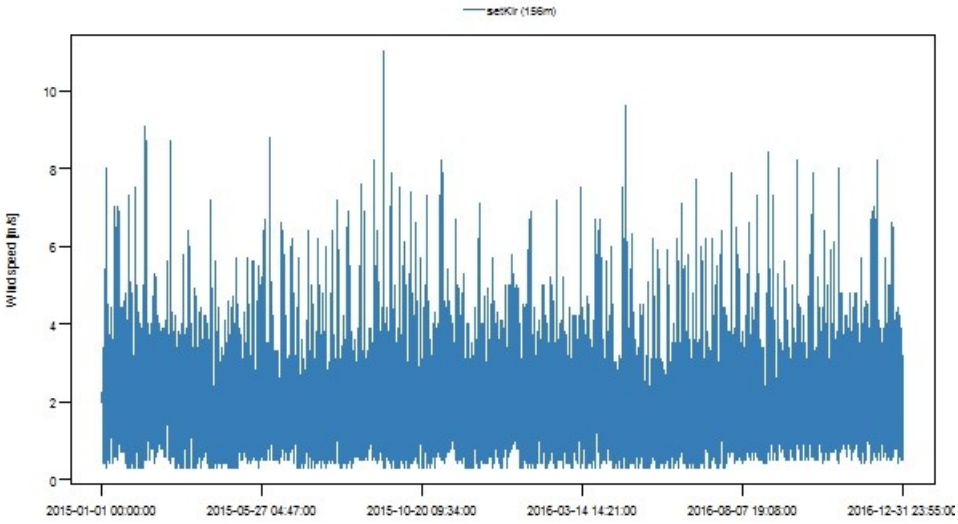

Figure 7.6: Wind speed variation for the Kirstenbosch station

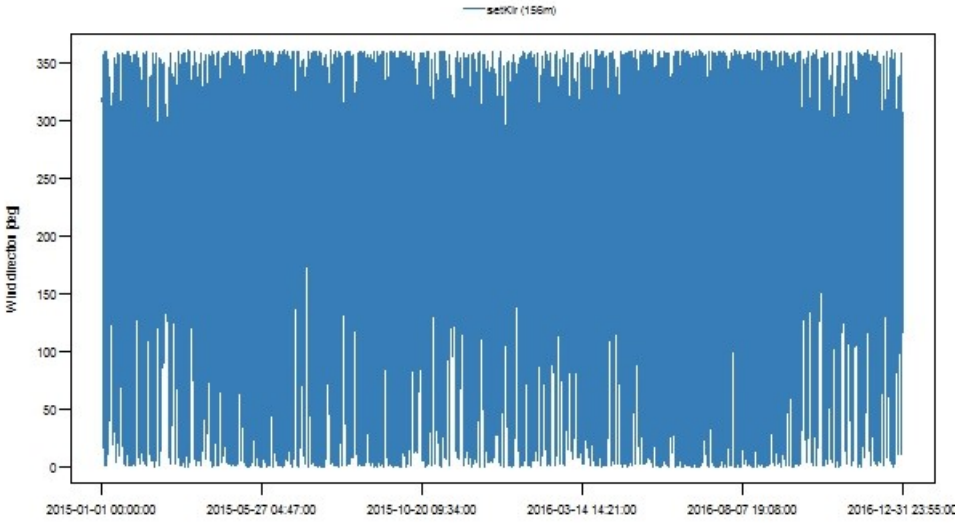

Figure 7.7: Wind direction variation at the Kirstenbosch recording station

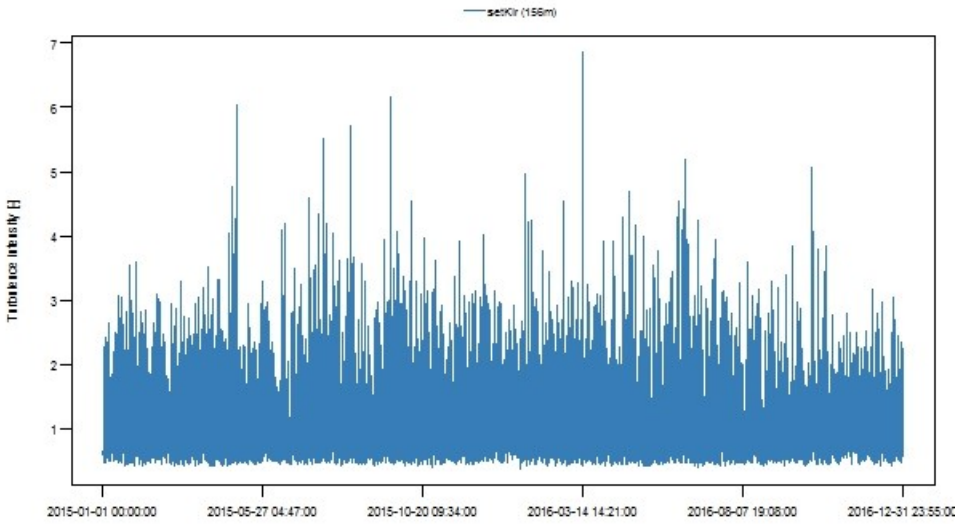

Figure 7.8: Turbulence intensity for the Kirstenbosch station

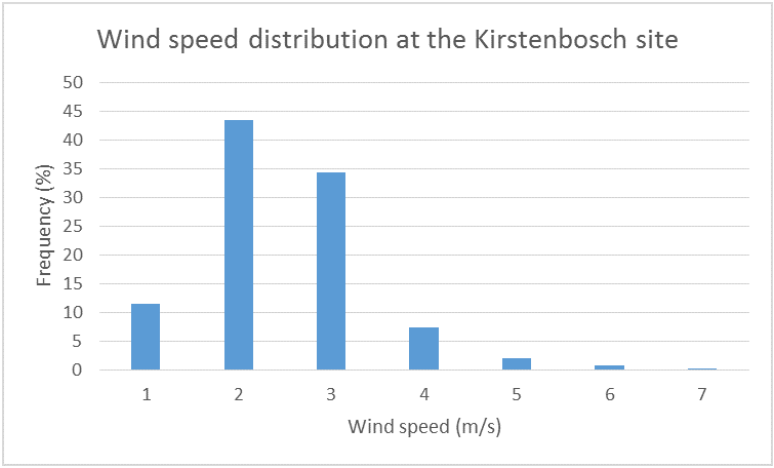

Figure 7.9: Kirstenbosch wind speed distribution

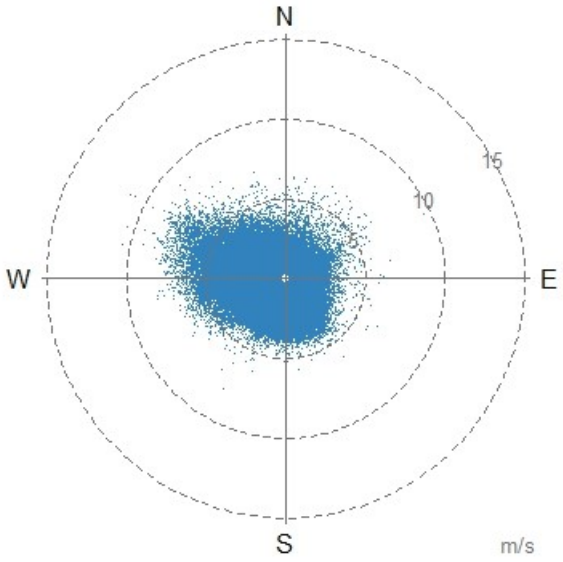

Figure 7.10: Polar plot for the Kirstenbosch station

see. This causes the Kirstenbosch station to have a low wind resource potential and therefore, it may not be economically viable to install a wind turbine at this location.

7.1.3 *Automatic Weather station*

The wind speed data recorded for the AWS station over the two year period is shown in Figure 7.11 below. In the figure the large range of wind speeds is evident, as the values range from 0m/s to nearly 14m/s. The majority of the data lies in the range between 2 and 8m/s. There is evidence of seasonal fluctuations in the wind data as there are slightly lower average wind speeds recorded in the winter months when compared to the summer months.

The variation in the wind direction is shown in Figure 7.12. The majority of the wind blows from between 100° and 250° clockwise from North, or in other words the wind blows mostly from the South.

The variability of the wind regime is further shown in Figure 7.13 which shows the Turbulence Intensity of the data recorded at the AWS station. The vast majority of the wind speeds have a TI of between 0% and 200% with some extreme values present which approach a TI of 600% in some cases.

Figure 7.14 shows the wind speed distribution for the AWS station over the two year period for wind speed bins of 1m/s. 57.6% of the wind speed data recorded was below 4m/s and a total of 91% of the data was below 7m/s.

The final plot that uses the AWS data is the polar plot and it is shown in Figure 7.15. This plot is similar to the wind rose which was depicted in Figure 4.10 however, while the wind rose plotted

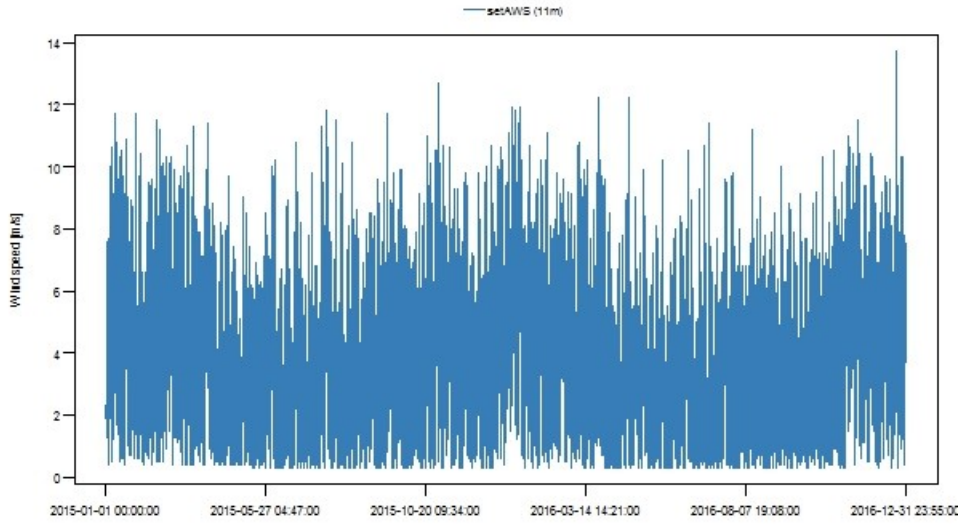

Figure 7.11: Wind speed measurements for the AWS station

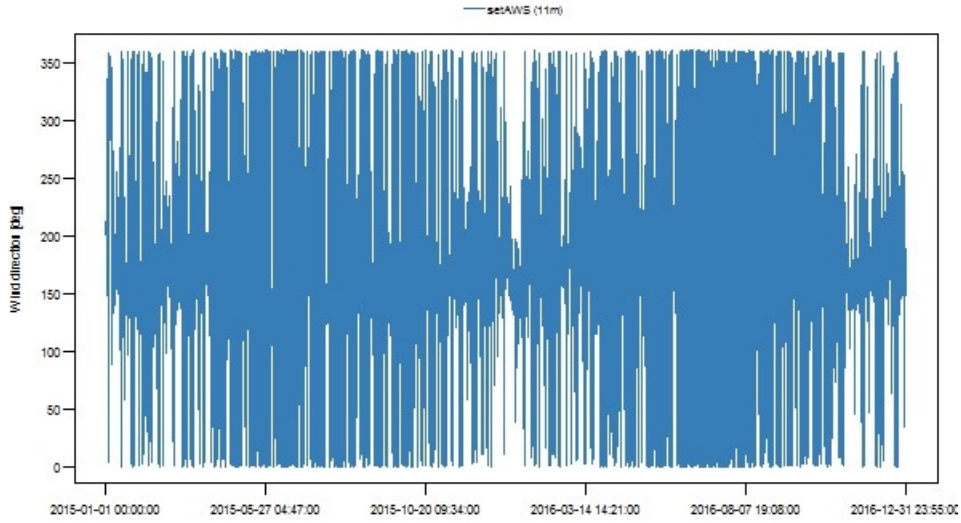

Figure 7.12: Wind direction variation for the AWS station

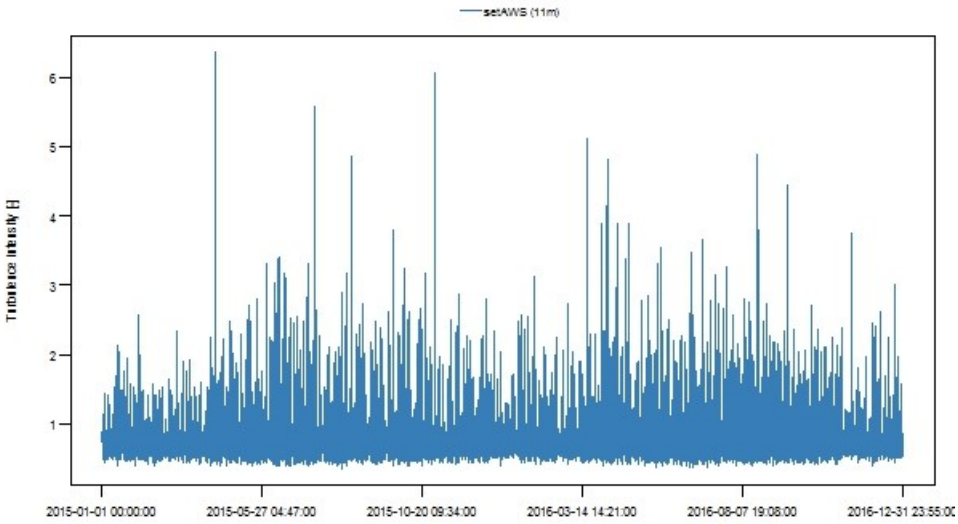

Figure 7.13: Turbulence Intensity for the AWS station

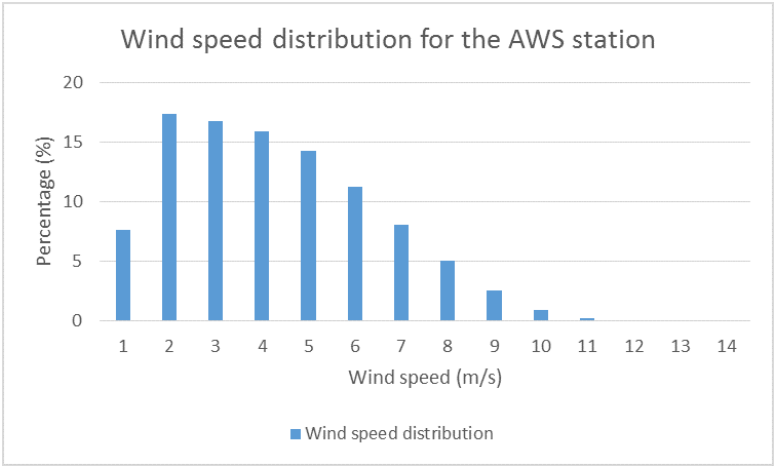

Figure 7.14: Automatic Weather Station wind speed distribution

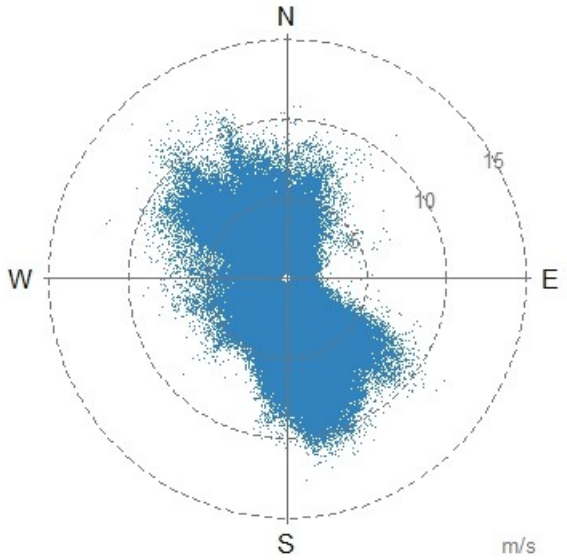

Figure 7.15: Polar plot for the AWS data

the frequencies of the wind speed and wind direction, the polar plot plots each data point with its corresponding wind speed and wind direction. The darker clustering of the data points show which wind speed and wind direction are most likely to occur. Again the prevailing wind is South and the majority of the data points fall between 0 and 10m/s.

7.1.4 *Molteno Reservoir*

The wind speed variation experienced at the site is shown in Figure 7.16. There is a slight seasonal variation in the wind speeds recorded, with the lower wind speeds being experienced in the winter months while the summer months experience higher average wind speeds. There is quite a large range of recorded wind speeds with the majority of recordings lying in the 0-5m/s range.

The next figure, Figure 7.17, shows the variation in the wind direction for the data recorded at the Molteno site for the two year period. There is significant variation in the wind direction with the majority of days experiencing wind from all directions. This may increase the turbulence around the recording station and lead to increased maintenance of the wind turbine should one be installed.

Showing further evidence of the large turbulence experienced at the Molteno reservoir site is Figure 7.18 which displays the Turbulence Intensity (TI) for the site over the entire recording period. The TI values for the majority of the recordings lie in the range of between 30% and 240%.

Figure 7.19 shows the wind speed distribution for the data recorded at the Molteno reservoir. The figure plots all values that occur that are

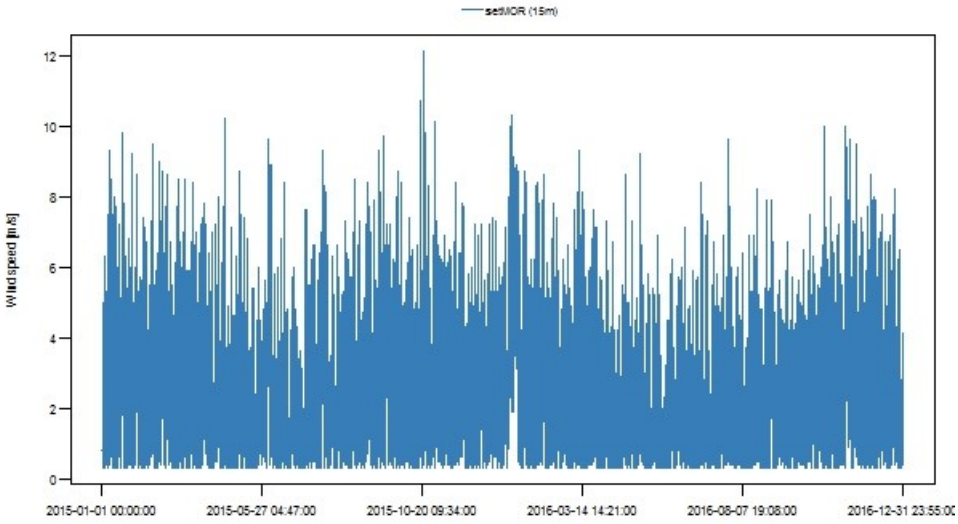

Figure 7.16: Wind speed variation at the Molteno reservoir site

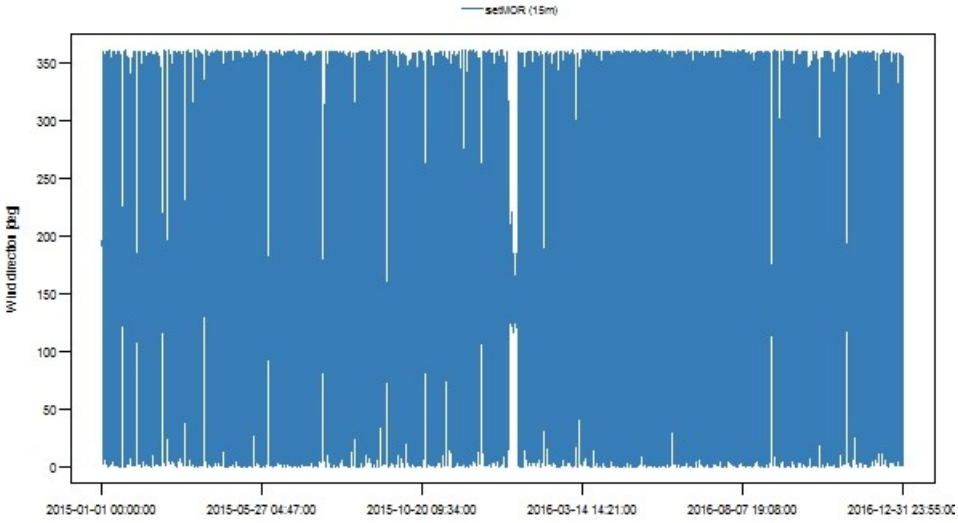

Figure 7.17: Wind direction variation for the Molteno reservoir

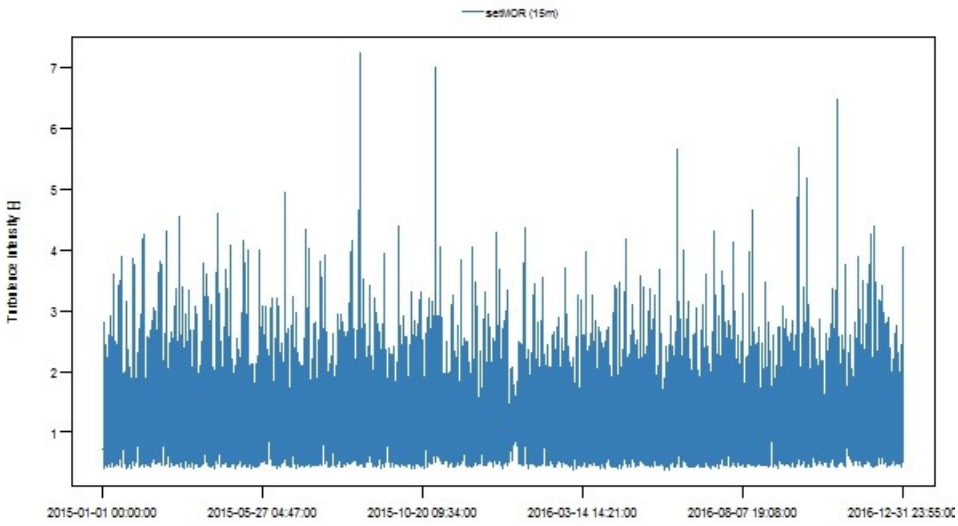

Figure 7.18: Turbulence Intensity for the Molteno reservoir

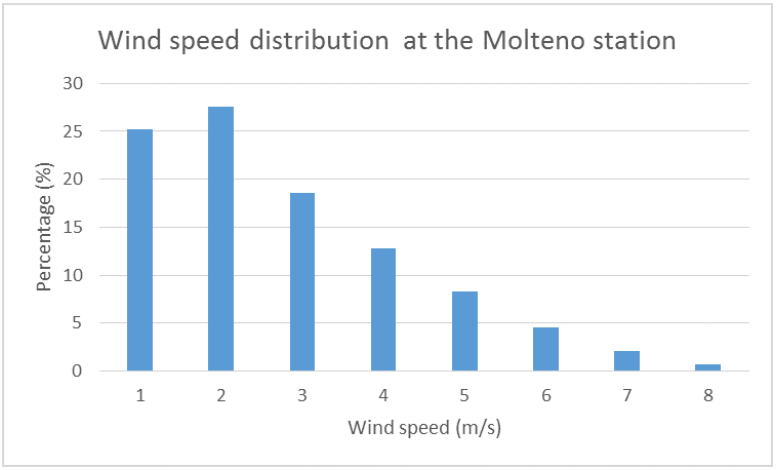

Figure 7.19: Molteno reservoir wind speed variation

lower than the wind speed bin. For example, the blue column corresponding to the 1m/s wind speed bin shows all the values that occur in the data that are between 0m/s and 1m/s. Using Figure 7.19, one can see that 71% of the wind speed data recorded had a speed of less than 3m/s which is lower than some of the wind turbine cut in speeds used in this study.

The polar plot for the Molteno site is shown in Figure 7.20. The figure shows that the vast majority of data falls in the 0-5m/s wind speed bin and thus this site will have a low wind energy resource potential.

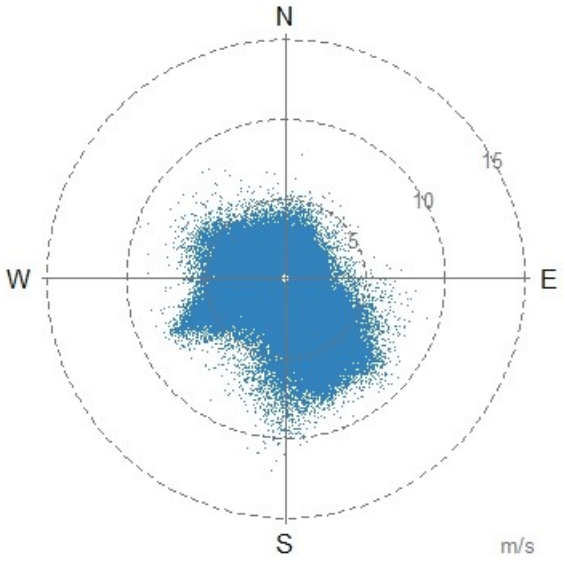

Figure 7.20: Polar plot for the Molteno reservoir

7.1.5 *South African Astronomical Observatory*

Figure 7.21 shows the wind speed variation for the station overt the two year recording period. The wind speeds vary from 0-6m/s and there is no wind speed that is above 8m/s. The seasonal effects of lower wind speeds during winter is visible from the data in Figure 7.21.

Figure 7.22 shows the wind direction variation that is present in the Observatory station data set. From the figure, there is a clear band between approximately 130° to 200° where the majority of the wind is coming from. This is consistent with the prevailing wind being from a southerly direction.

The next figure, Figure 7.23, shows the calculated Turbulence Intensity for the data observed at the Observatory station. In the first few months of 2015 there was significant variation in the turbulence but after around May 2015, the variation became less pronounced. After the initial wide range of TI values that were experienced in early 2015, the majority of the TI values lie in the 30% to 180% region.

The distribution of the wind speeds recorded at the Observatory station are shown in Figure 7.24. From the graph, 84% of the wind speeds recorded at the observatory are below 4m/s. This is an issue as many of the small scale wind turbines have a cut in wind speed near 4m/s. This means that the urban wind resource will be very limited for this station.

The final result to come from the Observatory data set is a polar plot of the data set which is shown in Figure 7.25. This figure plots each data point with its corresponding wind speed and wind direction to give an overall view of the wind regime at the station. Again

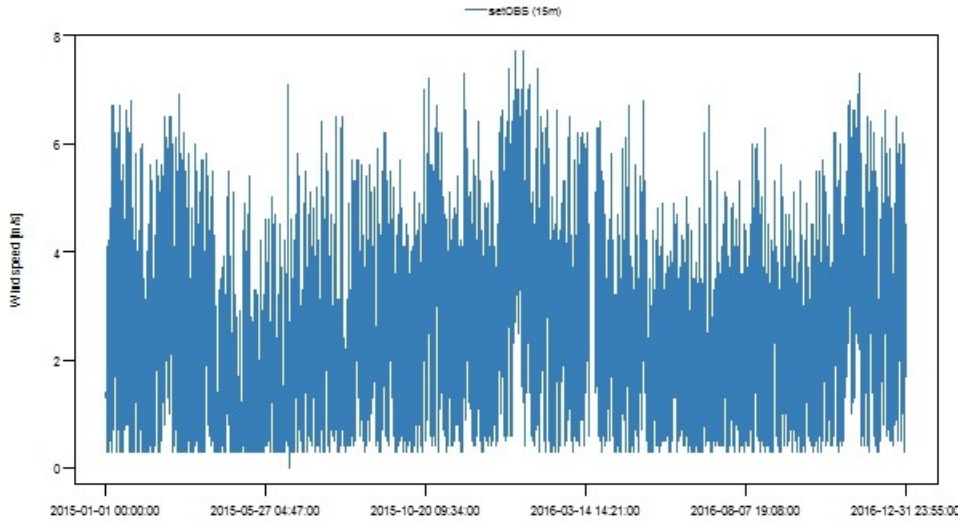

Figure 7.21: Wind speed variation for the Observatory station

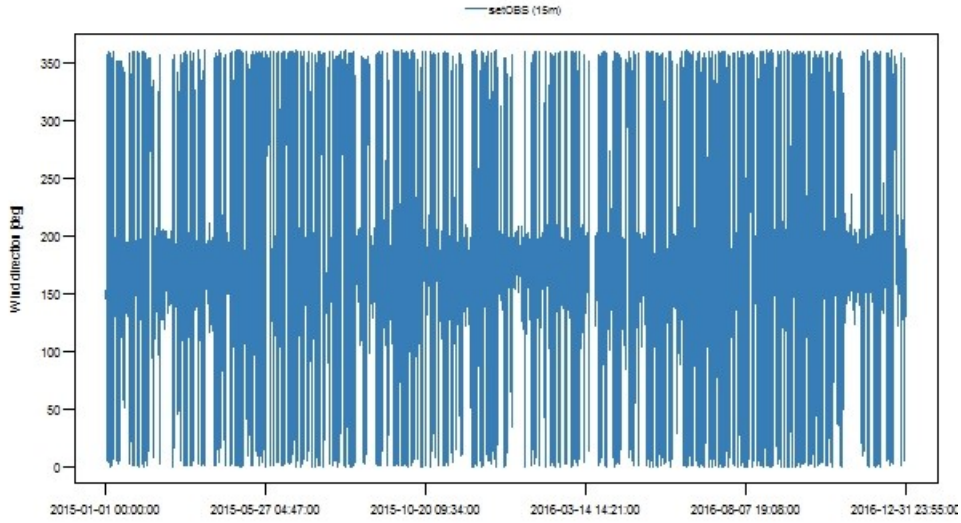

Figure 7.22: Wind direction variation for the Observatory station

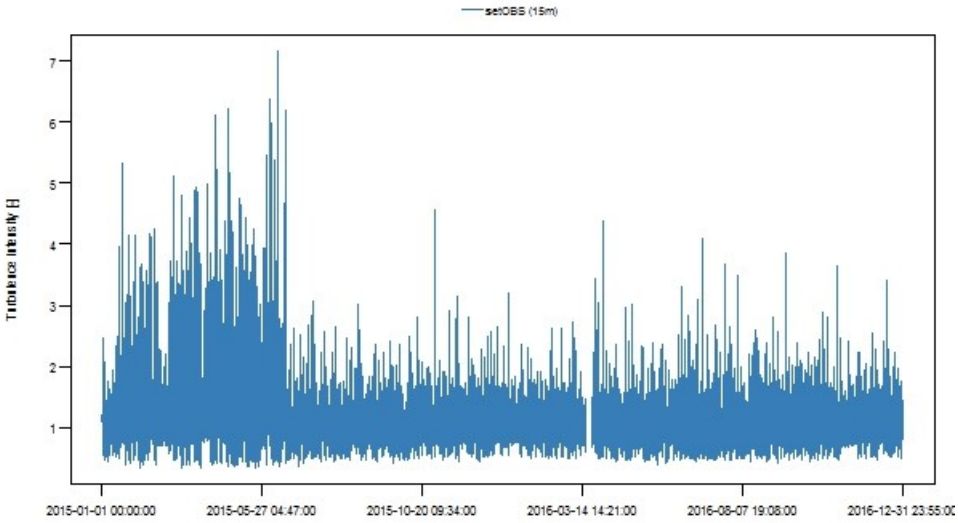

Figure 7.23: Turbulence Intensity for the Observatory station

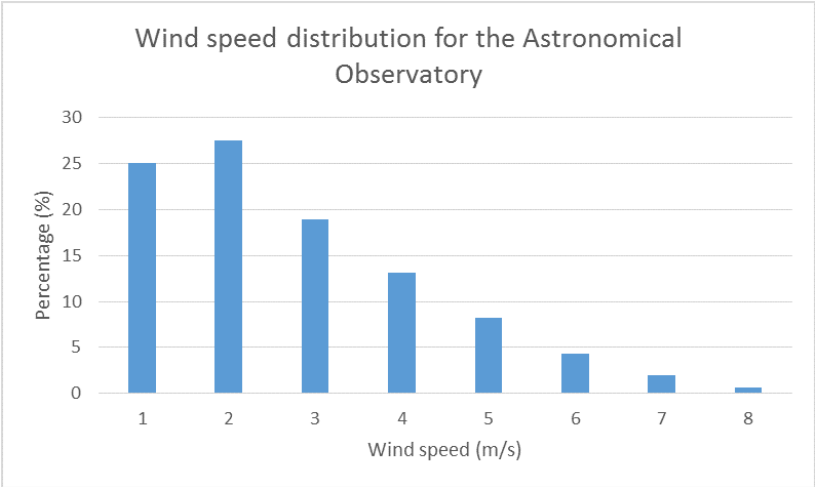

Figure 7.24: Astronomical Observatory wind speed distribution

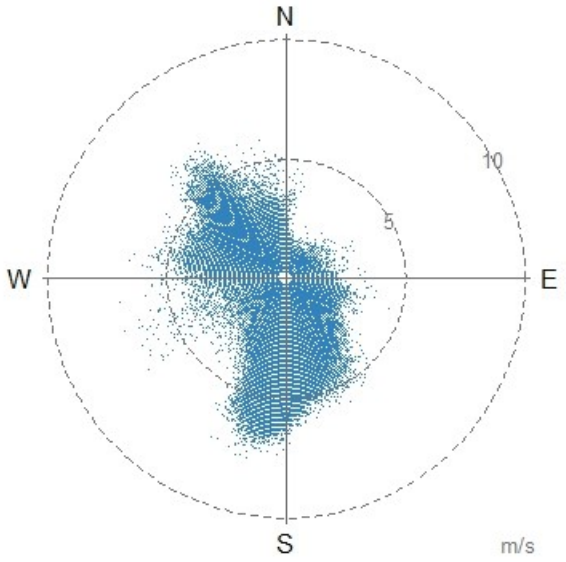

Figure 7.25: Polar plot for the Observatory station

the prevailing wind is from a southerly direction and the majority of the data points are below 5m/s.

7.1.6 *Cape Town Weather Office*

Figure 7.26 shows the wind speeds recorded at the WO station for the entire two year period. In the figure there is evidence of the seasonal fluctuations in the wind speed with lower wind speeds generally experienced in the winter months and higher wind speeds in the summer months. There are numerous occasions where the wind speed is above 10m/s which is a good indication that the site possess a high wind energy resource potential.

The next figure, Figure 7.27, shows the wind direction variation experienced at the WO station over the study period. Generally the wind comes from a direction between 130° and 230° from North which indicates that the prevailing wind comes from a southerly direction.

Evidence of the turbulence experienced at the WO station is shown by Figure 7.28 which highlights the Turbulence Intensity (TI) values for the station across the two year recording period. Apart from high outlying values, the TI values are mostly in the range of 30% to 200%.

Another graph of the wind speed distribution is shown by Figure 7.29 which shows the wind speed probability distribution for the data recorded at the WO station. There is an exceptionally good spread of wind speeds at this station with 51% of the wind speeds having a value of between 4m/s and 10m/s which is above the cut in speeds for a number of small scale wind turbines.

The final result from the WO data set is the polar plot of wind speed and wind direction over the two year period and is shown in

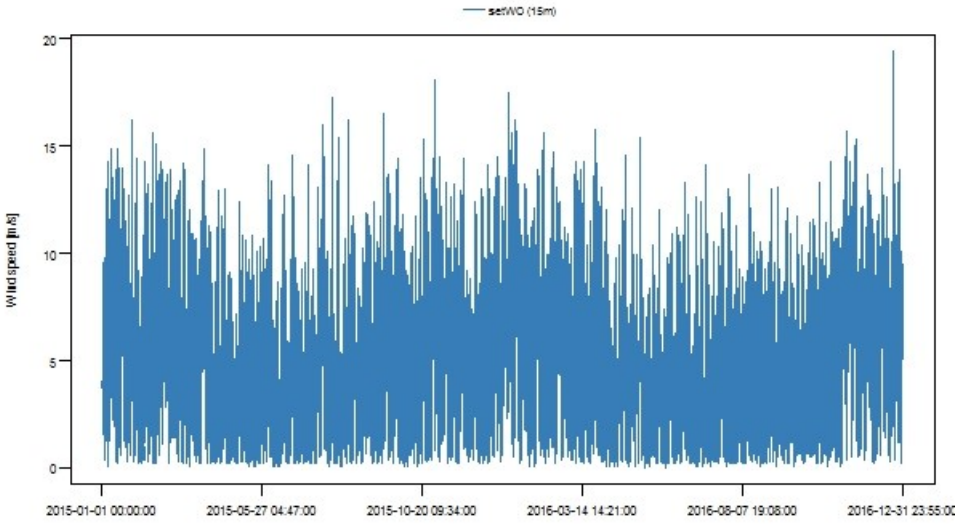

Figure 7.26: Wind speed variation recorded at the WO station

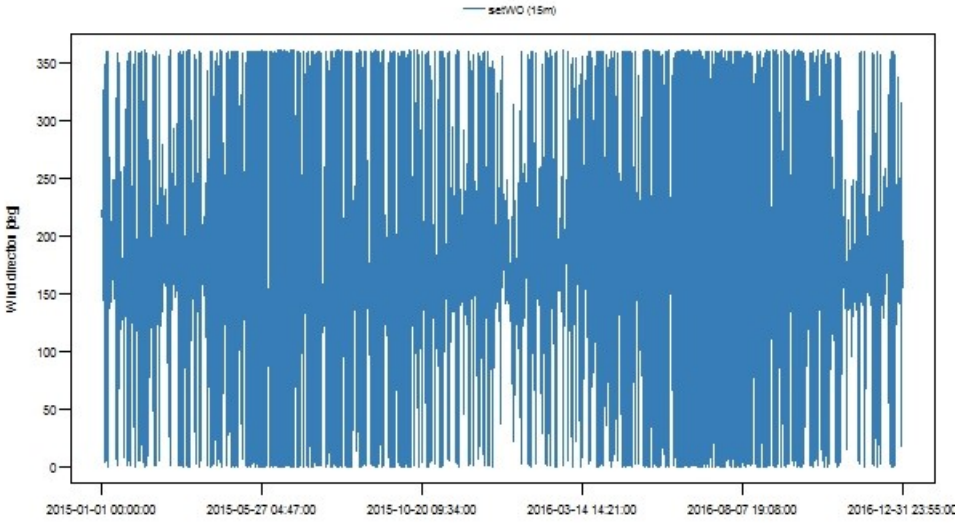

Figure 7.27: Wind direction variation for the WO station

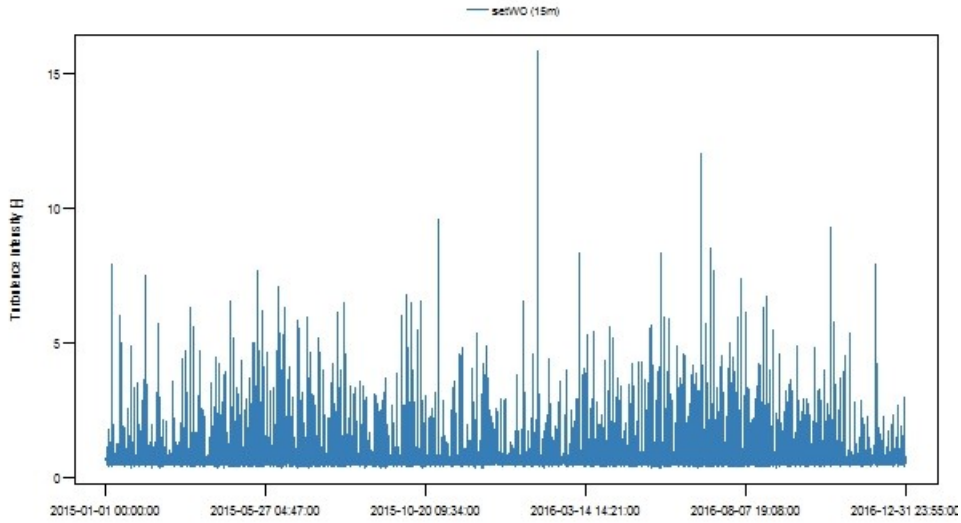

Figure 7.28: Turbulence Intensity for the WO station

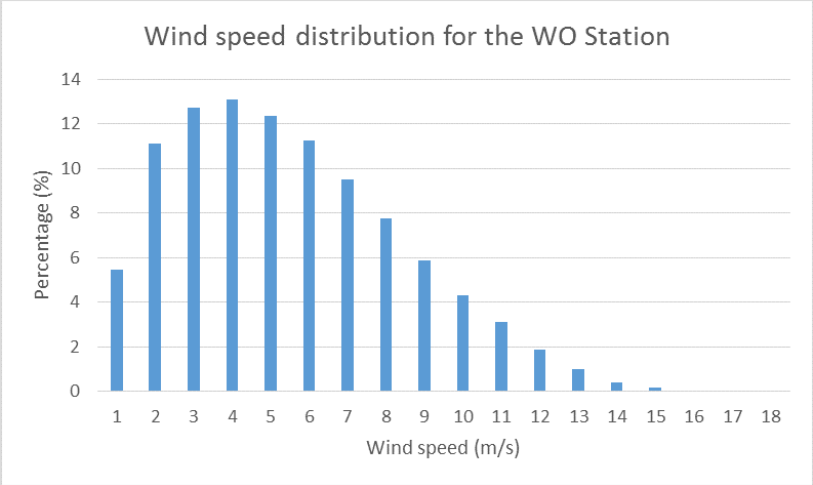

Figure 7.29: Weather Office wind speed distribution

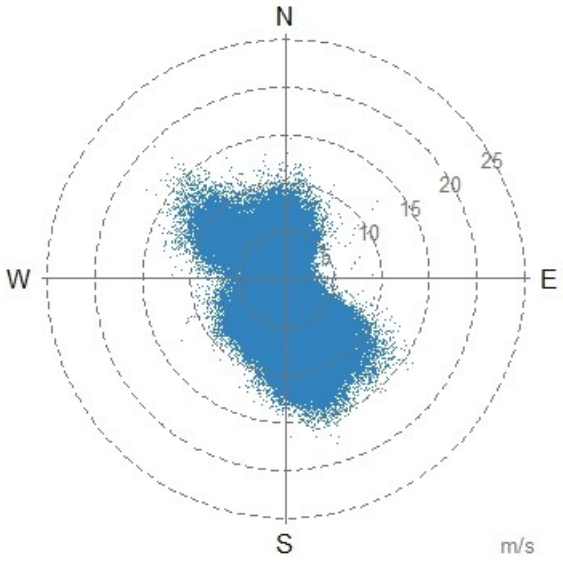

Figure 7.30: Polar plot for the WO station

Turbine Type	Kestrel e230i	eddyGT	Turby	SkyStream
Change in AEP from 15-20m (%)	16.4	19.1	26.2	19.1
Change in AEP from 20-25m (%)	12	14.3	18.9	13.7
Change in AEP from 25-30m (%)	9.4	11.2	14.7	11

Table 7.1: Sensitivity analysis for the AWS station

Figure 7.30. This figure plots the wind speed and wind direction of each of the data points that have been recorded over the 2 year period. This figure again shows that the prevailing wind direction is from the South and that the majority of the data points have a wind speed of between 5-10 m/s.

7.2 APPENDIX B: RESULTS OF THE HUB HEIGHT SENSITIVITY ANALYSIS

This section details the full results of the hub height sensitivity analysis. In the main body of this thesis, only the results from the Cape Town WO station were presented. However, the results from the other five locations reinforce the finding of a positive relationship between hub height and expected electricity generation and this relationship is characterised by decreasing returns of electricity generation relative to hub height.

Turbine Type	Kestrel e230i	eddyGT	Turby	SkyStream
Change in AEP from 15-20m (%)	10.2	12	14.1	11.0
Change in AEP from 20-25m (%)	7.3	8.7	9.9	7.8
Change in AEP from 25-30m (%)	5.6	6.5	7.5	5.9

Table 7.2: Sensitivity analysis for the RCYC station

Turbine Type	Kestrel e230i	eddyGT	Turby	SkyStream
Change in AEP from 15-20m (%)	18.8	21.1	32.7	23.7
Change in AEP from 20-25m (%)	13.9	17.2	23.1	17.4
Change in AEP from 25-30m (%)	11.2	12.5	17.9	13.7

Table 7.3: Sensitivity analysis for the Molteno reservoir

Turbine Type	Kestrel e230i	eddyGT	Turby	SkyStream
Change in AEP from 15-20m (%)	19.9	25.3	45.4	28.4
Change in AEP from 20-25m (%)	15.1	17.4	30.5	20.6
Change in AEP from 25-30m (%)	11.8	15	23.2	16.1

Table 7.4: Sensitivity analysis for the Observatory station

Turbine Type	Kestrel e230i	eddyGT	Turby	SkyStream
Change in AEP from 15-20m (%)	15.7	14	15.9	14.2
Change in AEP from 20-25m (%)	9.4	12.3	11.7	13
Change in AEP from 25-30m (%)	7.6	2.8	4.7	12.4

Table 7.5: Sensitivity analysis for the Kirstenbosch station

7.3 APPENDIX C: SAMPLES OF THE *r* SCRIPT

This section shows a sample of the *R* bReeze package that was used in the data analysis procedure after Graul & Poppinga (2015). The three parts of the script that are shown in this section of the document relate the the calcualtion of the Weibull parameters, the wind energy content, and the AEP values.

7.3.1 *Weibull parameters*

```
> weibull
function (mast, v.set, dir.set, num.sectors = 12, subset, digits = 3,
    print = TRUE)
{
    if (class(mast) != "mast")
        stop(substitute(mast), " is no mast object")
    num.sets <- length(mast$sets)
    if (!missing(v.set) && missing(dir.set))
        dir.set <- v.set
    if (missing(v.set) && !missing(dir.set))
        v.set <- dir.set
    if (!is.numeric(v.set))
        v.set <- match(v.set, names(mast$sets))
    if (is.na(v.set))
        stop("'v.set' not found")
    if (!is.numeric(dir.set))
        dir.set <- match(dir.set, names(mast$sets))
    if (is.na(dir.set))
        stop("'dir.set' not found")
    if (!is.numeric(num.sectors))
        stop("'num.sectors' must be numeric")
    if (num.sectors <= 1)
        stop("There must be at least 2 sectors")
    if (v.set <= 0 || v.set > num.sets)
        stop("'v.set' not found")
    if (dir.set <= 0 || dir.set > num.sets)
        stop("'dir.set' not found")
    if (is.null(mast$sets[[v.set]]$data$v.avg))
        stop("'set' does not contain average wind speed data")
    if (is.null(mast$sets[[dir.set]]$data$dir.avg))
        stop("'set' does not contain wind direction data")
    if (missing(subset))
        subset <- c(NA, NA)
    start.end <- subset.int(mast$timestamp, subset)
    start.end <- subset.int(mast$timestamp, subset)
    start <- start.end[1]
    end <- start.end[2]
    v <- mast$sets[[v.set]]$data$v.avg[start:end]
    d <- mast$sets[[dir.set]]$data$dir.avg[start:end]
    sector.width <- 360/num.sectors
    sectors <- seq(0, 360 - sector.width, by = sector.width)
    sector.edges <- c(sectors - sector.width/2, tail(sectors,
        n = 1) + sector.width/2)%%360
    weibull.tbl <- matrix(NA, nrow = num.sectors + 1, ncol = 4)
    for (s in 1:num.sectors) {
        low <- sector.edges[s]
        high <- sector.edges[s + 1]
        if (low < high)
            sector.idx <- d >= low & d < high
        else sector.idx <- d >= low | d < high
        weibull.param <- weibull.int(v[sector.idx], FALSE)
        weibull.tbl[s, 1] <- weibull.param$A
        weibull.tbl[s, 2] <- weibull.param$k
    }
    weibull.param <- weibull.int(v, TRUE)
    weibull.tbl[num.sectors + 1, 1] <- weibull.param$A
    weibull.tbl[num.sectors + 1, 2] <- weibull.param$k
    freq <- frequency(mast, v.set, dir.set, num.sectors, bins = NULL,
        subset = subset, digits = digits, print = FALSE)
    weibull.tbl[, 3] <- freq$wind.speed
    weibull.tbl[, 4] <- freq$total
    r.names <- c(paste0("s", 1:num.sectors), "all")
    if (num.sectors == 4)
        r.names <- c("n", "e", "s", "w", "all")
    if (num.sectors == 8)
        r.names <- c("n", "ne", "e", "se", "s", "sw", "w", "nw",
            "all")
    if (num.sectors == 12)
        r.names <- c("n", "nne", "ene", "e", "ese", "sse", "s",
```

```
            all")
    if (num.sectors == 12)
        r.names <- c("n", "nne", "ene", "e", "ese", "sse", "s",
            "ssw", "wsw", "w", "wnw", "nnw", "all")
    if (num.sectors == 16)
        r.names <- c("n", "nne", "ne", "ene", "e", "ese", "se",
            "sse", "s", "ssw", "sw", "wsw", "w", "wnw", "nw",
            "nnw", "all")
    weibull.tbl <- data.frame(weibull.tbl, row.names = r.names)
    names(weibull.tbl) <- c("A", "k", "wind.speed", "frequency")
    attr(weibull.tbl, "units") <- c("m/s", "-", attr(mast$sets[[v.set]]$data$v.avg,
        "unit"), "%")
    attr(weibull.tbl, "call") <- list(func = "weibull", mast = deparse(substitute(mast)),
        v.set = v.set, dir.set = dir.set, num.sectors = num.sectors,
        subset = subset, digits = digits, print = print)
    weibull.tbl <- round(weibull.tbl, digits)
    class(weibull.tbl) <- "weibull"
    if (print)
        print(weibull.tbl)
    invisible(weibull.tbl)
}
<environment: namespace:bReeze>
```

7.3.2 *Wind energy calculation*

```
> energy
function (wb, rho = 1.225, bins = c(5, 10, 15, 20), digits = 0,
    print = TRUE)
{
    if (class(wb) != "weibull")
        stop(substitute(wb), " is no weibull object")
    if (any(bins < 0))
        stop("'bins' must be NULL or a vector of positives")
    if (is.null(attr(wb, "call")$mast))
        stop("Source mast object of ", substitute(wb), " could not be found")
    mast <- get(attr(wb, "call")$mast)
    v.set <- attr(wb, "call")$v.set
    dir.set <- attr(wb, "call")$dir.set
    num.sectors <- attr(wb, "call")$num.sectors
    subset <- attr(wb, "call")$subset
    start.end <- subset.int(mast$timestamp, subset)
    start <- start.end[1]
    end <- start.end[2]
    lim <- c(0, 5 * (trunc(ceiling(max(mast$sets[[v.set]]$data$v.avg[start:end],
        na.rm = TRUE))/5) + 1))
    if (!is.null(bins))
        if (head(bins, 1) != 0)
            bins <- c(0, bins)
    num.classes <- length(bins)
    v.max <- max(mast$sets[[v.set]]$data$v.avg[start:end], na.rm = TRUE)
    if (num.classes > 2) {
        for (i in (num.classes - 1):2) {
            if (bins[i + 1] >= v.max && bins[i] >= v.max) {
                bins <- head(bins, -1)
                num.classes <- length(bins)
            }
        }
    }
    if (!is.null(bins))
        if (num.classes == 2 && bins[num.classes] >= v.max)
            stop("Only one wind class found")
    energy.tbl <- data.frame(matrix(NA, nrow = num.sectors +
        1, ncol = num.classes + 1))
    r.names <- c(paste0("s", 1:num.sectors), "all")
    if (num.sectors == 4)
        r.names <- c("n", "e", "s", "w", "all")
    if (num.sectors == 8)
        r.names <- c("n", "ne", "e", "se", "s", "sw", "w", "nw",
            "all")
    if (num.sectors == 12)
        r.names <- c("n", "nne", "ene", "e", "ese", "sse", "s",
            "ssw", "wsw", "w", "wnw", "nnw", "all")
    if (num.sectors == 16)
        r.names <- c("n", "nne", "ne", "ene", "e", "ese", "se",
            "sse", "s", "ssw", "sw", "wsw", "w", "wnw", "nw",
            "nnw", "all")
    row.names(energy.tbl) <- r.names
    c.names <- c("total")
    if (!is.null(bins)) {
        for (i in 1:(num.classes - 1)) c.names <- append(c.names,
            paste(bins[i], bins[i + 1], sep = "-"))
        c.names <- append(c.names, paste0(">", bins[num.classes]))
    }
    names(energy.tbl) <- c.names
    freq.l <- frequency(mast, v.set, dir.set, num.sectors, bins,
        subset, print = FALSE)
    freq <- freq.l[[2]]
    if (length(freq.l) > 2)
        for (i in 3:length(freq.l)) freq <- cbind(freq, freq.l[[i]])
    if (!is.null(bins))
        freq <- data.frame(freq)
```

```
        freq <- data.frame(freq)
    for (i in 1:num.sectors) {
        if (!is.null(bins)) {
            for (j in 2:dim(freq)[2]) energy.tbl[i, j] <- round(energy.int(lim,
                wb$k[i], wb$A[i], rho) * freq[i, j]/100, digits)
            energy.tbl[i, 1] <- round(energy.int(lim, wb$k[i],
                wb$A[i], rho) * freq[i, 1]/100, digits)
        }
        else {
            energy.tbl[i, 1] <- round(energy.int(lim, wb$k[i],
                wb$A[i], rho) * freq[i]/100, digits)
        }
    }
    for (i in 1:(num.classes + 1)) energy.tbl[num.sectors + 1,
        i] <- sum(energy.tbl[1:num.sectors, i], na.rm = TRUE)
    for (i in 1:length(energy.tbl)) energy.tbl[, i][is.nan(energy.tbl[,
        i]) | is.na(energy.tbl[, i])] <- 0
    if (!is.null(bins))
        if (tail(bins, 1) >= v.max)
            energy.tbl[, length(energy.tbl)] <- NULL
    if (sum(energy.tbl[, length(energy.tbl)], na.rm = TRUE) ==
        0)
        energy.tbl[, length(energy.tbl)] <- NULL
    attr(energy.tbl, "unit") <- "kWh/m^2/a"
    attr(energy.tbl, "call") <- list(func = "energy", wb = deparse(substitute(wb)),
        rho = rho, bins = bins, digits = digits, print = print)
    energy.tbl <- round(energy.tbl, digits)
    class(energy.tbl) <- "energy"
    if (print)
        print(energy.tbl)
    invisible(energy.tbl)
}
<environment: namespace:bReeze>
```

7.3.3 *AEP calculation*

```
> aep
function (profile, pc, hub.h, rho = 1.225, avail = 1, bins = c(5,
    10, 15, 20), sectoral = FALSE, digits = c(3, 0, 0, 3), print = TRUE)
{
    if (missing(profile))
        stop("Profile 'profile' is mandatory")
    if (missing(pc))
        stop("Power curve 'pc' is mandatory")
    if (missing(hub.h))
        stop("Hub heigth 'hub.h' is mandatory")
    if (missing(rho))
        rho <- 1.225
    if (missing(avail))
        avail <- 1
    if (missing(bins))
        bins <- c(5, 10, 15, 20)
    if (missing(sectoral))
        sectoral <- FALSE
    if (missing(digits))
        digits <- c(3, 0, 0, 3)
    if (missing(print))
        print <- TRUE
    if (class(profile) != "profile")
        stop(substitute(profile), " is no profile object")
    if (class(pc) != "pc")
        stop(substitute(pc), " is no power curve object")
    if (!is.numeric(hub.h))
        stop("'hub.h' must be numeric")
    if (!is.numeric(rho))
        stop("'rho' must be numeric")
    if (!is.numeric(avail))
        stop("'avail' must be numeric")
    if (avail < 0 || avail > 1)
        stop("'avail' must be a numeric value between 0 and 1")
    if (any(bins < 0))
        stop("'bins' must be NULL or a vector of positives")
```

```
    if (length(digits) != 4) {
        digits <- rep(digits, 4)
        warning("'digits' shall be a vector of four values (for wind speed, operation, aep and cap
acity)",
            call. = FALSE)
    }
    if (is.null(attr(profile, "call")$mast))
        stop("Source mast object of ", substitute(profile), " could not be found")
    mast <- get(attr(profile, "call")$mast)
    v.set <- attr(profile, "call")$v.set[1]
    dir.set <- attr(profile, "call")$dir.set
    num.sectors <- attr(profile, "call")$num.sectors
    subset <- attr(profile, "call")$subset
    rho.pc <- attr(pc, "rho")
    rated.p <- attr(pc, "rated.power")
    start.end <- subset.int(mast$timestamp, subset)
    start <- start.end[1]
    end <- start.end[2]
    sector.width <- 360/num.sectors
    sectors <- seq(0, 360 - sector.width, by = sector.width)
    sector.edges <- c(sectors - sector.width/2, tail(sectors,
        n = 1) + sector.width/2)%%360
    v.ref <- mast$sets[[v.set]]$data$v.avg[start:end]
    h.ref <- profile$h.ref
    dir <- mast$sets[[dir.set]]$data$dir.avg[start:end]
    idx <- !is.na(v.ref) & !is.na(dir)
    v.hh <- v.ref[idx]
    dir <- dir[idx]
    dir <- dir[idx]
    if (sectoral) {
        for (i in 1:num.sectors) {
            low <- sector.edges[i]
            high <- sector.edges[i + 1]
            if (low < high)
                sector.idx <- dir >= low & dir < high
            else sector.idx <- dir >= low | dir < high
            v.hh[sector.idx] <- v.hh[sector.idx] * exp(profile$profile[i,
                "alpha"] * log(hub.h/h.ref))
        }
    }
    else v.hh <- v.hh * exp(profile$profile["all", "alpha"] *
        log(hub.h/h.ref))
    v.max <- max(v.hh, na.rm = TRUE)
    if (!is.null(bins))
        if (head(bins, 1) != 0)
            bins <- c(0, bins)
    num.classes <- length(bins)
    if (num.classes > 2) {
        for (i in (num.classes - 1):2) {
            if (bins[i + 1] >= v.max & bins[i] >= v.max) {
                bins <- head(bins, -1)
                num.classes <- length(bins)
            }
        }
    }
    if (!is.null(bins))
        if (num.classes == 2 && bins[num.classes] >= v.max)
            stop("Only one wind class found")
    aep.tbl <- data.frame(matrix(NA, nrow = num.sectors + 1,
        ncol = num.classes + 3))
    r.names <- c(paste0("s", 1:num.sectors), "all")
    if (num.sectors == 4)
        r.names <- c("n", "e", "s", "w", "total")
    if (num.sectors == 8)
        r.names <- c("n", "ne", "e", "se", "s", "sw", "w", "nw",
            "total")
    if (num.sectors == 12)
        r.names <- c("n", "nne", "ene", "e", "ese", "sse", "s",
            "ssw", "wsw", "w", "wnw", "nnw", "total")
    if (num.sectors == 16)
        r.names <- c("n", "nne", "ne", "ene", "e", "ese", "se",
            "sse", "s", "ssw", "sw", "wsw", "w", "wnw", "nw",
            "nnw", "total")
    row.names(aep.tbl) <- r.names
    c.names <- c("wind.speed", "operation", "total")
    if (!is.null(bins)) {
        for (i in 1:(num.classes - 1)) c.names <- append(c.names,
            paste(bins[i], bins[i + 1], sep = "-"))
        c.names <- append(c.names, paste0(">", bins[num.classes]))
    }
    names(aep.tbl) <- c.names
    if (!is.null(bins))
        lim.max <- max(5 * (trunc(ceiling(max(v.hh, na.rm = TRUE))/5) +
            1), 5 * (trunc(ceiling(max(bins))/5) + 1))
    else lim.max <- 5 * (trunc(ceiling(max(v.hh, na.rm = TRUE))/5) +
        1)
    for (i in 1:num.sectors) {
        low <- sector.edges[i]
        high <- sector.edges[i + 1]
        if (low < high)
            sector.idx <- dir >= low & dir < high
        else sector.idx <- dir >= low | dir < high
        aep.tbl$wind.speed[i] <- round(mean(v.hh[sector.idx],
            na.rm = TRUE), digits[1])
        aep.tbl$operation[i] <- op <- round(length(v.hh[sector.idx])/length(v.hh) *
            8760, digits[2])
        wb.par <- weibull.int(v.hh[sector.idx], FALSE)
```

```
        wb.par <- weibull.fit(v.hh[sector.idx], FALSE)
        if (!is.null(bins)) {
            for (j in 2:num.classes) aep.tbl[i, j + 2] <- round(aep.int(wb.par,
                c(bins[j - 1], bins[j]), pc, rho.pc, op, rho,
                avail), digits[3])
            aep.tbl[i, num.classes + 3] <- round(aep.int(wb.par,
                c(bins[num.classes], lim.max), pc, rho.pc, op,
                rho, avail), digits[3])
        }
        aep.tbl$total[i] <- round(aep.int(wb.par, c(0, lim.max),
            pc, rho.pc, op, rho, avail), digits[3])
    }
    aep.tbl$wind.speed[num.sectors + 1] <- round(mean(v.hh, na.rm = TRUE),
        digits = digits[1])
    aep.tbl$operation[num.sectors + 1] <- 8760
    for (i in 3:(num.classes + 3)) aep.tbl[num.sectors + 1, i] <- sum(aep.tbl[1:num.sectors,
        i], na.rm = TRUE)
    for (i in 1:length(aep.tbl)) aep.tbl[, i][is.nan(aep.tbl[,
        i]) | is.na(aep.tbl[, i])] <- 0
    if (!is.null(bins))
        if (tail(bins, 1) >= v.max)
            aep.tbl[, length(aep.tbl)] <- NULL
    if (sum(aep.tbl[, length(aep.tbl)], na.rm = TRUE) == 0)
        aep.tbl[, length(aep.tbl)] <- NULL
    attr(aep.tbl$wind.speed, "unit") <- "m/s"
    attr(aep.tbl$operation, "unit") <- "h/a"
    attr(aep.tbl$total, "unit") <- "MWh/a"
    cap <- round(aep.tbl$total[num.sectors + 1]/(rated.p * 0.001 *
        8760), digits = digits[4])
    aep <- list(aep = aep.tbl, capacity = cap)
    attr(aep, "call") <- list(func = "aep", profile = deparse(substitute(profile)),
        pc = deparse(substitute(pc)), hub.h = hub.h, rho = rho,
        avail = avail, bins = bins, sectoral = sectoral, digits = digits,
        print = print)
    class(aep) <- "aep"
    if (print)
        print(aep)
    invisible(aep)
}
<environment: namespace:bReeze>
> 
```